

# Did the ancient Egyptians record the period of the eclipsing binary Algol – the Raging one? <sup>★</sup>

L. Jetsu<sup>1</sup>, S. Porceddu<sup>1</sup>, J. Lyytinen<sup>1</sup>, P. Kajatkari<sup>1</sup>, J. Lehtinen<sup>1</sup>, T. Markkanen<sup>1</sup>, and J. Toivari-Viitala<sup>2</sup>

<sup>1</sup> Department of Physics, P.O. Box 64, FI-00014 University of Helsinki, Finland (e-mail: lauri.jetsu@helsinki.fi)

<sup>2</sup> Department of World Cultures, P.O. Box 59, FI-00014 University of Helsinki, Finland

Received / Accepted

## ABSTRACT

The eclipses in binary stars give precise information of orbital period changes. Goodricke discovered the 2.867 days period in the eclipses of Algol in the year 1783. The irregular orbital period changes of this longest known eclipsing binary continue to puzzle astronomers. The mass transfer between the two members of this binary should cause a long-term increase of the orbital period, but observations over two centuries have not confirmed this effect. Here, we present evidence indicating that the period of Algol was 2.850 days three millennia ago. For religious reasons, the ancient Egyptians have recorded this period into the Cairo Calendar, which describes the repetitive changes of the Raging one. Cairo Calendar may be the oldest preserved historical document of the discovery of a variable star.

**Key words.** general: history and philosophy of astronomy — methods: statistical – stars: eclipsing binaries – stars: individual: Algol

## 1. Introduction

In eclipsing binaries, two stars rotate around a common centre of mass, and the orbital plane and the line of sight nearly coincide. A primary eclipse occurs when the dimmer member partially or totally covers the visible disk of the brighter member. In Algol type eclipsing binaries (hereafter EB), one member has evolved into a giant or subgiant. This has caused Roche-lobe overflow<sup>1</sup> leading to mass transfer (hereafter MT) to the other less evolved main sequence star (Pustynnik 1998). MT from the less massive to the more massive member should cause a long-term increase of the orbital period  $P_{\text{orb}}$  (Biermann & Hall 1973; Hall 1989). Many EBs show only positive or negative  $P_{\text{orb}}$  changes (Hall 1989). Both positive and negative  $P_{\text{orb}}$  changes seemed to occur only in EBs where at least one member displayed magnetic activity (Hall 1989). Applegate (1992) presented a theory, where magnetic activity causes such alternate period changes (hereafter APC). APC are still poorly understood (Zavala et al. 2002) and Applegate's theory has been questioned (Lanza 2005, 2006). APC were recently also observed in EBs that have no member displaying magnetic activity (Liao & Qian 2010).

Algol is the brightest EB. Montanari discovered Algol's eclipses in 1669 (Merrill 1938). Algol was the second variable star discovered, 73 years after the discovery of Mira by Fabritius. Goodricke (1783) determined  $P_{\text{orb}} = 2.867$  of Algol with naked eyes. On the same year, the Royal Society of London awarded him the Copley Medal for this outstanding achievement. However, the observed (O) eclipses could not be calculated (C) with any constant  $P_{\text{orb}}$  value (Argelander 1855). These

O minus C (hereafter  $O - C$ ) changes have shown APC cycles of 1.9, 32 and 180 years (Frieboes-Conde et al. 1970). Algol is actually a triple system (Csizmadia et al. 2009; Zavala et al. 2010). The eclipsing members in the 2.<sup>d</sup>867 close orbit are Algol A (B8 V) and Algol B (K2 IV). The brightness falls from 2.<sup>m</sup>1 to 3.<sup>m</sup>4 within 5 hours when the dimmer Algol B partially covers the brighter Algol A (Isles 1997). The third member Algol C (F1 IV) in the wide 1.<sup>y</sup>9 orbit causes the shortest  $O - C$  cycle. Applegate's theory may explain the 32<sup>y</sup> and 180<sup>y</sup> APC cycles, because Algol B displays magnetic activity (Applegate 1992). The observed MT (Richards 1992) from Algol B to Algol A should cause a long-term  $P_{\text{orb}}$  increase, but APC may have masked this effect (Biermann & Hall 1973). This problem was discussed when Kiseleva et al. (1998) compared Algol to another EB called U Cep, where the parabolic  $O - C$  trend has confirmed a long-term  $P_{\text{orb}}$  increase caused by MT. Evidence for this effect in Algol is lacking after nearly 230 years of observations. Thus, any  $P_{\text{orb}}$  information predating 1783 A.D. would be valuable.

Ancient Egyptian scribes wrote Calendars of Lucky and Unlucky Days that assigned good and bad prognoses for the days of the year. The prognoses were based on mythological and astronomical events considered influential for everyday life. The best preserved calendar is the Cairo Calendar (hereafter CC) in papyrus Cairo 86637 dated to 1271–1163 B.C. (Bakir 1966; Demaree & Janssen 1982; Helck et al. 1975–1992). The ancient Egyptian year had 365 days. It contained 12 months of 30 days each. The year was divided into the flood\* (Akhet), the winter\* (Peret) and the harvest\* (Shemu) seasons.<sup>2</sup> CC gave three prognoses a day, except for the 5 additional “epagomenal” days of the year. Our Table 1 follows the German notation G = “gut” = “good\*” and S = “schlecht” = “bad\*” (Leitz 1994). The notation for unreadable prognoses in CC is “–”. The Egyptian day began

<sup>★</sup> Table 3 is published only electronically at the CDS via anonymous ftp to cdsarc.u-strasbg.fr (130.79.128.5) or via <http://cdsarc.u-strasbg.fr/viz-bin/qcat?J/A+A/yyy/Axxx>

<sup>1</sup> The region of space, where orbiting material can not escape the gravitational pull of a star in a binary system, is called the Roche-lobe. Overflow occurs when a star in binary system expands past the Roche-lobe limit and material begins to escape.

<sup>2</sup> The symbol “\*” denotes the words given in ancient Egyptian language in the end of this paper after the list of references.

**Table 1.** CC prognoses for one Egyptian year.

	Akhet I	Akhet II	Akhet III	Akhet IV	Peret I	Peret II	Peret III	Peret IV	Shemu I	Shemu II	Shemu III	Shemu IV
<i>D</i>	<i>M</i> = 1	<i>M</i> = 2	<i>M</i> = 3	<i>M</i> = 4	<i>M</i> = 5	<i>M</i> = 6	<i>M</i> = 7	<i>M</i> = 8	<i>M</i> = 9	<i>M</i> = 10	<i>M</i> = 11	<i>M</i> = 12
1	GGG	GGG	GGG	GGG	GGG	GGG	GGG	GGG	GGG	GGG	GGG	GGG
2	GGG	GGG	—	GGG	GGG	GGG	GGG	GGG	—	—	GGG	GGG
3	GGG	GGG	GGG	SSS	GGG	—	—	SSS	GGG	GGG	SSS	SSS
4	GGG	SGS	—	GGG	GGG	GGG	SSS	GGG	SSS	SSS	GGG	SSG
5	GGG	SSS	—	GGG	GSS	GGG	GGG	SSS	—	GGG	SSS	GGG
6	SSG	GGG	GGG	SSS	GGG	—	GGG	SSS	GGG	—	—	SSS
7	GGG	SSS	GGG	SSS	SSS	GGG	SSS	GGG	GGG	SSS	SSS	—
8	GGG	GGG	—	GGG	GGG	GGG	GGG	GGG	—	GGG	SSS	GGG
9	GGG	GGG	SSS	GGG	GGG	GGG	GGG	—	GGG	GGG	GGG	GGG
10	GGG	GGG	GGG	GGG	SSS	SSS	SSS	—	—	GGG	SSS	GGG
11	SSS	GGG	GGG	GGG	SSS	GGG	GGG	SSS	—	SSS	SSS	SSS
12	SSS	SSS	—	SSS	—	GGG	GGG	SSS	—	GGG	—	GGG
13	GSS	GGG	SSS	GGG	GGG	SSS	GGG	SSS	—	GGG	—	GGG
14	—	GGG	SSS	GGG	SSS	SGG	—	—	—	GGG	SSS	GGG
15	GSS	GSS	SSS	—	GGG	—	SSS	GGG	—	SSS	GGG	SSS
16	SSS	GGG	GGG	GGG	GGG	—	SSS	GGG	GGG	GGG	SSS	GGG
17	SSS	GGG	—	—	SSS	GGG	SSS	SSS	GGG	SSS	—	GGG
18	GGG	SSS	SSS	SSS	GGG	SSS	GGG	—	GGG	SSS	SSS	SSG
19	GGG	GGG	SSS	SSS	SSS	GSS	—	GGG	GGG	SSS	SSS	GGG
20	SSS	SSS	SSS	SSS	SSS	SSS	SSS	—	SSS	SSS	SSS	—
21	GGG	SSG	GGG	SSG	GGG	—	—	—	SSS	SSG	GGG	GGG
22	SSS	—	—	GGG	GGG	GGG	SSS	SSS	GGG	SSS	SSS	GGG
23	SSS	—	SSS	GGS	GGG	GGG	GGG	—	GGG	GGG	SSS	SSS
24	GGG	SSS	GGG	—	GGG	SSS	SSS	SSS	—	GGG	GGG	GGG
25	GGS	SSS	GGG	—	GGG	GGG	—	SSS	GGG	GGG	GSG	GGG
26	SSS	SSS	GGG	GGG	SSS	—	SSS	—	GGG	SSS	GGG	GSG
27	GGG	SSS	GGG	GGS	GGG	—	SSS	SSS	—	SSS	SSS	SSS
28	GGG	GGG	GGG	SSS	GGG	GGG	GGG	GGG	—	GGG	SSS	GGG
29	SGG	GGG	GGG	SSS	GGG	SSS	GGG	GGG	GGG	GGG	GGG	GGG
30	GGG	GGG	GGG	GGG	GGG	SSS	GGG	GGG	GGG	GGG	GGG	GGG

**Notes.** All 12 months (*M*) are 30 days (*D*) long.

from dawn. For example, “GGS” for “I Akhet 25” means that the first two parts of this day were good, but the third part was bad. The synodic period of the Moon was detected in CC with the standard Rayleigh test (Porceddu et al. 2008, hereafter Paper I), as well as indications of numerous less significant periods. One of these less significant periods,  $2.^d85$ , was close, but not equal, to  $P_{\text{orb}}$  of Algol. However, the influence of Algol on CC had to be considered only tentative. It was, therefore, noted that affirmation of the identification of Algol would certainly require a more detailed study.

Paper I was published in an archeological journal. The current Paper II concentrates on statistics (period analysis), astrophysics and astronomy. The connections between Algol and the writers of CC, the ancient Egyptian scribes, are discussed in greater detail in Porceddu et al. (2012, hereafter Paper III). We have added a few footnotes to make this Paper II readable to the scientists, who are not specialized in astronomy. All acronyms used are given after the list of references, as well as a list of selected words translated to the ancient Egyptian language.

The analysed data are created from CC in Sect. 2. The normalized Rayleigh test is formulated in Sect. 3. This test reveals that after removing the good prognoses connected to the lunar cycle, the only significant real periodicity in CC is 2.850 days, which is 0.017 days shorter than the current orbital period of

Algol. The mass transfer in the Algol system could explain this 0.017 days orbital period increase during the past three millennia (Sect. 4). Finally, we show that out of all currently known over 40 000 variable stars, Algol is the only one whose periodic variability could have been discovered by the ancient Egyptians and recorded to CC (Sect. 5).

## 2. Data

The ancient Egyptian texts known as the Calendars of Lucky and Unlucky Days, or hemerologies, are literary works that assign prognoses to each day of the Egyptian year. These prognoses denote whether the day, or a part of the day, is considered “good\*” or “bad\*”. Nine different hemerologies, partial or full, have been found preserved from ancient Egyptian times. Only three of them, papyrus Cairo 86637 (Bakir 1966), papyrus Sallier IV (p. BM 10184) (Budge 1923) and papyrus BM 10474 (Budge 1922) are full hemerologies, such that assign each day of the Egyptian year a unique prognosis. For the major part, the texts and the prognoses are in agreement. It has been suggested that papyrus Sallier IV is in fact a writing exercise from the scribal school, since some writing mistakes have been corrected in the margins of the papyrus (Helck et al. 1975–1992). Because papyrus BM 10474 includes only the prognoses, but not the de-

scriptions of the dates, CC from papyrus Cairo 86637 is at the moment the best preserved Calendar of Lucky and Unlucky days available.

The CC prognoses for one Egyptian year have been tabulated in Table 1 according to the reproduction and German translation (Leitz 1994). Our notations are the same, i.e. “G” = “gut” = good and “S” = “schlecht” = bad. Damaged and unreadable prognoses in CC have been ignored, as well as the prognoses from other reproduced and translated papyri. These particular days with no prognoses are denoted with “–”.

The structure of the year, as presented in CC (Table 1), is in accordance with the ancient Egyptian civil calendar. It divided the year into 12 months of 30 days each. Additionally, each day was divided into three parts. However, the exact logic of this day division procedure has not been explained anywhere in the known Egyptian texts. Most of the time, the prognosis is same for all the different parts of the same day (i.e. GGG or SSS). However, 23 days of the year have been assigned a heterogeneous prognosis, e.g. such as GSS. The verbose descriptions of this kind of days have been used to infer how Egyptians divided the day into three parts. For example, the prognosis of the day “I Akhet 8” is GGS. The text regarding the day advises not to go out during the “night\*”. On the other hand, the day “I Akhet 25” has the same prognosis GGS, but the text advises to stay in for the “evening\*”. A study of all heterogeneous prognoses indicated that the first third of the day refers to the morning, the second third refers to mid-day and the last third refers to evening, but also possibly includes the night (Leitz 1994).

We decided to create 24 different samples of series of time points (hereafter SSTP) from the prognoses of Table 1 to check, if the period analysis results depend on the

1. transformation between the Egyptian and Gregorian year.
2. day division used.
3. prognoses selected.
4. prognoses removed.

The month ( $M = 1, 2, \dots, 12$ ) and the day of month ( $D = 1, 2, \dots, 30$ ) has been assigned for every prognosis in Table 1. For example, the three prognoses for the 6th day of the Egyptian year, “I Akhet 6” with  $M = 1$  and  $D = 6$ , were “SSG”. A suitable numbering for the days in an Egyptian year is

$$N_E = 30(M - 1) + D.$$

The full length of the Egyptian civil year was 365 days. The last five days,  $361 \leq N_E \leq 365$ , were not included into Table 1, nor were prognoses given for them. The transformation to the day number  $N_G$  in a Gregorian year is simply

$$N_G = \begin{cases} N_E + N_0 - 1, & N_E \leq 366 - N_0 \\ N_E + N_0 - 366, & N_E > 366 - N_0, \end{cases} \quad (1)$$

where  $N_0$  is a constant and  $N_G = 1$  is 1st of January. For example, it has been suggested that  $N_0 = 187$  is a suitable value (Leitz 1994). In this case, “I Akhet 1”  $\equiv N_E = 1$  would be  $N_G = 187$  in the Gregorian year.

The declination of the Sun ( $\delta_\odot$ ) determines the length of a day at any particular geographical latitude ( $\phi$ ). The declination is the angle between the solar rays and the plane of the Earth’s equator. The approximation

$$\delta_\odot = \delta_\odot(N_G) = -23.45^\circ \cos [360^\circ(N_G + 10)/365.25] \quad (2)$$

would be accurate, if the Earth’s orbit were a perfect circle, the orbital velocity were constant and the vernal equinox occurred

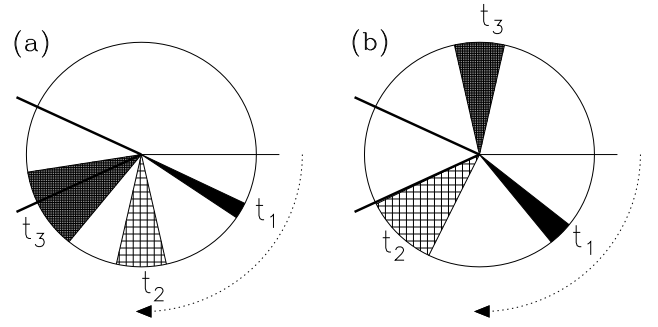


**Fig. 1.** (a) First (Eq. 4) and (b) second (Eq. 4) day division alternative. The horizontal continuous line crossing the right hand side of the circle denotes the sunrise. The dotted arrow shows the clockwise direction of time from sunrise to mid-day. The two thick lines crossing the left hand side of the circle denote the range of sunset times in a year. The three sectors show the ranges of the three daily time point values  $t_1$  (dark),  $t_2$  (crossed) and  $t_3$  (shaded) in a year.

at  $N_G = 80$ . The maximum error of this approximation is  $\pm 3^\circ$  in declination, which equals a maximum error of 0.01 days in the sunrise and sunset. However, this accuracy is sufficient for this study, because the selected geographical latitude (see Eq. 3) and especially the selected day division (see Eqs. 4 and 5) introduce considerably larger uncertainties in the calculated SSTP.

The time interval between sunrise and sunset is

$$l_D = l_D(N_G) = a \{ \arccos[-\tan(\phi) \tan(\delta_\odot)] \}, \quad (3)$$

where  $[l_D]$  = hours and the constant  $a = 24/180^\circ$  transforms degrees into hours. For this study, we selected the intermediate latitude of Middle Egypt, i.e.  $\phi = 26^\circ 41'$ .

It is not known, what part of the day each of the three daily prognoses referred to (Leitz 1994). As a first alternative, we assumed that the daytime was divided into three intervals having an equal length of  $l_D/3$  hours (Fig. 1a). The epochs of the mid-points of each interval occurred  $l_D/6$ ,  $3l_D/6$  and  $5l_D/6$  hours after the sunrise. The time points  $t_1(N_E)$ ,  $t_2(N_E)$  and  $t_3(N_E)$  calculated for the 1st, 2nd and 3rd prognosis of the  $N_E$ :th day of the Egyptian year were

$$\begin{aligned} t_1(N_E) &= (N_E - 1) + b \left\lfloor \frac{l_D(N_G)}{6} \right\rfloor \\ t_2(N_E) &= (N_E - 1) + b \left\lfloor \frac{3l_D(N_G)}{6} \right\rfloor \\ t_3(N_E) &= (N_E - 1) + b \left\lfloor \frac{5l_D(N_G)}{6} \right\rfloor, \end{aligned} \quad (4)$$

where the constant  $b = 24^{-1}$  transformed hours into days.

As a second alternative, we assumed that the daytime was divided into two intervals of  $l_D/2$  hours, while the third interval was the nighttime of  $24 - l_D$  hours (Fig. 1b). The epochs of the mid-points of these three intervals gave the following time points  $t_1(N_E)$ ,  $t_2(N_E)$  and  $t_3(N_E)$  for the 1st, 2nd and 3rd prognosis of the  $N_E$ :th day:

$$\begin{aligned} t_1(N_E) &= (N_E - 1) + b \left\lfloor \frac{l_D(N_G)}{4} \right\rfloor \\ t_2(N_E) &= (N_E - 1) + b \left\lfloor \frac{3l_D(N_G)}{4} \right\rfloor \\ t_3(N_E) &= (N_E - 1) + b \left\lfloor 12 + \frac{l_D(N_G)}{2} \right\rfloor. \end{aligned} \quad (5)$$

The prognoses of Table 1 would have offered an infinite number of alternatives for creating a series of time points. We decided to create 24 different SSTP (Table 2: Col. 1). Our aim was to check, if the results of the period analysis depended on the following choices.

- What was the chosen  $N_0$  value in Eq. 1? The transformation between Egyptian and Gregorian year alters the length of the daytime. This parameter  $N_0$  shifts the time points within each day of the year (Table 2: Col. 2,  $N_0$ ). Three different  $N_0$  values were tested. The values  $N_0 = 307$  and 62 were obtained by adding four months (120<sup>d</sup>) and eight months (240<sup>d</sup>) to the value of  $N_0 = 187$  suggested earlier (Leitz 1994).
- What was the chosen day division? This division alters the values of the time points within each day even more than the choice of  $N_0$ . The day divisions of Eqs. 4 and 5 were both tested (Table 2: Col. 3, Div). These two divisions represent the extremes that can be used in selecting these three epochs within 24 hours (see Fig. 1). The value of the Rayleigh test statistic does not change, if a constant value  $t_0$  is added to all time points (see Eq. 7). We did not, therefore, test the alternative of three nighttime points only, because it would have represented the alternative, where all three time points of the first day division (Fig. 1a) are shifted by about  $t_0 = 0.5$  days. Furthermore, the texts regarding the prognoses of  $t_1(N_E)$  and  $t_2(N_E)$  in CC referred to daytime.
- Which were the chosen prognoses? SSTP were calculated for different prognoses (Table 2: Col. 4, X). SSTP=1–12 were calculated from the “G” prognoses and SSTP=13–24 from the “S” prognoses.
- What would happen, if some prognoses were removed from the analysis? The days  $D = 1$  and 20 had the same prognoses GGG and SSS in every Egyptian month (Table 1). This introduced an obvious periodicity of 30 days. The time points of prognoses of these two particular days were removed from all SSTP with an even value (Table 2: Col. 5, Remove). The selected cases were “none” (no prognoses were removed), “ $D = 1$ ” (GGG of  $D = 1$  were removed) and “ $D = 20$ ” (SSS of  $D = 20$  were removed).

Cols. 6 and 7 in Table 2 give the number of time points ( $n$ ) and the time span ( $\Delta T = t_n - t_1$ ) of each SSTP.

The calculated  $t_i$  values for all prognoses are given in Table 3, which is only published electronically<sup>3</sup>. Cols. 1–4 of this Table 3 give the day ( $D$ ), month ( $M$ ), day number of the Egyptian year ( $N_E$ ) and the prognosis (X). Cols. 5–10 give the  $t_i$  [days] calculated with  $N_0 = 62, 187$  and 307 in Eq. 1 using the day divisions of Eqs. 4 or 5.

Table 2 summarizes the information all SSTP=1–24. For example, the first and last time point of SSTP=1 were  $t_1 = 0.080$  and  $t_n = 359.393$  (Table 3: Col. 5). The value of  $N_0$  was 62 (Eq. 1). The day division (Div) was that of Eq. 4, which is illustrated in Fig. 1a. This SSTP=1 was calculated from the X = G prognoses of Table 1. All G prognoses were used, i.e. “none” of them was removed. The number of time points was  $n = 564$ . The time span of SSTP=1 was  $\Delta T = t_n - t_1 = 359.3$  days.

In other words, the data were divided into two categories. The uneven numbered SSTP=1, 3, ..., 23 were created using all G or S prognoses of Table 1, while the prognoses of 1st and 20th day of every Egyptian month were removed from the even numbered SSTP=2, 4, ..., 24. The period analysis of these 24 different SSTP is performed in the next section.

**Table 2.** SSTP=1, 2, 3, ..., 23 and 24 created from Table 1.

SSTP	$N_0$	Div	X	Remove	$n$	$\Delta T$ (days)
1	62	Eq. 4	G	none	564	359.3
2	62	Eq. 4	G	$D = 1$	528	358.3
3	187	Eq. 4	G	none	564	359.4
4	187	Eq. 4	G	$D = 1$	528	358.4
5	307	Eq. 4	G	none	564	359.3
6	307	Eq. 4	G	$D = 1$	528	358.3
7	62	Eq. 5	G	none	564	359.6
8	62	Eq. 5	G	$D = 1$	528	358.6
9	187	Eq. 5	G	none	564	359.6
10	187	Eq. 5	G	$D = 1$	528	358.6
11	307	Eq. 5	G	none	564	359.6
12	307	Eq. 5	G	$D = 1$	528	358.6
13	62	Eq. 4	S	none	351	354.0
14	62	Eq. 4	S	$D = 20$	321	354.0
15	187	Eq. 4	S	none	351	354.0
16	187	Eq. 4	S	$D = 20$	321	354.0
17	307	Eq. 4	S	none	351	354.0
18	307	Eq. 4	S	$D = 20$	321	354.0
19	62	Eq. 5	S	none	351	354.0
20	62	Eq. 5	S	$D = 20$	321	354.0
21	187	Eq. 5	S	none	351	354.0
22	187	Eq. 5	S	$D = 20$	321	354.0
23	307	Eq. 5	S	none	351	354.0
24	307	Eq. 5	S	$D = 20$	321	354.0

**Notes.** The transformation constant  $N_0$  from Egyptian to Gregorian year (Eq. 1), the day division Div (Eq. 4 or 5), the selected prognoses (X), the removed prognoses (Remove), the number of time points ( $n$ ) and the time span ( $\Delta T = t_n - t_1$ ).

### 3. Analysis

In this section, we show that the standard Rayleigh test statistics are not reliable for the CC data. To achieve reliable statistics, we apply the normalized Rayleigh test. This test gives indisputable evidence for the significance of the 2.85 period in CC.

The following six subsections give a detailed description of all the procedures that were applied in our period analysis. This enables anybody to repeat our analysis – especially the many steps of simulations. The section begins with the formulation of the Rayleigh test. Aperiodic data imitating the real data is then simulated to check, if the statistics of the standard Rayleigh test are reliable. The main result of these simulations is that the standard Rayleigh test statistics are certainly not reliable for the CC data. When this problem has been solved, the best periods detected in the G and S prognoses of the real data are discussed separately. The main conclusion is that after the G prognoses at  $D = 1$  are removed, the only significant real periodicity in these good prognoses is 2.85 days. No significant periodicity is detected in the S prognoses. None of these results depend on the value of  $N_0$  in Eq. 1 or on the chosen day division of Eqs. 4 and 5.

#### 3.1. Rayleigh test

The period analysis began with the standard Rayleigh test (Jetsu & Pelt 2000; Kruger et al. 2002). The tested period interval was between  $P_{\min} = f_{\max}^{-1} = 1.5$  and  $P_{\max} = f_{\min}^{-1} = 90$  days. The chosen lower limit  $P_{\min}$  was comfortably larger than the spacing of the data, i.e. three time points, or less, within one day (Eqs. 4 and 5). The upper limit  $P_{\max}$  was four times shorter

<sup>3</sup> Table 3 is published only electronically at the CDS.

**Table 4.** Number of different daily prognosis combinations in Table 1.

combination	SSTP=1, 3, ..., 35			SSTP=2, 4, ..., 36		
	days	G	S	days	G	S
GGG	177	531	0	165	495	0
GGS	6	12	6	6	12	6
GSG	2	4	2	2	4	2
GSS	6	6	12	6	6	12
SSS	105	0	315	95	0	285
SSG	6	6	12	6	6	12
SGG	2	4	2	2	4	2
SGS	1	1	2	1	1	2
Total	305	564	351	283	528	321
“—”	55	0	0	53	0	0
Total	360	564	351	336	528	321
	→ Table 5			→ Table 6		

**Notes.** The columns used in calculating the probabilities given in Tables 5 and 6 are denoted with →.

than the 360 days time span of the data. The *phases* for the time points  $t_1 < t_2 < \dots < t_n$  were computed from

$$\phi_i = \text{FRAC}[(t_i - t_0)P^{-1}] = \text{FRAC}[(t_i - t_0)f], \quad (6)$$

where  $\text{FRAC}[x]$  removed the integer part of its argument  $x$ ,  $t_0$  was an arbitrary epoch and  $f = P^{-1}$  was the tested frequency. The Rayleigh test statistic is

$$z(f) = n^{-1} \left[ \left( \sum_{i=1}^n \cos \theta_i \right)^2 + \left( \sum_{i=1}^n \sin \theta_i \right)^2 \right], \quad (7)$$

where the *phase angles* are  $\theta_i = 2\pi\phi_i \equiv 2\pi f t_i$ . The value of  $z(f)$  is rotationally invariant, i.e. this combination of the unit vectors  $[\cos \theta_i, \sin \theta_i]$  does not depend on the chosen epoch  $t_0$  for the time points.

The *standard* significance estimates for the periodicities detected with the Rayleigh test rely on the null hypothesis

$H_0$ : “The phases  $\phi_i$  calculated with an arbitrary tested period  $P$  have a random distribution between 0 and 1”

Under  $H_0$ , the probability density function for one ( $m = 1$ ) arbitrary tested frequency is  $f(z) = e^{-z}$  and the cumulative distribution function is  $P(z \leq z_0) = F(z_0) = 1 - e^{-z_0}$  (Kruger et al. 2002). If the tested frequencies are between  $f_{\min}$  and  $f_{\max}$ , the number of independent statistical tests is  $m = \text{INT}[(f_{\max} - f_{\min})/f_0]$ , where  $\text{INT}[x]$  removes the decimal part of its argument  $x$  and  $f_0 = (t_n - t_1)^{-1}$  is the distance between two independent tested frequencies (Jetsu & Pelt 1996, 2000). The probability that  $z(f)$  reaches, or exceeds, the value  $z_0$  at least once in all these  $m$  independent statistical tests is

$$Q = Q(z_0) = P(z(f) \geq z_0) = 1 - (1 - e^{-z_0})^m. \quad (8)$$

This probability  $Q$  is hereafter referred to as the *standard critical level* of the Rayleigh test. The null hypothesis  $H_0$  is rejected if

$$Q < \gamma = 0.001, \quad (9)$$

where  $\gamma$  is called the *preassigned significance level*. This parameter  $\gamma$  expresses the probability of falsely rejecting  $H_0$  when it is in fact true. We used simulations to check, if the above standard critical level estimates were reliable for the CC data.

**Table 5.** Simulation of aperiodic data similar to the real data of SSTP=1, 3, ..., 23.

Stage A: Event	P(Event)
$X^*(t_1) = G$	191/305
$X^*(t_1) = S$	114/305
Stage B: Event	P(Event)
$X^*(t_1) = G \Rightarrow X^*(t_2) = G$	183/191
$X^*(t_1) = G \Rightarrow X^*(t_2) = S$	8/191
$X^*(t_1) = S \Rightarrow X^*(t_2) = S$	111/114
$X^*(t_1) = S \Rightarrow X^*(t_2) = G$	3/114
Stage C: Event	P(Event)
$X^*(t_1) = G$ and $X^*(t_2) = G \Rightarrow X^*(t_3) = G$	177/183
$X^*(t_1) = G$ and $X^*(t_2) = G \Rightarrow X^*(t_3) = S$	6/183
$X^*(t_1) = G$ and $X^*(t_2) = S \Rightarrow X^*(t_3) = G$	2/8
$X^*(t_1) = G$ and $X^*(t_2) = S \Rightarrow X^*(t_3) = S$	6/8
$X^*(t_1) = S$ and $X^*(t_2) = S \Rightarrow X^*(t_3) = S$	105/111
$X^*(t_1) = S$ and $X^*(t_2) = S \Rightarrow X^*(t_3) = G$	6/111
$X^*(t_1) = S$ and $X^*(t_2) = G \Rightarrow X^*(t_3) = G$	2/3
$X^*(t_1) = S$ and $X^*(t_2) = G \Rightarrow X^*(t_3) = S$	1/3

**Notes.** The probabilities P(event) are based on columns marked with “→” Table 5” in Table 4.

### 3.2. Simulation of aperiodic data similar to SSTP=1, 3, ..., 23

The number of different daily prognosis combinations in the *real* data are given in Table 4. We *simulated* aperiodic data, where these combinations occurred with the same probabilities. According to Table 4, the event  $X(t_1) = G$  occurred with the probability of  $(177+6+2+6)/305 = 191/305$  in the *real* data of SSTP=1, 3, ..., 23. The probability for the complementary event  $X(t_1) = S$  was  $(105+6+2+1)/305 = 114/305$ . The notations like  $X^*(t_1) = G$  or  $X^*(t_1) = S$  are hereafter used to refer to the events that the *simulated* prognosis for the first time point  $t_1$  of some arbitrary day is either good or bad.

Table 4 summarizes the information of the uneven and even numbered SSTP. It gives the number of “days” (Col. 2 and 5) having the same prognosis “combination” (Col. 1), as well the number of individual “G” (Cols. 3 and 6) and “S” prognoses (Cols. 4 and 7) in these combinations. Table 4 was used to calculate the probabilities given in our next Table 5. Aperiodic *simulated* data similar to the *real* data in SSTP=1, 3, ..., 23 was generated with the following procedure:

1. The simulated SSTP=1, 3, ... or 23 was chosen.
2. The  $N_0$  and Div values were fixed to the values of this SSTP which are given in Table 2.
3. The  $t_1, t_2$  and  $t_3$  values were calculated for every day of the year with these fixed  $N_0$  and Div values (Eqs. 1 – 5).
4. The time points of 55 randomly selected days were removed (see the “—” days in Table 4).
5. The random prognoses for each day were assigned using the probabilities given in Table 5.

Stage A: The random prognosis  $X^*(t_1)$  was assigned with the given probabilities P(event).

Stage B: The result for  $X^*(t_1)$  then determined the probabilities P(event) used in assigning the random prognosis  $X^*(t_2)$ .

Stage C: The results for  $X^*(t_1)$  and  $X^*(t_2)$  then determined the probabilities P(event) used in assigning the random prognosis  $X^*(t_3)$ .

6. The time points  $t_i$  having a prognosis different from the fixed prognosis of SSTP were removed, i.e.  $t_i$  having  $X^*(t_i) = S$

for  $SSTP=1, 3, \dots, 11$  and  $t_i$  having  $X^*(t_i) = G$  for  $SSTP=13, 15, \dots, 23$ .

This procedure was used to simulate 10 000 samples of aperiodic random series of time points similar to every  $SSTP=1, 3, \dots, 23$ .

The standard Rayleigh test periodogram  $z(f)$  for the *real* data of  $SSTP=1$  is shown in Fig. 2a (continuous line). The two highest peaks are at  $f_1 = 0.0340 \text{ d}^{-1}$  and  $f_2 = 0.351 \text{ d}^{-1}$ , i.e. at  $P_1 = 29.^{\text{d}}4$  and  $P_2 = 2.^{\text{d}}850$ . The standard critical level estimates for these two periodicities were  $Q = 0.0000034$  and  $0.0012$  (Eq. 8). Hence the null hypothesis  $H_0$  should be rejected with  $P_1$ , but it should not be rejected with  $P_2$  (Eq. 9).

The *noise periodogram*  $z^*(f)$  for all 10 000 simulated aperiodic data samples similar to  $SSTP=1$  is shown in Fig. 2b (continuous line). This noise periodogram is the *median* of periodograms for all 10 000 simulated data samples at any particular frequency. The reason for using the median, instead of the *mean*, was that the probability density function of the Rayleigh test statistic,  $f(z) = e^{-z}$ , is not Gaussian. This density function predicts that for a sample containing  $n$  time points, half of the  $z$  values are distributed between 0 and 0.693, while the distribution of the other half is between 0.693 and  $n$ . Hence the median, not the mean, was used in the calculation of the noise periodogram  $z^*(f)$ . At the higher frequency end, this  $z^*(f)$  periodogram approached the standard critical level of  $Q = 0.5 = P(z(f) > z_0)$ , where  $z_0 = 0.693$  (Fig. 2b: dotted line). However, the deviation of the noise periodogram  $z^*(f)$  from this 0.693 level increased towards the lower frequency end, i.e. the standard critical level estimates of Eq. 8 were not reliable.

Because the ratio  $\Delta T/P_{\max} \approx 360/90 = 4$  was quite small, the noise periodogram  $z^*(f)$  began to fluctuate at the lowest frequencies. It displayed peaks at the frequencies corresponding to the long periods

$$P(\Delta T, k) = \Delta T / (k + 1/2), \quad (10)$$

where  $k \geq 4$  is an integer (Fig. 2b). All simulated data samples contained several hundred time points, more or less evenly spaced over 360 days. With these particular longer periods  $P(\Delta T, k)$ , most of the data, about  $(2nk)/(2k + 1)$  time points, were evenly distributed between the phases 0 and 1, i.e. the sum of their phase angle vectors  $[\cos \theta_i, \sin \theta_i]$  was close to zero. But the rest of the data, about  $n/(2k + 1)$  time points, were within a phase interval having a width of 0.5. All these remaining data had phase angle vectors  $[\cos \theta_i, \sin \theta_i]$  pointing to the same side of a unit circle, which yielded a large value of  $z^*(f)$  for the frequencies  $f = 1/P(\Delta T, k)$ . These  $P(\Delta T, k)$  periodicities were not “real” periodicities. This phenomenon gave us another good reason for rejecting the use of the standard critical level estimates  $Q$  of the Rayleigh test.

In the power spectrum analysis, the observed power at any tested frequency is the “signal–power to noise–power ratio” (Scargle 1982). The simulated noise periodogram  $z^*(f)$  of the Rayleigh test can be computed for any arbitrary time point distribution at any tested frequency. We divided the standard Rayleigh test  $z(f)$  periodogram for the real data with the noise periodogram  $z^*(f)$  for similar simulated aperiodic data. This gave us the normalized periodogram

$$z_N(f) = z(f) / z^*(f) \quad (11)$$

at every tested frequency. The normalized periodogram  $z_N(f)$  of  $SSTP=1$  is shown in Fig. 2c. This normalization eliminated several unreal peaks, especially at the lower frequency range of  $z(f)$ . The two highest peaks of  $z_N(f)$  were at  $f_1 = 0.0337 \text{ d}^{-1}$

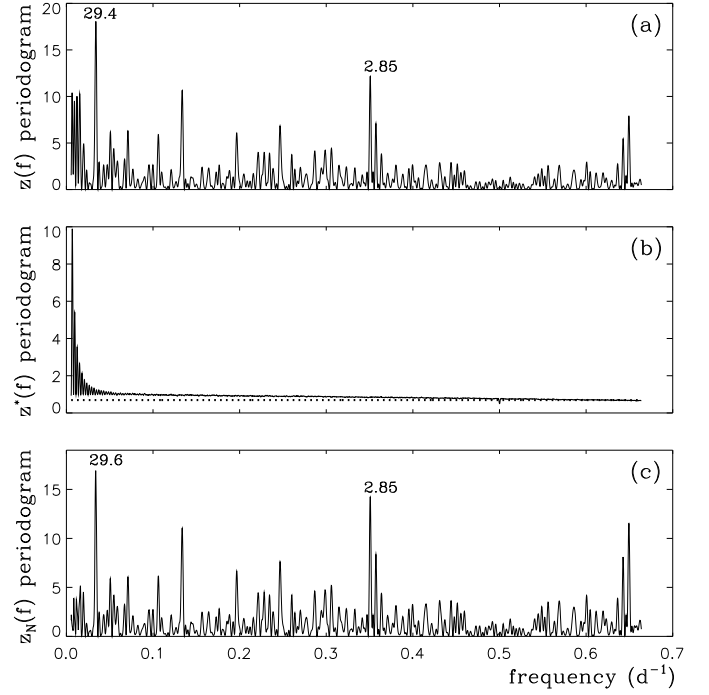


**Fig. 2.** Three periodograms of  $SSTP=1$ . **(a)** The  $f(z)$  periodogram for the *real* data of  $SSTP=1$ . The two best periods are  $P_1 = 29.4$  days and  $P_2 = 2.85$  days. **(b)** The noise periodogram  $z^*(f)$  (continuous line) determined from the aperiodic 10 000 samples of *simulated* data similar to the real data of  $SSTP=1$  and the level  $z_0 = 0.693$  corresponding to the standard Rayleigh test critical level  $Q = 0.5 = P(z(f) > z_0)$  (dotted line). **(c)** The normalized periodogram  $z_N(f)$  for the *real* data of  $SSTP=1$ : The two best periods are  $P_1 = 29.6$  days and  $P_2 = 2.85$  days.

and  $f_2 = 0.351 \text{ d}^{-1}$ , i.e. the two best periods were  $P_1 = 29.^{\text{d}}6$  and  $P_2 = 2.^{\text{d}}850$ . We compared these two best periods to the two best periods determined from  $f(z)$  in Fig. 2a. This comparison revealed that normalization had shifted the best period from  $29.^{\text{d}}4$  to  $29.^{\text{d}}6$ , but the second best period of  $2.^{\text{d}}850$  was not shifted. Our Fig. 3 displays how this shift of the best period occurred. The highest peak of  $z(f)$  was at  $f_1^{-1} = P_1 = 29.^{\text{d}}4$  (i.e. the dashed periodogram: open circle). After normalization with  $z^*(f)$  (i.e. the dotted periodogram), the highest peak of  $z_N(f)$  was at  $f_1^{-1} = P_1 = 29.^{\text{d}}6$  (i.e. the continuous periodogram: closed circle).

The best periods for  $SSTP=1$  were determined from the highest peaks of the normalized periodogram  $z_N(f)$ . It was clear that the standard critical level estimates  $Q$  of Eq. 8 were not reliable. Hence, the critical levels for the detected periods had to be also solved from simulations. For example, the highest peak of the normalized periodogram for  $f_1^{-1} = P_1 = 29.^{\text{d}}6$  reached  $z_1 = z_N(f_1) = 16.68$  (Fig. 3: closed circle). A total of ten million simulated aperiodic data samples similar to the real data of  $SSTP=1$  were generated using the probabilities of Table 5. The  $z_N(f)$  periodogram was calculated for each of these 10 000 000 simulated data samples within the frequency interval  $[f_1 - f_0/2, f_1 + f_0/2]$ . The number of simulated data samples, where the highest peak of the normalized periodogram satisfied  $z_N(f) > z_1 = 16.68$ , was then determined. There were only 120 such simulated data samples, i.e. the *simulated critical level* for  $P_1 = 29.^{\text{d}}6$  was  $Q^* = 120/10\,000\,000 = 0.000012$ . The same simulation procedure gave  $Q^* = 0.00014$  for the second best

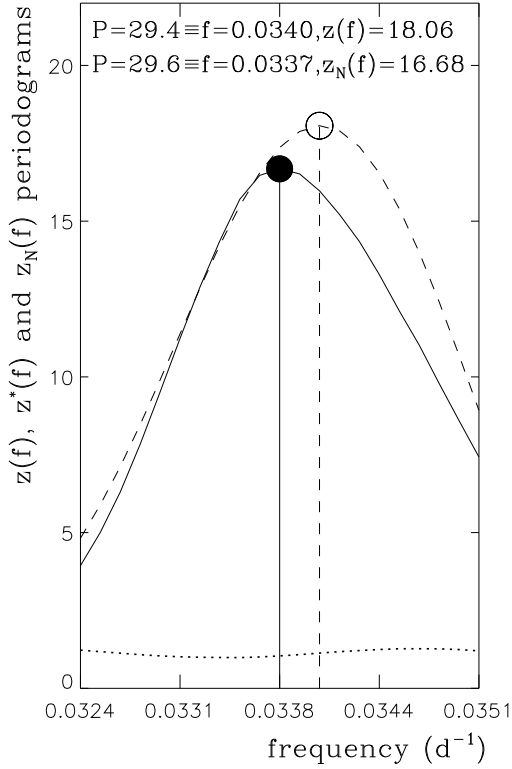


**Fig. 3.** Periodicity shift caused by normalization in SSTP=1. The  $z(f)$  (dashed line),  $z^*(f)$  (dotted line) and  $z_N(f)$  (continuous line) periodograms of Fig. 2 are shown in the frequency range  $[f_1 - f_0/2, f_1 + f_0/2]$ , where  $f_1^{-1} = 29.^d6$ ,  $f_0 = 1/\Delta T$  and  $\Delta T = 360.^d$ .

period  $P_2 = 2.^d850$ . This simulated critical level fulfilled the condition  $Q^* < \gamma = 0.001$ . We emphasize that the relation between the standard and simulated critical level estimates for the two best periods was not the same, i.e.  $Q < Q^*$  for  $P_1 = 29.^d6$  and  $Q > Q^*$  for  $P_2 = 2.^d850$ . Because the standard critical level estimates of the Rayleigh test were not reliable, the  $H_0$  rejection criterion of Eq. 9 was revised to

$$Q^* < \gamma = 0.001. \quad (12)$$

In addition to the above periodicities  $P_1 = 29.^d6$  and  $P_2 = 2.^d850$ , two other periodicities,  $P_3 = 1.^d5401$  ( $Q^* = 0.00091$ ) and  $P_4 = 7.^d48$  ( $Q^* = 0.00091$ ), satisfied this  $H_0$  rejection criterion of Eq. 12 in SSTP=1. The origin of these two periodicities will be discussed later.

All SSTP=3, 5, 7, ..., 23 were analysed using exactly the same simulation procedures as described for SSTP=1. The periods detected in the G prognoses of SSTP=1, 3, ...and 11 are given in Table 7. It contains all those periodicities that satisfied the  $H_0$  rejection criterion of Eq. 12. Cols. 1–4 of Table 7 give  $N_0$ , Div and Remove values of each SSTP. The next columns give the detected periods ( $P \pm \sigma_P$ ) in the order of increasing simulated critical level ( $Q^*$ ), i.e. the best period is given first. The periods detected in the S prognoses of SSTP=13, 15, ...and 23 are given in Table 8. The contents of Cols. 1–4 are the same as in Table 7, but only the two best periods are given for the S prognoses, because none these periodicities satisfied the  $H_0$  rejection criterion of Eq. 12. The error estimates  $\sigma_P$  for all these periods in Tables 7 and 8 were determined from the normalized periodogram  $z_N(f)$  with the bootstrap method (Jetsu & Pelt 1996). The error estimate for each periodicity is the standard deviation of all period estimates given by the bootstrap.

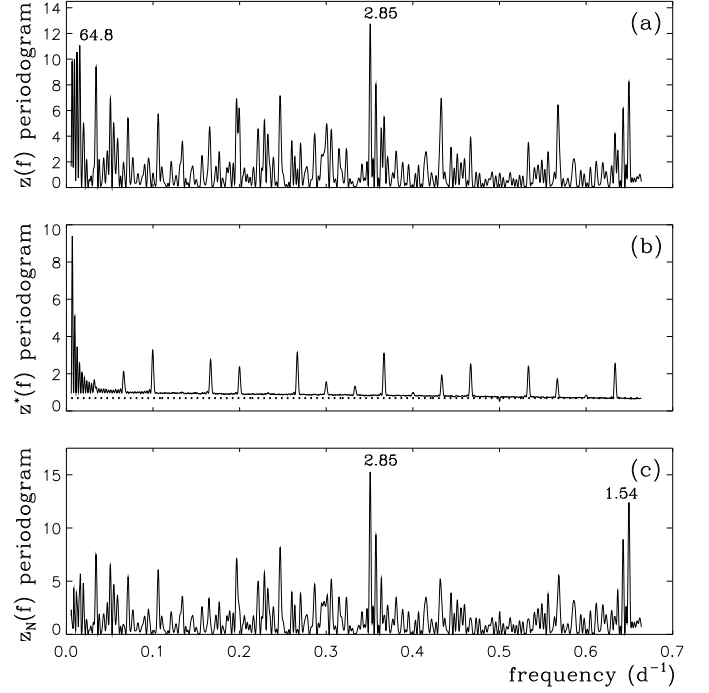


**Fig. 4.** Three periodograms of SSTP=2. The notations are the same as in Fig. 2.

### 3.3. Simulation of aperiodic data similar to SSTP=2, 4, ..., 24

The generation of aperiodic data similar to the even numbered SSTP=2, 4, ..., 24 of real data could not rely on the simulation probabilities given in Table 5, because the number of  $t_i$  decreased after removing the twelve “GGG” prognoses at  $D = 1$  and the ten “SSS” prognoses at  $D = 20$ . The last three right hand columns of Table 4 (marked “→ Table 6”) were used to calculate the simulation probabilities  $P(\text{Event})$  given in Table 6. The procedure in generating simulated aperiodic data similar to the real data in SSTP=2, 4, ..., 24 was the following:

1. The simulated SSTP=2, 4, ... or 24 was chosen.
2. The  $N_0$  and Div values were fixed to the values of this SSTP which are given in Table 2.
3. The  $t_1, t_2$  and  $t_3$  values were calculated for every day of the year with these fixed  $N_0$  and Div values (Eqs. 1 – 5).
4. The time points at  $D = 1$  and 20 of each month were removed.
5. The time points of 53 randomly selected days were removed (see the “—” days in Table 4).
6. The random prognoses  $X^*(t_1), X^*(t_2)$  and  $X^*(t_3)$  for each day were assigned as in Sect. 3.2, except that the  $P(\text{Event})$  probabilities at Stages A, B and C were now taken from Table 6.
7. The time points  $t_i$  having a prognosis different from the fixed prognosis of SSTP were removed, i.e.  $t_i$  having  $X^*(t_i) = S$  for SSTP=2,4, ..., 12 and  $t_i$  having  $X^*(t_i) = G$  for SSTP=14, 16, ..., 24.

The analysis then proceeded as for SSTP=1, 3, ..., 23.

The two highest peaks of the standard Rayleigh test periodogram  $f(z)$  for the real data of SSTP=2 were at  $P_1 = 2.^d850$  and  $P_2 = 64.^d8$  (Fig. 4a). Again, the noise periodogram  $z^*(f)$  displayed fluctuations at the lower frequency range (Fig. 4b). Comparison with  $z^*(f)$  of SSTP=1 (Fig. 2b) showed that several additional new high peaks of noise periodogram  $z^*(f)$  had

**Table 6.** Simulation of aperiodic data similar to the real data of SSTP=2, 4, ..., 24.

Stage A: Event	P(Event)
$X^*(t_1) = G$	179/283
$X^*(t_1) = S$	104/283
Stage B: Event	P(Event)
$X^*(t_1) = G \Rightarrow X^*(t_2) = G$	171/179
$X^*(t_1) = G \Rightarrow X^*(t_2) = S$	8/179
$X^*(t_1) = S \Rightarrow X^*(t_2) = S$	101/104
$X^*(t_1) = S \Rightarrow X^*(t_2) = G$	3/104
Stage C: Event	P(Event)
$X^*(t_1) = G \text{ and } X^*(t_2) = G \Rightarrow X^*(t_3) = G$	165/171
$X^*(t_1) = G \text{ and } X^*(t_2) = G \Rightarrow X^*(t_3) = S$	6/171
$X^*(t_1) = G \text{ and } X^*(t_2) = S \Rightarrow X^*(t_3) = G$	2/8
$X^*(t_1) = G \text{ and } X^*(t_2) = S \Rightarrow X^*(t_3) = S$	6/8
$X^*(t_1) = S \text{ and } X^*(t_2) = S \Rightarrow X^*(t_3) = S$	95/101
$X^*(t_1) = S \text{ and } X^*(t_2) = S \Rightarrow X^*(t_3) = G$	6/101
$X^*(t_1) = S \text{ and } X^*(t_2) = G \Rightarrow X^*(t_3) = G$	2/3
$X^*(t_1) = S \text{ and } X^*(t_2) = G \Rightarrow X^*(t_3) = S$	1/3

**Notes.** The probabilities P(event) are based on columns marked with "→ Table 6" in Table 4.

appeared over the whole tested frequency interval. These additional new  $z^*(f)$  peaks were caused by the removal of  $t_i$  at  $D = 1$ . The standard critical level estimates  $Q$  based on Eq. 8 were therefore certainly not reliable. The two highest peaks of the normalized periodogram  $z_N(f)$  (Fig. 4c) were at  $P_1 = 2.^d850$  ( $Q^* = 0.000094$ ) and  $P_2 = 1.^d540$  ( $Q^* = 0.00059$ ). Now the normalization did not shift the best period  $P_1$ , but the value of the second best period  $P_2$  was revised from  $64.^d8$  to  $1.^d540$ . The former long  $64.^d8$  period was in fact an unreal period  $P(\Delta T, k = 5)$  predicted by Eq. 10 and it was nicely eliminated when  $z(f)$  was divided with the strongly fluctuating  $z^*(f)$  at these low frequencies.

The most striking *difference* between the period analysis results for SSTP=1 and 2 was that the highly significant periodicity of  $29.^d6$  ( $Q^* = 0.000012$  in SSTP=1) had vanished. This was caused by the removal of the "GGG" prognoses of the first day of every month. The 6th best period in SSTP=2 was  $29.^d3$ , but the critical level had fallen to  $Q^* = 0.019$ . The same prognosis combination "GGG" was also given for the second day  $D = 2$  of nine months, while the other three months had "—" at  $D = 2$  (see Table 1). Had we also removed these particular "GGG" prognoses at  $D = 2$ , all traces of periodicities close to 30 days would have been totally eliminated.

The most important *similarity* in the results was that the  $2.^d850$  periodicity fulfilled the  $H_0$  rejection criterion of Eq. 12 in both SSTP=1 and 2. When the "GGG" prognoses at  $D = 1$  were removed, the significance of this periodicity even increased, because the simulated critical level decreased from  $Q^* = 0.00014$  to  $0.000094$ . The second highest peak at  $P_2 = 1.^d540$  in Fig. 4c was an unreal period, as will be explained later (see Eq. 13). Hence the period of  $P_1 = 2.^d850$  was certainly the only strong real periodicity peak detected in SSTP=2 over the whole period interval from 1.5 to 90 days. In conclusion, the removal of the "GGG" prognoses of the first day of every month eliminated the  $29.^d6$  periodicity detected in SSTP=1. After this elimination, the  $2.^d850$  periodicity was the best period in SSTP=2 and it also had become more significant.

### 3.4. Results of the period analysis of all G prognoses

Four periods detected from the G prognoses satisfied the  $H_0$  rejection criterion of Eq. 12 (Table 7:  $29.^d6$ ,  $7.^d48$ ,  $2.^d85$ , and  $1.^d54$ ).

The odd numbered SSTP= 3, 5, 7, 9 and 11 were similar to SSTP=1 in the sense that the G prognoses at  $D = 1$  were not removed. The two best periods detected in all these other five SSTP were the same as those detected in SSTP=1. These two best periods were always within the error limits of  $P_1 = 29.^d6 \pm 0.^d2$  and  $P_2 = 2.^d850 \pm 0.^d02$  (Table 7). This general result did not depend on the chosen  $N_0$  (Eq. 1), nor on the two different day divisions (Eqs. 4 – 5).

The even numbered SSTP=4, 6, 8, 10 and 12 were similar to SSTP=2, where the  $D = 1$  prognoses were removed. The best period detected in these other five SSTP were the same as in SSTP=2, i.e. within the error limits of  $P_1 = 2.^d850 \pm 0.^d002$  (Table 7). Again, this general result did not depend on  $N_0$  or on the day division.

The results between SSTP=1 and 2 were already compared above. Comparison of pairs SSTP=3 and 4, SSTP=5 and 6, SSTP=7 and 8, SSTP=9 and 10 or SSTP=11 and 12 showed that removing the G prognoses at  $D = 1$  always lead to the same result: *The best period  $29.^d6$  lost its significance, while  $2.^d850$  became the new best period and the significance of this periodicity increased.* Once again, this result of the period analysis did not depend on  $N_0$  or on the day division.

The period  $1.^d5401 \pm 0.0008$  ( $Q^* = 0.00091$ ) detected in SSTP=1 was also the third best period in SSTP=3 and 5. When the G prognoses at  $D = 1$  were removed, this  $1.^d54$  periodicity became the second best period in SSTP=2, 4 and 6. However, it was an unreal (i.e. spurious) period caused by the regular one day window in the spacing of the data. If the real period is  $P$  and the analysed time points are approximate multiples of a "window" period  $P_0$ , then unreal periods will occur at

$$P'(P_0, k_1, k_2) = [P^{-1} + (k_1/(k_2 P_0))]^{-1}, \quad (13)$$

where  $k_1 = \pm 1, \pm 2, \dots$  and  $k_2 = 1, 2, \dots$  (Tanner 1948). The combination of the period  $P = P_1 = 2.^d850$  and the window period  $P_0 = 1.^d0$  induced this unreal period  $P'(P_0 = 1.^d0, k_1 = -1, k_2 = 1) = -1.^d5405$ . The negative sign before this period value merely indicates that the phases  $\bar{\phi}_1$  calculated for the data with  $P_1 = 2.^d850$  and the respective phases  $\bar{\phi}_2$  calculated with  $P_2 = -1.^d5405$  fulfill  $\bar{\phi}_1 \approx -\bar{\phi}_2$ . This unreal  $1.^d540$  period was also detected in SSTP=2, 3, 4, 5 and 6. But this unreal period was not detected in SSTP=7, 8, 9, 10, 11 and 12, because the time points were more evenly distributed over 24 hours with the day division of Eq. 5 than with that of Eq. 4, where all time points occurred during daytime. In other words, the spacing of Fig. 1a induced a one day window period  $P_0 = 1.^d0$ , but the spacing of Fig. 1b did not.

The period  $7.^d48 \pm 0.^d02$  was detected in odd numbered SSTP=1, 5, 7, 9 and 11. But it vanished when the G prognoses at  $D = 1$  were removed, i.e. it was not detected in SSTP=2, 6, 8, 10 and 12. The obvious explanation was that this period is nearly equal to  $\delta t/4 = 7.50$ , where  $\delta t = 30^d$  is the regular distance between the G prognoses at  $D = 1$ .

The normalization of the  $z(f)$  periodogram to  $z_N(f)$  shifted the best period  $P_1$  from  $29.^d4$  to  $29.^d6$  in SSTP=1 (Figs. 2 and 3). Normalization caused a similar period shift also in SSTP=3, 5, 7, 9 and 11. It is probably not a coincidence that all these revised periods  $29.^d5$  or  $29.^d6$  were shifted closer to the length of the synodic month,  $P_{\text{syn}} = 29.^d53$ . This average value of  $P_{\text{syn}}$  would have been the most practical one for prediction purposes of the



**Table 7.** Best periods for the G prognoses.

SSTP	$N_0$	Div	Remove	$P$ (days)	$Q^*$	$P$ (days)	$Q^*$	$P$ (days)	$Q^*$	$P$ (days)	$Q^*$
1	62	Eq. 4	none	$29.6 \pm 0.2$	0.000012	$2.850 \pm 0.002$	0.00014	$1.5401 \pm 0.0008$	0.00091	$7.48 \pm 0.02$	0.00091
2	62	Eq. 4	$D = 1$	$2.850 \pm 0.002$	0.000094	$1.5400 \pm 0.0008$	0.00059	...	...	...	...
3	187	Eq. 4	none	$29.6 \pm 0.2$	0.000015	$2.850 \pm 0.002$	0.00024	$1.5401 \pm 0.0008$	0.00057	...	...
4	187	Eq. 4	$D = 1$	$2.851 \pm 0.002$	0.00016	$1.5401 \pm 0.0008$	0.00037	...	...	...	...
5	307	Eq. 4	none	$29.6 \pm 0.2$	0.000013	$2.851 \pm 0.002$	0.00015	$1.5404 \pm 0.0008$	0.00081	$7.48 \pm 0.02$	0.00089
6	307	Eq. 4	$D = 1$	$2.851 \pm 0.002$	0.000094	$1.5401 \pm 0.0008$	0.00054	...	...	...	...
7	62	Eq. 5	none	$29.5 \pm 0.2$	0.000012	$2.850 \pm 0.002$	0.00010	$7.48 \pm 0.02$	0.00079	...	...
8	62	Eq. 5	$D = 1$	$2.850 \pm 0.002$	0.000060	...	...	...	...	...	...
9	187	Eq. 5	none	$29.6 \pm 0.2$	0.000012	$2.851 \pm 0.002$	0.00016	$7.48 \pm 0.02$	0.00090	...	...
10	187	Eq. 5	$D = 1$	$2.851 \pm 0.002$	0.000096	...	...	...	...	...	...
11	307	Eq. 5	none	$29.6 \pm 0.2$	0.000013	$2.851 \pm 0.002$	0.000076	$7.48 \pm 0.02$	0.00088	...	...
12	307	Eq. 5	$D = 1$	$2.851 \pm 0.002$	0.000051	...	...	...	...	...	...

**Notes.** These periods satisfied the  $H_0$  rejection criterion of Eq. 12.

ancient Egyptians. However, the length of the synodic month is not constant, but varies between  $29.^d3$  and  $29.^d8$  during one year (Stephenson & Baolin 1991).

### 3.5. Results of the period analysis of all S prognoses

None of the best periods detected from the S prognoses satisfied the  $H_0$  rejection criterion of Eq. 12 (see Table 8), i.e. no significant periodicity was detected in these SSTP of bad prognoses.

The two best periods for the S prognoses of SSTP = 13, 15, ..., 23 were always the same within their error limits (Table 8). These two periods were  $30.^d3 \pm 0.^d2$  and  $7.^d48 \pm 0.^d02$ . But both of them vanished when the S prognoses at  $D = 20$  were removed. They were replaced by the new periods of  $1.^d557$ ,  $2.^d795$  and  $2.^d822$ .

The two periods  $30.^d3$  and  $7.^d48$  clearly originated from the S prognoses at  $D = 20$ . After removing these  $D = 20$  prognoses, the two new periods  $2.^d822$  and  $2.^d795$  were both very close to, but not exactly equal to, the period  $2.^d850$  already detected from the G prognoses. There is only a difference of one cycle between  $2.^d822$  and  $2.^d850$  during 287 days. The periods  $2.^d797$  and  $2.^d850$  give the same difference within 145 days. The third new period  $1.^d557$  in the S prognoses was present only in SSTP=14 and 18. It was clearly an unreal period connected to  $2.^d795$  through the window period  $P_0 = 1.^d0$  (i.e.  $k_1 = 1$  and  $k_2 = -1$  in Eq. 13). All these general period analysis results for the S prognoses did not depend on  $N_0$  or day division.

### 3.6. General remarks about the results of period analysis

As already mentioned before, there was an infinite number of alternatives for creating different series of time points from Table 1. Here we have given the results for 24 alternative SSTP. For example, when a prognosis was available for  $D = 2$  in Table 1, it was always "GGG". We performed additional period analysis tests, where the  $D = 2$  time points were also removed together with those already mentioned above. The results remained the same: the best periods for the G prognoses were always  $2.^d85$ . Apart from the 24 different SSTP analysed here, we simply could not invent any other realistic alternative transformations of the CC prognoses into a series of time points that would have altered this main period analysis result.

We also mentioned that the use of the approximation of Eq. 2 caused an inaccuracy of  $0.^d01$ , or less, in the sunrise and sunset. The applied  $N_0$  combined to the two alternative day divisions caused much larger shifts to the time points. Yet, the general results remained the same. This was an additional proof for that the approximation of Eq. 2 had no influence to results of our period analysis.

Unreal periods appeared in the data. These unreal periods could be divided into two categories. In the first category, the regular windows in the data spacing induced unreal periodicity even with aperiodic data, i.e. with noise. The unreal periods given by Eq. 10 were a typical example. These first category unreal periods could be eliminated with the normalization of Eq. 11. In the second category, the interplay of real periodicity and the windows of the data spacing induced unreal periods. Many of these unreal periods could be predicted by Eq. 13. A typical example was the unreal 1.54 days period caused by the interplay of the real 2.85 days period and the window period of 1.0 day. These second category unreal periods could not be eliminated with the normalization of Eq. 11. However, they vanished when the real periodicity was removed. This was the case for the unreal 7.48 days period when the real 29.6 days period was removed. All these results for the unreal periods of both categories therefore indicated that the 29.6 and 2.85 days periods were real.

Our simulations imitating the real data revealed that the standard Rayleigh test critical level estimates,  $Q(z_0)$ , based on inserting the value of  $z_0 = z(f)$  into Eq. 8, were not correct for CC data. If we had not applied the simulated statistics based on the normalized periodogram  $z_N(f)$  of Eq. 11, the previous mistake of using the standard Rayleigh test statistics (Paper I) would have been repeated. The case of SSTP=1 is briefly described below, because it illustrates how this bias would have mislead our period analysis.

The 2.85 days period in SSTP=1 did not satisfy the criterion  $Q < \gamma = 0.001$  (Eq. 9), which was required for rejecting  $H_0$ , i.e. the evidence for this period was not indisputable. However, the significance of this 2.85 days period was *underestimated* in SSTP=1, because  $Q = 0.0012$  was larger than  $Q^* = 0.00014$ . The opposite happened to the 29.4 days period in SSTP=1, the significance was *overestimated*, because  $Q = 0.0000034$  was smaller than  $Q^* = 0.000012$ . Normalization also shifted this periodicity from 29.4 to 29.6 days (Figs. 2 and 3), which is closer to the 29.53 days synodic period of the Moon. The peaks of the normalized periodogram for the  $29.^d6$  and  $2.^d85$  periods in SSTP=1

**Table 8.** Best periods for the S prognoses.

SSTP	$N_0$	Div	Remove	$P$ (days)	$Q^*$	$P$ (days)	$Q^*$
13	62	Eq. 4	none	$30.3 \pm 0.2$	0.0021	$7.48 \pm 0.02$	0.0028
14	62	Eq. 4	$D = 20$	$2.795 \pm 0.003$	0.0066	$1.5570 \pm 0.0009$	0.0095
15	187	Eq. 4	none	$30.3 \pm 0.2$	0.0018	$7.48 \pm 0.02$	0.0026
16	187	Eq. 4	$D = 20$	$2.822 \pm 0.002$	0.0079	$2.795 \pm 0.003$	0.0084
17	307	Eq. 4	none	$30.3 \pm 0.2$	0.0020	$7.49 \pm 0.02$	0.0031
18	307	Eq. 4	$D = 20$	$2.796 \pm 0.002$	0.0053	$1.5487 \pm 0.0008$	0.011
19	62	Eq. 5	none	$30.2 \pm 0.2$	0.0018	$7.48 \pm 0.02$	0.0024
20	62	Eq. 5	$D = 20$	$2.795 \pm 0.003$	0.0053	$2.822 \pm 0.002$	0.011
21	187	Eq. 5	none	$30.3 \pm 0.2$	0.0019	$7.48 \pm 0.02$	0.0028
22	187	Eq. 5	$D = 20$	$2.822 \pm 0.002$	0.0061	$2.795 \pm 0.003$	0.0068
23	307	Eq. 5	none	$30.3 \pm 0.2$	0.0021	$7.48 \pm 0.02$	0.0024
24	307	Eq. 5	$D = 20$	$2.795 \pm 0.003$	0.0041	$2.824 \pm 0.002$	0.012

**Notes.** None of these periods satisfied the  $H_0$  rejection criterion of Eq. 12.

had the heights  $z_N(f) = 16.7$  and  $14.6$ . We then tested what would happen, if these two  $z_0 = z_N(f)$  values were inserted into Eq. 8. The results for  $Q(z_0)$  were those given on Col. 5 below

$P$	$f$	$m$	$z_0 = z_N(f)$	$Q(z_0)$	$Q^*$
$29.^d6$	$0.034d^{-1}$	235	16.7	0.000013	0.000012
$2.^d85$	$0.351d^{-1}$	235	14.6	0.00011	0.00014

These  $Q(z_0)$  values agreed well with the simulated critical  $Q^*$  levels for these two periods, which are given on Col. 6 above. This result was one additional indication of that our period analysis of CC data, based on the normalized periodogram  $z_N(f)$  and the simulated critical level estimates  $Q^*$ , was correct. We emphasize that the relation of Eq. 8 should be applied only for the standard Rayleigh test statistic  $z(f)$ , but not for the normalized test statistic  $z_N(f)$ . Regardless of this, inserting the test statistic  $z_0 = z_N(f)$  into Eq. 8 would have given nearly the same critical level estimates  $Q(z_0)$  as our simulations of  $Q^*$ . This indicated that our simulated statistics were robust.

Normalization allowed us to imitate the prognosis coding rules applied by the ancient Egyptians, although we did not know those rules. This procedure gave us the simulated critical level estimates  $Q^*$  and it also eliminated unreal periods. However, the best idea of all was to test what happens, if the lunar cycle is removed. This resulted in the 2.85 days period being the only significant real period and the significance of this period was even increased. After that it was only necessary to prove that this main result did not depend on the chosen  $N_0$  of Eq. 1 or on the chosen day division.

The main conclusion of our period analysis was that if the most obvious repetitive prognoses ( $D = 1$  always GGG) and ( $D = 20$  always SSS) were removed, the S prognoses did not reveal significant real periodicity, but the G prognoses certainly did. The best period in all these cases was within  $2.^d850 \pm 0.^d002$  for the good prognoses. This result did not depend on the chosen value of  $N_0$ , nor on the chosen day division. CC does not give explicit clues as to why the ancient Egyptians assigned the prognoses with such regularity, but this value differs by  $0.^d017 \pm 0.^d002$  from the current orbital period  $2.^d867328$  of the eclipsing binary Algol ( $\beta$  Per). If this is indeed the reason for finding this periodicity in CC, the orbital period of Algol should have increased about 25 minutes during the past three millennia. The astrophysics connected to this alternative are discussed in the next section.

#### 4. Astrophysics

This section begins with a general description of the triple system Algol. The solution for the ‘‘Algol paradox’’ (Pustynnik 1998, i.e. Roche-lobe overflow) and the current evolutionary status of this EB are then described. The observed long-term APC, and the physical mechanisms that may cause these APC, are then explained (Hall 1989; Applegate 1992). An increase of  $P_{\text{orb}}$  from  $2.^d850$  to  $2.^d867$  within the past three millennia could be explained by MT (Biermann & Hall 1973). Our estimated rate of this MT also agrees with the predictions of an evolutionary model for Algol (Sarna 1993). The inclination of Algol may also have changed in the past three millennia. The uncertainty in the period (Soderhjelm 1975, 1980; Csizmadia et al. 2009; Zavala et al. 2010) of these inclination changes does not rule out the possibility that the Egyptians may even have witnessed total eclipses, where Algol almost disappeared from the sky for about half an hour. In all following calculations, the date 1224 B.C. is used for the CC, which is a reasonable estimate (see Paper III). A shift of this date by a few centuries forward or backward would not alter any of our main results in this Sect. 4, or in the next Sect. 5.

Geminiano Montanari discovered the brightness variations of Algol in the year 1669 (Merrill 1938). John Goodricke (1783) determined the 2.87 days period of these variations 114 years later. He proposed that an eclipse of another object or a darker area on the stellar surface could be the cause of the observed variability. These two close orbit stars eclipsing each other are usually referred to as Algol A and Algol B. According to Aitken (1935), the third member in the wide orbit of this system, Algol C, was already discovered by Chandler (1888). The credit of this discovery could also have been given to Curtiss (1908), as has been recently pointed out by Csizmadia et al. (2009). The presence of one, two or even three additional members in this system was proposed later (Eggen 1948; Pavel 1949). More recently, it was confirmed that there are only three members in this system and that the orbital period of the third member Algol C is  $P_2 = 1.862$  years (Frieboes-Conde et al. 1970). The spectral types are Algol A: B8 V, Algol B: K2 IV and Algol C: F1 IV (Csizmadia et al. 2009). The diameter of the dimmer Algol B is larger than that of the brighter Algol A. The observed visual brightness of Algol falls from  $2.^m1$  to  $3.^m4$  during the primary eclipse (Isles 1997). This partial eclipse of Algol A by Algol B lasts a little less than 10 hours (see Figs. 5 and

**Table 9.** Some of the recently determined physical parameters of the Algol system (Zavala et al. 2010).

A–B: Orbital elements	AB–C: Orbital elements	Masses
$a_1 = 2.3 \pm 0.1$ mas	$a_2 = 93.8 \pm 0.2$ mas	$m_A = 3.7 \pm 0.2 M_\odot$
$i_1 = 98.6$ degrees	$i_2 = 83.7 \pm 0.1$ degrees	$m_B = 0.8 \pm 0.1 M_\odot$
$\Omega_1 = 7.4 \pm 5.2$ degrees	$\Omega_2 = 132.7 \pm 0.1$ degrees	$m_C = 1.5 \pm 0.1 M_\odot$
$e_1 = 0$	$e_2 = 0.225 \pm 0.005$	
$P_1 = 2.867328$ days	$P_2 = 679.85 \pm 0.04$ days	

6). Algol is the closest EB to the Sun at the distance of 28.5 pc (Perryman & ESA 1997). The physical parameters of Algol given in our Table 9 are those recently determined from optical interferometry (Zavala et al. 2010). The notation is

$a$	=	semiaxis major of the orbit
$i$	=	orbital inclination
$\Omega$	=	position angle of the ascending node
$e$	=	eccentricity of the orbit
$P$	=	orbital period
$m$	=	mass.

The subscripts “1” and “2” for these parameters denote the “A–B” and “AB–C” systems, respectively. The units are  $[a_1] = [a_2] =$  milli arc seconds = mas,  $[i_1] = [i_2] = [\Omega_1] = [\Omega_2] =$  degrees,  $[e_1] = [e_2] =$  dimensionless,  $[P_1] = [P_2] =$  days and  $[m_A] = [m_B] = [m_C] = M_\odot =$  the mass of the Sun.

Algol seemed to defy the general rule of astrophysics that more massive stars evolve faster, because the more massive Algol A has not evolved away from the main sequence, but the less massive Algol B has already evolved to the subgiant stage. This famous “Algol paradox” was finally resolved only about half a century ago (Pustynnik 1998). Algol A was less massive than Algol B when this system was formed. For example, the zero age main sequence masses for these two stars in the “best-fitting” evolutionary model were  $m_B = 2.81 M_\odot$  and  $m_A = 2.50 M_\odot$  (Sarna 1993). In this particular model, Algol B evolved to the subgiant stage in 450 million years and filled its Roche-lobe. This happened only about 3 million years ago. Roche-lobe overflow caused substantial MT to Algol A which became more massive than Algol B within less than 700 000 years. At the current quiescent evolutionary stage, this MT has become weaker and will continue to weaken. We will later compare our results to the MT prediction of this particular evolutionary model of Sarna (1993). Circumstellar material with transient characteristics, a low density transient asymmetric accretion disk and a gas stream have been observed in Algol (Richards 1993). More recently, interferometric radio observations of a large coronal loop structure extending from pole to pole of Algol B were published (Peterson et al. 2010). This persistent co-moving magnetic field structure is aligned towards Algol A.

The  $O - C$  of Algol have revealed complex short- and long-term  $P_{\text{orb}}$  changes. Frieboes-Conde et al. (1970) noted that Algol showed three more or less regular  $O - C$  cycles.

- 1 The “great inequality” with a full amplitude of over 3 hours and a period of about 180 years. Their study ruled out the presence of an additional invisible fourth member as a cause of this periodicity.
- 2 The period of 32 years with a full amplitude of about 20 minutes which they attributed to the apsidal motion of the eclipsing A–B system.

- 3 The period of 1.9 years with a full amplitude of about 9 minutes resulting from the Light Travel Time Effect (hereafter “LTTE”) caused by the orbital motion of the AB–C system.

They concluded that the orbital period had also changed abruptly two times, i.e. by  $+3.^s5$  close to the year 1944 and  $-2.^s1$  in the year 1952. The cause of the 1.9 years cycle was soon confirmed (Hill et al. 1971). But apsidal motion did not explain the 32 year periodicity, because the orbit of the A–B system is circular (Soderhjelm 1980). The orbital periods in different EBs had been observed to decrease, increase or remain constant. Hall (1989) noticed that APC occurred *only* in those EBs where at least one member had a convective envelope. Applegate (1992) presented a theory where the magnetic activity of the late-type K2 IV star Algol B could induce APC. His relation between the orbital period and  $O - C$  changes was

$$\Delta P/P = 2\pi (A_{O-C}/P_{\text{mod}})$$

where  $A_{O-C}$  was half of the full amplitude of the  $O - C$  variations and  $P_{\text{mod}}$  was the cycle of these variations. The time units in this relation were the same for all parameters, i.e.  $[\Delta P] = [P] = [O - C] = [P_{\text{mod}}]$ . For Algol, Applegate used

$$A_{O-C} = 0.^d03, P_{\text{mod}} = 30^y \Rightarrow \Delta P/P = 1.7 \times 10^{-5}, \Delta P = 4.^s3$$

$$A_{O-C} = 0.^d15, P_{\text{mod}} = 200^y \Rightarrow \Delta P/P = 1.3 \times 10^{-5}, \Delta P = 3.^s2.$$

The observed range of orbital period changes of Algol between the years  $t_1 = 1784$  and  $t_2 = 1952$  had been between  $P_1 = 2.^d8672506$  and  $P_2 = 2.^d86734862$  (Hoffleit 1984). These values gave

$$\Delta P = P_2 - P_1 = 8.^s5$$

$$\Delta P/P = 3.4 \times 10^{-5}$$

$$\dot{P} = (P_2 - P_1)/(t_2 - t_1) = 1.6 \times 10^{-9}$$

$$\dot{P}/P = 5.6 \times 10^{-10} \text{ d}^{-1}.$$

The above  $\dot{P}$  and  $\dot{P}/P$  estimates were actually lower limits, because the full range of these period changes was observed during a time span shorter than  $t_2 - t_1$ . Thus, the order of all these estimates showed that the interplay between the  $P_{\text{mod}}$  cycles of 30 and 200 years could explain the observed  $O - C$  changes. The physical causes of APC in EBs, which typically have an amplitude of  $\Delta P/P \approx 10^{-5}$ , are still unknown, but the Applegate mechanism or LTTE are regarded as two most probable causes (Zavala et al. 2002; Liao & Qian 2010). The validity of the Applegate mechanism has also been questioned (Lanza 2005, 2006). The original sample of 101 EBs studied by Hall (1989) was recently reanalysed by Liao & Qian (2010) using supplementary more accurate new data. This study revealed that APC occur *also* in some EB not having a star with a convective envelope, i.e. a star of a spectral type later than F5. The conclusion was that magnetic activity is one, but not the only, cause of APC.

In addition to APC, an unnoticed long-term increasing trend in the  $P_{\text{orb}}$  changes of Algol may exist. The large APC in many EBs may have “masked” (Biermann & Hall 1973) the presence of a small long-term period increase or decrease that should have been observed as parabolic  $O - C$  changes. This particular problem was nicely illustrated when the  $O - C$  changes of Algol were compared to those of another EB called U Cep (Kiseleva et al. 1998). Under stationary conditions, MT from the less massive to the more massive component leads to a long-term  $P_{\text{orb}}$  increase of an EB (Biermann & Hall 1973). This should also have been the case with Algol which is currently in

a quiescent stage of MT. The estimated long-term average rate of period change is

$$\dot{P}/P = -[3 \dot{m}_B (m_A - m_B)] / (m_A m_B) \quad (14)$$

where  $\dot{P}$  is the rate of change of the orbital period,  $m_A$  and  $m_B$  are the masses of the gainer and the loser, and  $\dot{m}_B$  is the rate of MT per orbital cycle (Biermann & Hall 1973; Chaubey 1993; Qian 2000). The units in this relation are  $[\dot{P}] = \text{dimensionless}$ ,  $[P] = \text{days}$ ,  $[m_A] = [m_B] = M_\odot$  and  $[\dot{m}] = M_\odot$  per orbital cycle. Let us assume that the orbital period of Algol was  $P_1 = 2.^d850$  in  $t_1 = 1224$  B.C. and it has since then increased to  $P_2 = 2.^d867328$  in  $t_2 = 2012$  A.D. For a constant rate of period change  $\dot{P}$ , this would have been 43 seconds in a century or about half a second a year, which gives

$$\begin{aligned} \dot{P} &= 1.5 \times 10^{-8} \\ \dot{P}/P &= 5.1 \times 10^{-9} \text{ d}^{-1} \\ \dot{m}_B &= -1.7 \times 10^{-9} M_\odot \text{ per orbital cycle} = -2.2 \times 10^{-7} M_\odot \text{ per year.} \end{aligned}$$

Hence, the total mass transferred during the past three thousand years would have been about 74% of the mass of Jupiter. Our MT estimate for Algol agrees well with the “best-fitting” theoretical evolutionary model, which predicted  $\dot{m}_B = -2.9 \times 10^{-7} M_\odot$  per year (Sarna 1993). It was already concluded earlier that MT in Algol “is unlikely to be less than  $10^{-7} M_\odot \text{ y}^{-1}$ ” (Soderhjelm 1980). Our result also agrees with the  $\dot{m}$  estimates obtained for other EBs (Chaubey 1993; Šimon 1999; Qian 2000). Constant MT rate is only an approximation (Biermann & Hall 1973), because there are both quiescent periods and short bursts of MT. Such a burst may have occurred in Algol in the year 1975 (Mallama 1978). The relation of Eq. 14 may also underestimate the actual MT in Algol and other EBs (Zavala et al. 2002). However, much more conservative MT estimates having a range between  $10^{-13} M_\odot \text{ y}^{-1}$  and  $10^{-8} M_\odot \text{ y}^{-1}$  have also been published for Algol itself (Harnden et al. 1977; Cugier & Chen 1977; Hadrava 1984; Richards 1992).

We have discussed why  $P_{\text{orb}}$  of Algol might have changed during the past three millennia, but we have assumed that eclipses occurred in 1224 B.C. Another physical parameter connected to the eclipses may also have changed during this time interval, namely the inclination  $i_1$  of Algol. Partial eclipses occur when  $63^\circ < i_1 < 117^\circ$ . The diameter of the brighter Algol A is smaller than that of Algol B. Hence, the flux from the brighter Algol A is fully obstructed during a total eclipse by the dimmer Algol B. Total eclipses occur when  $87.^m3 < i_1 < 92.^m7$ . They cause light curve minima having a depth of  $2.^m8$ . The effect of a total eclipse is dramatic, if compared to the currently occurring partial eclipses with a depth of  $1.^m3$  (see Figs. 5 and 6). In a total eclipse, the brightness falls to  $5.^m0$  and a naked eye observer gets the impression that for half an hour Algol almost disappears from the sky (Csizmadia et al. 2009).

Luyten (1938) argued that perturbations caused by Algol C were slowly changing  $i_1$ . This should have been observed as a change in the depth of the eclipse. He therefore noted that the eclipse of Algol need not always occur, because this depends on the instantaneous value of  $i_1$ . His estimates were  $i_1 = 78^\circ$  for Montanari in the year 1669,  $i_1 = 83^\circ$  for Goodricke in the year 1783 and he also computed that in the year 1938 the  $i_1$  decrease was one arc second per year.

Soderhjelm (1975) derived the following period

$$P_{i_1} = \frac{\frac{4}{3} \left(1 + \frac{m_A + m_B}{m_C}\right) \frac{P_2^2}{P_1^2} (1 - e_2^2)^{3/2}}{\left(\frac{G_1^2}{G_2^2} + \frac{2G_1}{G_2} \cos \Phi + 1\right)^{1/2} \cos \Phi}, \quad (15)$$

where

$$\begin{aligned} G_1 &= \frac{m_A m_B}{m_A + m_B} [Ga_1(1 - e_1)^2(m_A + m_B)]^{1/2}, \\ G_2 &= \frac{(m_A + m_B) m_C}{m_A + m_B + m_C} [Ga_2(1 - e_2)^2(m_A + m_B + m_C)]^{1/2}, \end{aligned}$$

$G$  is the gravitational constant and  $\Phi$  is the angle between the orbital planes of A–B and AB–C systems, which is

$$\Phi = \cos i_1 \cos i_2 + \sin i_1 \sin i_2 \cos(\Omega_1 - \Omega_2). \quad (16)$$

The units are  $[P_{i_1}] = \text{s}$ ,  $[m_A] = [m_B] = [m_C] = \text{kg}$ ,  $[a_1] = [a_2] = \text{m}$ ,  $[e_1] = [e_2] = \text{dimensionless}$  and  $[G] = 6.67 \times 10^{-11} \text{ m}^3 \text{ kg}^{-1} \text{ s}^{-2}$ . Soderhjelm (1975) used  $m_A$ ,  $m_B$ ,  $m_C$ ,  $a_1$ ,  $a_2$ ,  $e_1$  and  $e_2$  values that were very close to those given in our Table 9. He used  $\Phi = 11^\circ$  which gave  $P_{i_1} = 1\,900$  years. These relatively fast  $i_1$  changes should have been eventually observed as changes in the depth of eclipses. Because this effect could not be confirmed, Soderhjelm (1975, 1980) concluded that the two orbital planes were most likely coplanar. Polarimetric measurements (Rudy 1979) and VLBI interferometry (Lestrade et al. 1993) indicated the opposite, i.e. perpendicularity. This latter alternative has been confirmed by the two most recent interferometric studies. The first one gave  $\Theta = 95^\circ \pm 3^\circ$  (Csizmadia et al. 2009) and the second one gave  $\Theta = 96^\circ \pm 5^\circ$  (Zavala et al. 2010). Using these two  $\Theta$  values and the  $m_A$ ,  $m_B$ ,  $m_C$ ,  $a_1$ ,  $a_2$ ,  $e_1$  and  $e_2$  values in Table 9 gave  $P_{i_1} = 25\,000$  and  $31\,000$  years (Eq. 15). Hence, the inclination  $i_1$  of the A–B system may have been quite stable during the past three millennia. The relation of Eq. 15 also shows that the period  $P_{i_1}$  approaches infinity when  $\Phi$  (Eq. 16) approaches 90 degrees, i.e. the changes of  $i_1$  become slower. Numerical integrations of the orbits of Algol A, B and C have also been performed (Csizmadia et al. 2009). The estimated amplitude of the  $i_1$  variations in these integrations was 170 degrees with a period of 20 000 years. These integrations indicated that no eclipses of Algol occurred in 1224 B.C. (Csizmadia et al. 2009, their Fig. 9). However, there were at least two reasons, why partial or even total eclipses of Algol may very well have occurred in those days.

The change of  $\Theta$  from  $85^\circ$  to  $86^\circ$  increases the period of inclination changes from 25 000 to 31 000 years (Eq. 15). The effect of this one degree increment shows how much uncertainty in this period is caused by  $\pm 3^\circ$  and  $\pm 5^\circ$  errors of  $\Theta$ . A minor increment of this angle  $\Theta$  in the input for the numerical integrations would have decreased the slope of  $i_1$  changes shown in Fig. 9 by Csizmadia et al. (2009) and this slope could also have predicted partial, or even total, eclipses in 1224 B.C.

The solutions for the orbital elements of Algol were different in the two most recent interferometric studies (Csizmadia et al. 2009; Zavala et al. 2010). For example, the latter study showed that the orientation for the close binary orbit is retrograde, instead of prograde. The numerical integrations of the long-term inclination changes of Algol were described as “rough approximations only”, because “the position of the node” could not be determined very accurately (Csizmadia et al. 2009).

From the astrophysical point of view,  $P_{\text{orb}}$  of Algol could have increased from 2.850 to 2.867 days in the past three millennia. The estimated MT that could have caused this effect agreed with the MT prediction of the best evolutionary model for Algol (Sarna 1993), as well as with MT observed in other EBs

(Chaubey 1993; Šimon 1999; Qian 2000). The inclination  $i_1$  of Algol may have changed (Soderhjelm 1975), but the uncertainty of the available estimates for the angle  $\Theta$  between the orbital planes of the A–B and AB–C systems (Csizmadia et al. 2009; Zavala et al. 2010) did not allow us to eliminate any of the three different alternatives: total, partial or no eclipses at all in 1224 B.C.

Finally, we note that the rotation period of the Earth has increased since the writing of CC. The average increase has been about 1.7 ms in a century (Stephenson 1997). This phenomenon had no effect to the values of our computed SSTP within one year, because the length of a day in 1224 B.C. was only about 0.06 seconds, or  $7 \times 10^{-7}$  days, shorter than today. However, the tracing of the  $O - C$  changes of Algol back to 1224 B.C. would require that the consequences of this phenomenon are considered, because the accumulated  $O - C$  effect is a few hours. Accumulated long-term  $O - C$  changes caused by the motion of the centre of mass of the Algol AB–C system with respect to the Sun could also be estimated. Yet, the past unknown APC of Algol will always prevent an accurate tracing of the  $O - C$  changes back to 1224 B.C.

## 5. Astronomy

A naked eye observer can discover periodicity in the Sun, the Moon, the planets and the stars. The one year period of the Sun and the synodic periods of the planets (Mercury, Venus, Mars, Jupiter and Saturn) exceed our period analysis upper limit of 90 days. The 29.5 days synodic period of the Moon was detected in CC. Therefore, the only remaining class of celestial objects, where the ancient Egyptians could have detected periodicity between 1.5 and 90 days, were the stars.

If the ancient Egyptians discovered the eclipses of Algol and then determined the period of these eclipses, this was achieved with naked eye observations. In this section, we show that Algol in particular would have been the variable star that caught their attention. We present a logical sequence of ten clearly stated astronomical criteria. These criteria lead to the inevitable conclusion that Algol was a star, where the ancient Egyptians would have been able to record periodic variability with naked eyes, i.e. to achieve a reasonable level of predictability.

We searched for the best variable star candidate from the General Catalogue of Variable Stars (hereafter GCVS).<sup>4</sup> It contains all the over 40 000 stars currently confirmed to be variable. Before going into details, we shortly describe our elimination process in this paragraph. There were only 109 variables that reach the maximum visual brightness of 4.<sup>m</sup>0 and vary with an amplitude greater than 0.<sup>m</sup>4. This variability could be discovered with naked eyes in ideal observing conditions. Of all these variable star candidates, only 13 undergo periodic brightness variations with a period below 90 days. At least four multiples of such periodicities could be contained in CC. Proper motion and precession corrections showed that three of these variable star candidates could not have been observed in Egypt around 1224 B.C. Three other candidates were eliminated, because their brightness variations can not be predicted even today. The variability of two of the seven remaining variables could not be discovered from naked eye observations during one night. Then the possibility was considered that the constellation pattern changes from one night to another would have revealed the variability of

these seven objects. We described this tedious elimination process in great detail, because we wanted to *prove* that Algol is the best variable star candidate, where the constellation pattern changes could certainly be observed during one night with naked eyes. For those interested, our suggestion is that they would read through the original determination of the period of Algol made by (Goodricke 1783), because it was based on the same technique as described here by us. The determination of the period of variability would have been a difficult task with naked eye observations, even if variability would have been detected. We could show that the ancient Egyptians might have succeeded in this only with the two EBs,  $\lambda$  Tau and Algol. There were numerous reasons why it is much easier to determine the epochs of the eclipses of Algol than those of  $\lambda$  Tau. This has also been the case in the modern history of variable stars. If the eclipses of Algol were total or nearly total three thousand years ago, the period could have easily been determined with a very high accuracy.

We used the maximum visual brightness ( $m_{\max}$ ), the amplitude of the light curve ( $\Delta m = m_{\min} - m_{\max}$ ) and the period of variability ( $P$ ) to select those GCVS objects, where predictable variability could be detected with naked eye observations. Except at the epoch of maximum brightness, the variables are always dimmer than  $m_{\max}$ . If this value is larger than 4, it becomes rather difficult to observe the variable in typical observing conditions or when it is closer to the horizon.<sup>5</sup>

Our first criterion was:

$C_1$ : The maximum brightness of the variable is  $m_{\max} \leq 4.0$ .

It selected those 237 GCVS objects that are clearly visible to the unaided eye at least during the epoch of their maximum brightness.

The human eye can detect brightness differences of a few tenths of a magnitude by comparing the brightness of the variable to that of a nearby comparison star (Goodricke 1783; Argelander 1855). Suitable comparison star magnitudes are therefore between  $m_{\min}$  and  $m_{\max}$  of the variable star. To eliminate differences in atmospheric extinction, these constant brightness comparison stars should not be located more than about 15 degrees away from the variable star. A much larger angular separation prevents reliable brightness comparison. The observer tries to determine whether the variable is brighter or dimmer than each particular comparison star. This method was also applied by Goodricke (1783) when he determined the period of Algol. An experienced observer can in our times determine the brightness of a variable with an accuracy of 0.<sup>m</sup>1 by using the known brightnesses of the comparison stars (Isles 1997; Turner 1999). It is unlikely that the Egyptians could have reached this accuracy, especially in the determination of their comparison stars magnitudes. Our second criterion was:

$C_2$ : The amplitude of the variable is  $\Delta m > 0.4$ .

It selected those variables, where periodic brightness variations may be detected with the comparison star technique (Goodricke 1783; Argelander 1855; Isles 1997; Turner 1999) described above. The criteria  $C_1$  and  $C_2$  selected 109 GCVS objects.

The observed changes of a variable star can be used for prediction purposes only if these changes are periodic. Our third

<sup>4</sup> The GCVS at <http://www.sai.msu.su/groups/cluster/gcvs/gcvs/> was accessed in November 2008.

<sup>5</sup> In the astronomical magnitude system, the brightness decreases when the magnitude  $m$  increases. The scale of visual magnitude system is defined so that  $m = 6$  is the upper limit for the human eye detection in ideal observing conditions.

**Table 10.** Thirteen variable star candidates not rejected with the  $C_1, \dots, C_4$  criteria.

Name	Number	$P$ (days)	Type	$m_{\max}$ (mag)	$\Delta m$ (mag)	$\delta_{-1224}$ (deg)	$a_0$ (h)	$a_{30}$ (h)	$a_{60}$ (h)	$a_{\max}$ (deg)
$\zeta$ Pho	HR 338	1.6697671	EB	3.91	0.51	-73	0	0	0	...
$\rho$ Per	HR 921	50	S	3.30	0.70	+23	14	10	6	86
Algol	HR 936	2.8673043	EB	2.12	1.27	+25	14	10	6	88
$\lambda$ Tau	HR 1239	3.9529478	EB	3.37	0.54	-1	12	8	4	62
$\mu$ Lep	HR 1702	2	Cp	2.97	0.44	-25	10	5	0	38
$\beta$ Dor	HR 1922	9.8426	C	3.46	0.62	-65	0	0	0	...
$\zeta$ Gem	HR 2650	10.15073	C	3.62	0.56	+18	13	9	6	82
l Car	HR 3884	35.53584	C	3.28	0.90	-50	7	0	0	14
$\beta$ Lyr	HR 7106	12.913834	EB	3.25	1.11	+34	15	10	6	82
R Lyr	HR 7157	46	S	3.88	1.12	+43	16	11	7	73
$\kappa$ Pav	HR 7107	9.09423	C	3.91	0.87	-60	4	0	0	3
$\eta$ Aql	HR 7570	7.176641	C	3.48	0.91	-1	12	8	4	62
$\delta$ Cep	HR 8571	5.366341	C	3.48	0.89	+44	16	11	7	73

**Notes.** Cols 1 and 2: The names and BSC numbers, Col. 3: Period of variability ( $P$ ), Col. 4: Variable type (Type: EB = eclipsing binary, S = semiregular pulsating star, Cp = chemically peculiar or C = cepheid), Cols. 5 and 6: The maximum visual brightness ( $m_{\max}$ ) and the amplitude of variability ( $\Delta m$ ), Col. 7: Declinations for the epoch 1224 B.C ( $\delta_{-1224}$ ), Cols. 8–11: The time the object was above altitudes  $0^\circ$ ,  $30^\circ$  and  $60^\circ$  ( $a_0$ ,  $a_{30}$  and  $a_{60}$ ) and the altitude of upper culmination ( $a_{\max}$ ), if the object rose above horizon.

selection criterion was:

$C_3$ : The brightness of the variable changes with a known period  $P$ .

The criteria  $C_1, \dots, C_3$  gave 30 GCVS objects.

Periods comparable to, or longer than, the time span of the data simply can not be contained in CC. The length of CC was about 360 days. Our fourth selection criterion was:

$C_4$ : The period of the variable is shorter than 90 days.

It ensured that the variable underwent at least four cycles during 360 days. The 13 GCVS candidates that fulfilled the criteria  $C_1, \dots, C_4$  are given in Table 10.

The intermediate geographical latitude of Middle Egypt is  $\phi = 26^\circ 41' \approx 27^\circ$ . Stars with a declination of  $\delta < \phi - 90^\circ = -63^\circ$  are never visible at this latitude. On the other hand, circumpolar stars with  $\delta > 90^\circ - \phi = 63^\circ$  will never set. The altitude of a star is highest when it passes the south meridian. The altitude at this “upper culmination” is  $a_{\max} = 90^\circ - \phi + \delta$ , if the star culminates south of zenith. The respective value is  $a_{\max} = 90^\circ + \phi - \delta$  for stars culminating north of zenith. The proper motion and precession corrections were calculated for the epoch 1224 B.C. There are no circumpolar stars in Table 10, but the variables  $\zeta$  Pho ( $\delta_{-1224} = -73^\circ$ ) and  $\beta$  Dor ( $\delta_{-1224} = -65^\circ$ ) could not be observed at the selected epoch. Atmospheric extinction prevents accurate photometry close to the horizon. It was therefore also impossible to notice the variability of  $\kappa$  Pav ( $\delta_{-1224} = -60^\circ$ ), because this star never rose more than 3 degrees above the horizon. Furthermore, the yearly nighttime visibility of  $\kappa$  Pav was 4 hours (4 months), less than 4 hours (5 months) and not at all (3 months). Our fifth selection criterion was:

$C_5$ : The variable was not below, or too close to, the horizon of Middle Egypt in 1224 B.C.

It rejected  $\zeta$  Pho,  $\beta$  Dor and  $\kappa$  Pav, i.e. the criteria  $C_1, \dots, C_5$  reduced the sample size into 10 GCVS objects.

The periods of three variables in Table 10 are not very accurate. This is due to their irregular variability. Reliable predic-

tions are possible only with a regular periodicity. Even modern astronomers fail to detect regular periodicity in some of the remaining variables. These three variables in Table 10, where no regular periodicity has been detected, are now shortly discussed.

$\rho$  Per is a semi-regular pulsating star. This M4 II star “shows little or no periodicity” (Percy et al. 1993). There are indications of periodicity “in the 70- to 100-day range”, but “no evidence for a 50-day period” given in GCVS. Other periodicities have been reported later (Percy et al. 1996).

$\mu$  Lep is a chemically peculiar B9p star. There were indications of a periodicity of  $P \approx 2^d$  (Renson et al. 1976), which is given in GCVS, as well as  $\Delta m = 0.44$ . But the light curve and this periodicity are not regular. Photometry has indicated constant brightness (Heck et al. 1987), but also variability of  $\Delta m = 0.39$  (Perry et al. 1987). No other reports of periodicity after the original detection (Renson et al. 1976) were found. For example,  $\mu$  Lep “could not be classified as variable or constant with any degree of certainty” in the Hipparcos Catalogue (Perryman & ESA 1997).

The period of the semi-regular pulsating star R Lyr is 46 days in GCVS. Another reported period is 53.41 days (Percy et al. 1996). The photometry has also revealed “complex variability” with periods of 46 and 64 days (Percy et al. 2001). The changes of the visual light curve have been highly irregular.

Our sixth selection criterion was:

$C_6$ : The brightness of the variable can be predicted.

This criterion eliminated these three variables  $\rho$  Per,  $\mu$  Lep, and R Lyr, because their brightness changes are simply unpredictable. Thus the criteria  $C_1, \dots, C_6$  gave 7 GCVS objects.

The light curves of these seven remaining variables are shown in Fig. 5. This group contains four cepheids ( $\zeta$  Gem, l Car,  $\eta$  Aql and  $\delta$  Cep) and three EBs (Algol,  $\lambda$  Tau and  $\beta$  Lyr). The cepheid light curves display smooth changes as a function of phase (Figs. 5c, 5d, 5f and 5g). Steeper changes are seen in the light curves of EBs (Figs. 5a, 5b, and 5e). The steepest changes, as a function of phase, occur in the light curves of Algol and  $\lambda$  Tau. All three EB light curves show a deeper primary eclipse. A less deep secondary eclipse can be clearly seen only in the light

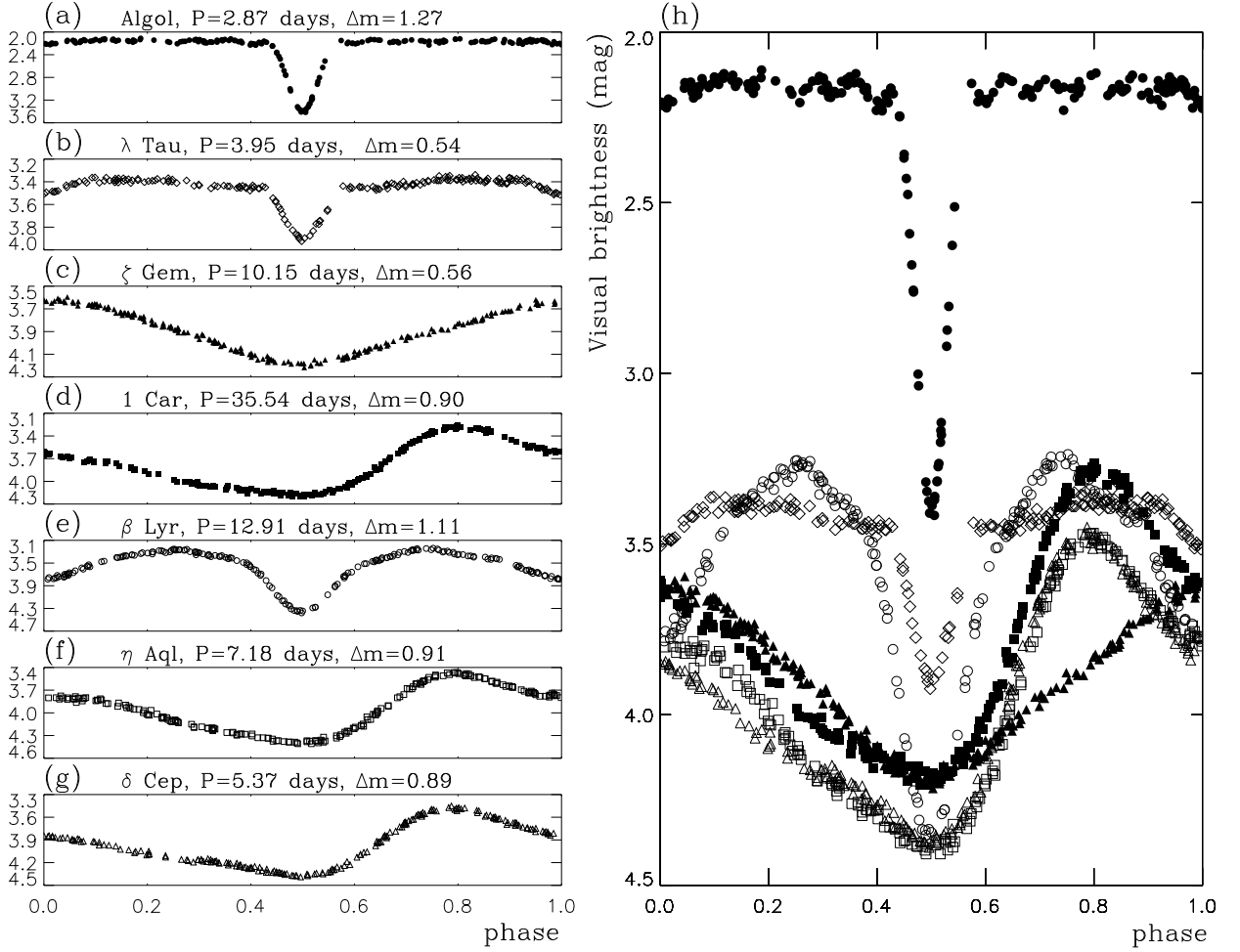


**Fig. 5.** Light curves of the seven best variables star candidates as function of phase. The phases were calculated with the given period  $P$  (days): (a) Algol (closed circles), (b)  $\lambda$  Tau (open diamonds), (c)  $\zeta$  Gem (closed triangles), (d) l Car (closed squares), (e)  $\beta$  Lyr (open circles), (f)  $\eta$  Aql (open squares) and (g)  $\delta$  Cep (open triangles). (h) All these light curves in the same magnitude scale: Algol is more than one magnitude brighter than the other six variables, and it also undergoes the largest changes of brightness.

curves of  $\lambda$  Tau and  $\beta$  Lyr. Algol is the brightest of these seven variables and also has the largest amplitude  $\Delta m$  (Fig. 5h).

The largest brightness changes that these variables can undergo during a single night are shown in Fig. 6. The nightly variability of  $\zeta$  Gem (closed triangles) and l Car (closed squares) is never more than about  $0.^m1$  (Figs. 6c and 6d). Such variability simply can not be detected with naked eyes over the time span of one night. The respective ranges of  $\beta$  Lyr (open circles),  $\eta$  Aql (open squares) and  $\delta$  Cep (open triangles) are between  $0.^m2$  and  $0.^m4$ . In ideal observing conditions, a variable star observer might be able to detect the gradual dimming or brightening of these three variables in less than 12 hours, but the variations in atmospheric extinction would make this task difficult. This would be possible, *if* the observer selected suitable comparison stars very close to these variables. However, the vertical lines in the smaller panels of Fig. 6 show that the brightness changes of  $\beta$  Lyr,  $\eta$  Aql and  $\delta$  Cep could not be perceived during most nights (Figs. 6e, 6f and 6g). The two variables with the largest nightly changes of  $0.^m54$  and  $1.^m27$  are the two EBs,  $\lambda$  Tau and Algol, respectively (Figs. 6a and 6b). However, Algol is the only EB, whose entire primary eclipse can be observed during a single night.

Our seventh criterion was:

*C<sub>7</sub>: The variability can be detected during a single night.*

This criterion would eliminate  $\zeta$  Gem and l Car.

Kottamia Observatory ( $\phi = 30^\circ$ ) is located on plateau 470 meters above the sea level between Cairo and Suez. The observing conditions at this site help us understand what kind of observations the ancient Egyptians might have been able to perform. The site has nearly 300 clear nights a year, half of these being suitable for photometric observations (Mikhail & Haubold 1995). The measured atmospheric extinction coefficient is typically  $k_V = 0.^m25$ , but it undergoes large seasonal variations (Mikhail 1979). Since the ancient Egyptian observations were made in proximity of the Nile, we can assume that the photometric conditions were not better than those at the Kottamia Observatory located higher on a desert plateau. This assumption is supported by a study by Schmidt (1994), which showed that  $k_V = 0.^m30$  would be an appropriate value for Alexandria, Egypt in the times of Ptolemy (about 100–160 A.D). Atmospheric extinction changes the brightness of stars. It is weakest at the zenith, i.e. at the altitude  $a = 90^\circ$ . The effects of extinction were estimated by using the visual extinction coefficient  $k_V = 0.^m25$ . With this value, the apparent visual brightness of a star falls only about  $0.^m1$  when it descends from  $a = 90^\circ$  to  $45^\circ$ , but extinction becomes much stronger at lower altitudes. When  $a$  goes from  $45^\circ$

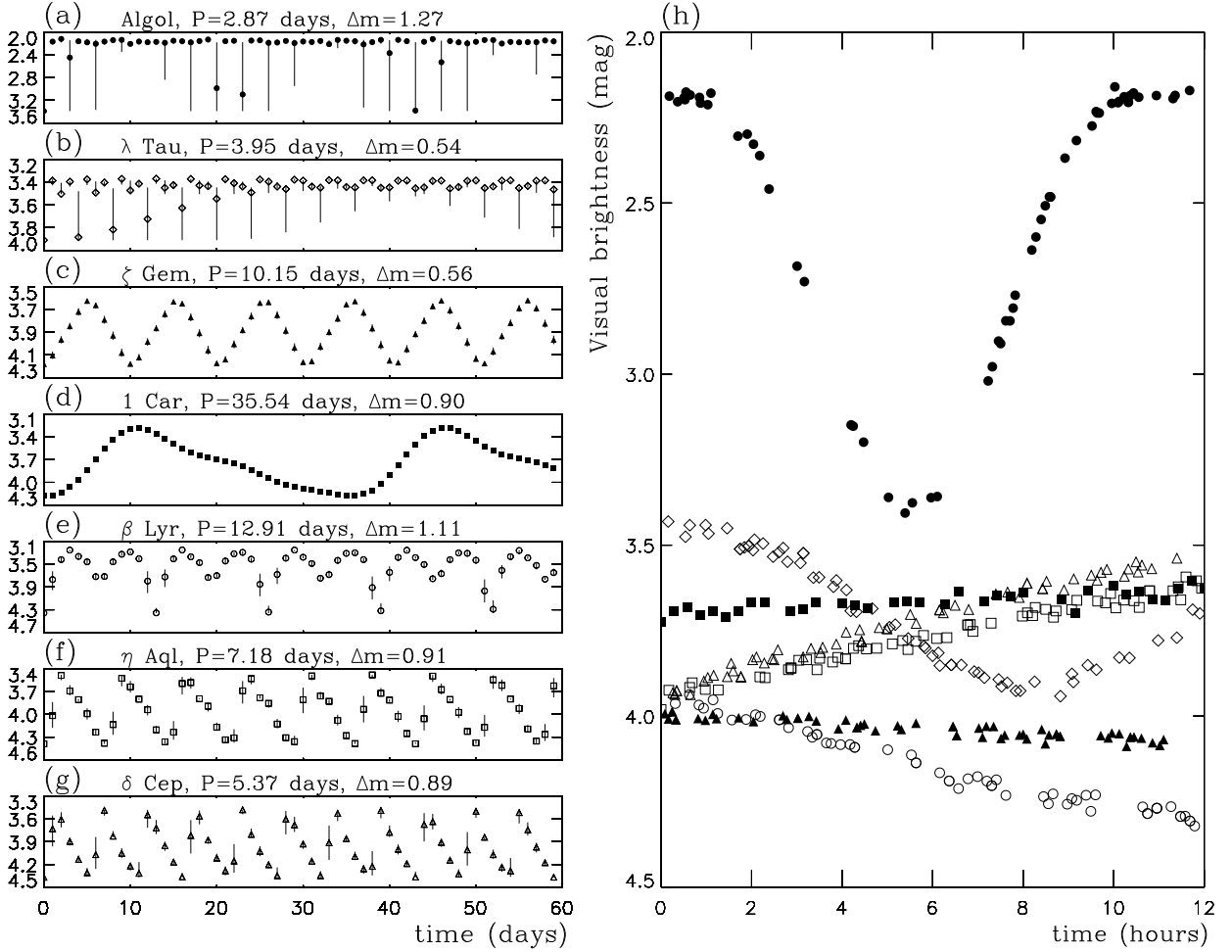


**Fig. 6.** Light curves of the seven best variable star candidates as a function of time. The magnitudes are shown for a time interval of 60 days. (a–g) The symbols are the same as Fig. 5, but here they denote the brightness at mid-night. The vertical lines (when visible) display the total range of the brightness changes during a night lasting 12 hours. (h) The nightly changes of all these variables in the same magnitude scale. The selected phase interval of each light curve is the one that would induce the largest possible brightness changes during a single night.

to  $10^\circ$ , the brightness of a star already falls by  $1.^m05$ . Finally, the fall is  $1.^m15$  over the short  $a$  range between  $10^\circ$  and  $5^\circ$ .

The bright stars close to the seven remaining variable star candidates are shown in Fig. 7. The left hand y-axis of every panel in Fig. 7 gives the declination  $\delta$ , while the right hand y-axis shows the corresponding altitude of upper culmination  $a_{\max}$ . In 1224 B.C. at Middle Egypt, 1 Car never rose higher than  $a_{\max} = 14^\circ$ , while Algol rose to  $a_{\max} = 88^\circ$  close to the zenith. The  $a_{\max}$  values of the other five variables were between these two extremes (Table 10).

Egyptians were probably not interested in science for the sake of pure theoretical knowledge. However, our next criterion would require several nights of dedicated observations of the constellations around the remaining variable star candidates. Variability could be detected from such long-term observations, e.g. as a change in the constellation pattern of the variable. This requires that suitable comparison stars are first *identified* close to the seven variables. These variables are denoted with \* in Table 11 and Fig. 7. All bright stars close to these seven remaining variable star candidates were classified into the following four categories:

- ★ = This star belongs to the same modern constellation as the variable (\*). The brightness  $m$  of this star in the Bright Star Catalogue (hereafter BSC in Hoffleit & Jaschek 1991) fulfills  $m \leq m_1$ , where  $m_1 = m_{\max} + 0.1$ . To a naked eye observer, the variable never appears brighter than this star.
- ★ = This star belongs to the same modern constellation as the variable (\*). The brightness  $m$  of this star in BSC fulfills  $m_1 < m < m_2$ , where  $m_2 = m_{\min} - 0.1$ . To a naked eye observer, the variable sometimes appears dimmer or brighter than this star.
- = This star does not belong to the same modern constellation as the variable (\*), but it is not located more than 15 degrees away from the variable. The brightness  $m$  of this star in BSC fulfills  $m \leq m_1$ . To a naked eye observer, the variable never appears brighter than this star.
- = This star does not belong to the same modern constellation as the variable (\*), but it is not located more than 15 degrees away from the variable. The brightness  $m$  of this star in BSC fulfills  $m_1 < m < m_2$ . To a naked eye observer, the variable sometimes appears dimmer or brighter than this star.

The stars with  $m \geq m_2$  are of no interest here, because they never appear brighter than the variable.



**Table 11.** Brightest stars close to the seven best variable star candidates.

Name	Number	$m$ (mag)	$\Delta m$ (mag)	$d$ (da)	Name	Number	$m$ (mag)	$\Delta m$ (mag)	$d$ (da)	Name	Number	$m$ (mag)	$\Delta m$ (mag)	$d$ (da)
★ $\alpha$ Per	HR 1017	1.79	–	9.4	* $\beta$ Per	HR 936	2.12	1.27		★ $\zeta$ Per	HR 1203	2.85	–	12.9
★ $\epsilon$ Per	HR 1220	2.88	0.12	9.5	★ $\gamma$ Per	HR 915	2.93	–	12.6	★ $\delta$ Per	HR 1122	3.01	–	9.2
● $\gamma$ And	HR 603	2.26	–	12.1	● $\beta$ Tri	HR 622	3.00	–	13.1					
★ $\alpha$ Tau	HR 1457	0.75	0.20	9.4	★ $\beta$ Tau	HR 1791	1.65	–	25.7	★ $\eta$ Tau	HR 1165	2.87	–	12.1
★ $\zeta$ Tau	HR 1910	2.88	0.29	24.7	★ 78 Tau	HR 1412	3.35	0.07	7.5	* $\lambda$ Tau	HR 1239	3.37	0.54	
★ $\epsilon$ Tau	HR 1409	3.53	–	9.4	★ $o$ Tau	HR 1030	3.60	–	9.4	★ 27 Tau	HR 1178	3.63	–	11.9
★ $\gamma$ Tau	HR 1346	3.65	–	5.5	★ 17 Tau	HR 1142	3.70	–	12.2	★ $\xi$ Tau	HR 1038	3.70	0.09	8.7
★ $\delta$ Tau	HR 1373	3.76	–	7.3	● 1 Ori	HR 1543	3.19	–	12.9	● 3 Ori	HR 1552	3.69	–	14.2
★ $\beta$ Gem	HR 2990	1.14	–	12.4	★ $\alpha$ Gem	HR 2891	1.59	–	13.4	★ $\gamma$ Gem	HR 2421	1.93	–	7.5
★ $\mu$ Gem	HR 2286	2.75	0.27	9.8	★ $\epsilon$ Gem	HR 2473	2.98	–	6.5	★ $\eta$ Gem	HR 2216	3.15	0.75	11.6
★ $\xi$ Gem	HR 2484	3.36	–	8.7	★ $\delta$ Gem	HR 2777	3.53	–	4.0	★ $\kappa$ Gem	HR 2985	3.57	–	10.1
★ $\lambda$ Gem	HR 2763	3.58	–	5.2	★ $\theta$ Gem	HR 2540	3.60	–	13.7	* $\zeta$ Gem	HR 2650	3.62	0.56	
★ $\iota$ Gem	HR 2821	3.79	–	8.9	★ $\nu$ Gem	HR 2905	4.06	–	9.7	● $\beta$ CMi	HR 2845	2.84	0.08	13.5
★ $\alpha$ Car	HR 2326	-0.72	–	27.8	★ $\beta$ Car	HR 3685	1.68	–	7.9	★ $\epsilon$ Car	HR 3307	1.86	–	10.4
★ $\iota$ Car	HR 3699	2.25	–	4.7	★ $\theta$ Car	HR 4199	2.76	–	6.7	★ $\nu$ Car	HR 3890	3.01	–	2.6
★ $\omega$ Car	HR 4037	3.32	–	8.0	★ p Car	HR 4140	3.27	0.10	5.5	★ q Car	HR 4050	3.36	0.08	3.9
★ a Car	HR 3659	3.44	–	5.5	★ $\chi$ Car	HR 3117	3.47	–	17.1	* 1 Car	HR 3884	3.28	0.90	
★ U Car	HR 4257	3.78	–	9.0	★ S Car	HR 4114	3.82	–	6.4	★ c Car	HR 3571	3.84	–	6.2
★ X Car	HR 4337	3.84	0.18	10.7	★ i Car	HR 3663	3.97	–	3.9	★ 1 Car	HR 4102	4.00	–	12.0
● $\delta$ Vel	HR 3485	1.96	0.40	11.1	● $\kappa$ Vel	HR 3734	2.50	–	8.1	● n Vel	HR 3803	3.13	–	5.7
● $\phi$ Vel	HR 3940	3.54	–	8.1	● o Vel	HR 3447	3.55	0.12	12.8	● $\lambda$ Cen	HR 4467	3.13	–	12.6
● $\pi$ Cen	HR 4390	3.89	–	14.7	● $\beta$ Vol	HR 3347	3.77	–	9.3	● $\alpha$ Vol	HR 3615	4.00	–	6.0
● $\lambda$ Mus	HR 4520	3.64	–	13.4										
★ $\alpha$ Lyr	HR 7001	-0.02	0.09	5.9	★ $\gamma$ Lyr	HR 7178	3.24	–	2.0	* $\beta$ Lyr	HR 7106	3.25	1.11	
★ R Lyr	HR 7157	3.88	1.12	10.6	● $\mu$ Her	HR 6623	3.42	–	14.3	● $\xi$ Her	HR 6703	3.70	–	12.0
● o Her	HR 6779	3.80	0.07	10.2	● 109 Her	HR 6895	3.84	–	12.9	● $\theta$ Her	HR 6695	3.86	–	11.6
● 110 Her	HR 7061	4.19	–	12.6	● $\beta$ Cyg	HR 7417	3.08	–	10.3	● $\eta$ Cyg	HR 7615	3.39	–	13.8
● $\chi$ Cyg	HR 7564	3.30	10.9	12.7										
★ $\alpha$ Aql	HR 7557	0.77	–	7.6	★ $\gamma$ Aql	HR 7525	2.72	–	9.7	★ $\zeta$ Aql	HR 7235	2.99	–	17.4
★ $\theta$ Aql	HR 7710	3.23	–	4.7	★ $\delta$ Aql	HR 7377	3.36	–	7.2	★ $\lambda$ Aql	HR 7236	3.44	–	12.9
★ $\beta$ Aql	HR 7602	3.71	–	5.9	* $\eta$ Aql	HR 7570	3.48	0.91		★ $\epsilon$ Aql	HR 7176	4.02	–	19.2
★ i Aql	HR 7193	4.02	–	14.3	● $\alpha$ Cap	HR 7754	0.08	–	15.0	● $\epsilon$ Del	HR 7852	4.03	–	14.4
★ $\alpha$ Cep	HR 8162	2.44	–	9.6	★ $\gamma$ Cep	HR 8974	3.21	–	20.0	★ $\beta$ Cep	HR 8238	3.16	0.11	13.7
★ $\zeta$ Cep	HR 8465	3.35	–	2.4	★ $\eta$ Cep	HR 7957	3.43	–	13.3	★ $\iota$ Cep	HR 8694	3.52	–	8.3
* $\delta$ Cep	HR 8571	3.48	0.89		★ $\mu$ Cep	HR 8316	3.43	1.67	5.9	★ $\epsilon$ Cep	HR 8494	4.15	0.06	2.5
★ $\theta$ Cep	HR 7850	4.22	–	15.2	● $\beta$ Cas	HR 21	2.25	0.06	12.7	● $\alpha$ Lac	HR 8585	3.77	–	8.2
● 81 Cyg	HR 8335	4.23	–	11.0										

**Notes.** The Name, BSC number and magnitude ( $m$ ) of stars close to Algol,  $\lambda$  Tau,  $\zeta$  Gem, 1 Car,  $\beta$  Lyr,  $\eta$  Aql and  $\delta$  Cep: The amplitude of photometric variability ( $\Delta m$  in GCVS) is given, if it exceeds  $0.^m05$ . In these cases of variability, the  $m$  value from BSC has been substituted with the  $m_{\max}$  value from GCVS. The notation “–” means that  $\Delta m < 0.^m05$ . The angular distance ( $d$ ) of the star from the variable is given in degrees of arc (da). The notations \*, ★, ★, ● and ● are explained in Sect. 5. The same notations are used in Fig. 7.

The ancient Egyptian scribes known as the “hour-watchers” might have noticed major constellation pattern changes, as explained in Paper III. Their ancient constellations were not the same as ours (Clagett 1995). The two categories of brighter stars (★ and ●) are relevant, because these stars have influenced the constellation patterns in modern and ancient times. The other two categories (★ and ●) are relevant, because they represent the suitable comparison stars for naked eye observers. All stars belonging to the above four categories in BSC are given in Table 11. Note that we also give  $\Delta m$  of these stars, if it exceeds  $0.^m05$  in the GCVS. With such variable comparison stars, it is impossible to determine the brightness of the variable with an accuracy of  $0.^m1$ . The  $m$  values in BSC can be anywhere between the  $m_{\max}$  and  $m_{\max} + \Delta m$  values given in GCVS. Hence the  $m$  values from BSC have been substituted with the  $m_{\max}$  values from GCVS for every star with  $\Delta m \geq 0.05$ . The seven constellations of the remaining variable star candidates are shown in Fig. 7, where we

have excluded those ★ and ★ category stars, which are over 20 degrees away from the variable in Table 11.

Let us assume that there would exist a hypothetical constellation pattern, e.g. three stars forming a triangle, where the periodic variable star fades more than half a magnitude below the other two constant brightness stars. If the angular separation of the stars in this triangle were only one or two degrees, differential extinction would not mislead observations. Hence, the changes of such a constellation pattern could be reliably observed even at lower altitudes. This hypothetical constellation pattern would be ideal for the detection of a variable star. But in reality the pattern in the field around many variables has too few suitable comparison stars or some apparently suitable comparison stars are variables themselves. The field around and the light curve of the seven remaining variables have their own individual characteristics. Thus the checking of our next criterion required a rather tedious description for each object, but this elimination process was necessary from the astronomical point of view. This process revealed how easy or difficult it would have been for the

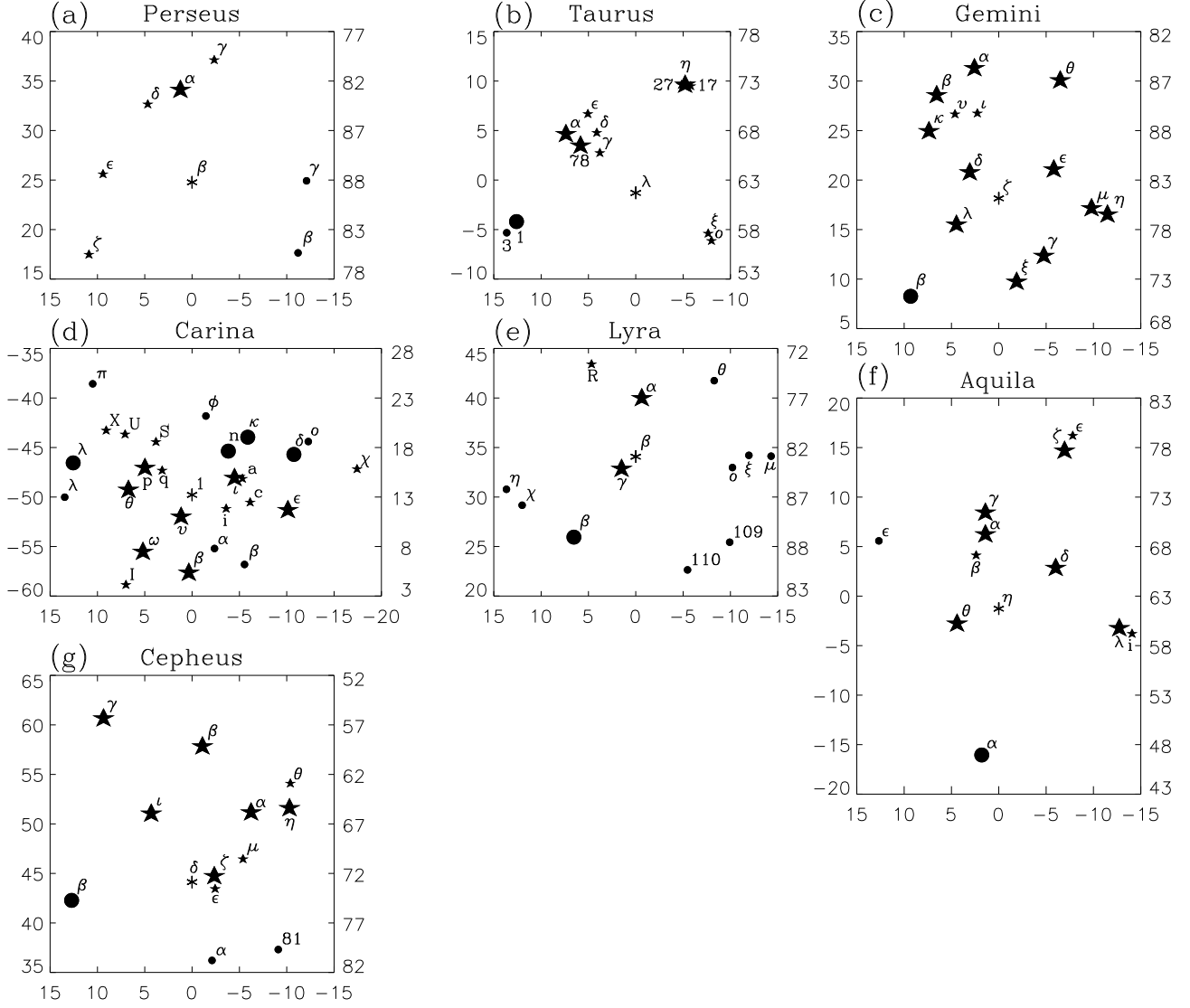


**Fig. 7.** Star maps close to the seven best variable star candidates. The stars (★ and ☆) in the same modern constellation with the variables (\*) are shown in panels: (a) Algol, (b)  $\lambda$  Tau, (c)  $\zeta$  Gem, (d)  $\iota$  Car, (e)  $\beta$  Lyr, (f)  $\eta$  Aql and (g)  $\delta$  Cep. Only those stars in the same modern constellation are shown which fulfill  $d \leq 20^\circ$  in Table 11. In addition, the stars (● and •) not belonging to the same modern constellation are also shown, if they fulfill  $d \leq 15^\circ$  in Table 11. The right ascension (x-axis:[°]), declination (left hand y-axis:[°]) and the altitude of upper culmination  $a_{\max}$  (right hand y-axis:[°]) have been calculated for the epoch 1224 B.C., i.e. all units are degrees of arc [da].

ancient Egyptians to notice the constellation pattern changes in the field close to each of the seven remaining variable star candidates. We advise those who intend to read our description of this process to take a magnified copy of Fig. 7. Comparing this copy to our next description of the field around these seven remaining variables will elaborate how much effort would have been required to discover each candidate with naked eyes only.

The field around the first EB, Algol ( $\beta$  Per), has only one brighter star and it also belongs to the modern constellation of Perseus (Fig. 7a:  $\alpha$  Per). Of the six comparison stars, only  $\epsilon$  Per is variable (Table 7:  $\Delta m = 0.^m12$ ). During the primary eclipse, Algol fades  $1.^m1$  below  $\gamma$  And,  $0.^m5$  below  $\zeta$  Per and  $\gamma$  Per,  $0.^m4$  below  $\delta$  Per and  $\beta$  Tri, as well as between  $0.^m4$  and  $0.^m5$  below  $\epsilon$  Per. All these magnitude differences can be easily observed with naked eyes. Extinction posed no problems in 1224 B.C., because the upper culmination occurred nearly at the zenith. During the best observing nights the time that Algol spent above  $a = 30^\circ$

was 10 hours. Because Algol is the 2nd brightest star in the field around it, the eclipse causes an abrupt change in the constellation pattern (ancient or modern), as Algol fades dimmer than the six bright stars around it. The brightness falls from  $2.^m1$  to  $3.^m4$  in less than 5 hours (Figs. 5 and 6: closed circles). The entire eclipse can be observed during a single night, because it lasts a little less than 10 hours. The eclipses are very obvious events (Goodricke 1783; Argelander 1855; Isles 1997), because for two hours the brightness remains more than one magnitude below  $m_{\max}$ . When the primary eclipse begins to occur at some particular night, it will repeat itself for every third night, but each time about 3 hours earlier. Then for about one week, the brightness of Algol appears constant, because the eclipse occurs at daytime (Fig. 6a: closed circles and vertical lines). We emphasize that the above description of constellation pattern changes caused by the variability of Algol is valid only for the partial eclipses of the current epoch. The possibility of total eclipses in 1224 B.C.,

which would have made Algol nearly invisible for about half an hour, was already discussed in Sect. 4.

The second EB,  $\lambda$  Tau, is the 5th brightest star in the field around it (Fig. 7b). One of the four brighter stars, 1 Ori, does not belong to the modern constellation of Taurus. Of the eight comparison stars, only  $\xi$  Tau is a variable star (Table 11:  $\Delta m = 0.^m09$ ). The depth of the secondary eclipse of this variable star candidate  $\lambda$  Tau is about  $0.^m1$  and it would therefore go unnoticed by naked eye observers. The primary eclipse of  $\lambda$  Tau lasts 14 hours, having a magnitude range between  $3.^m4$  and  $3.^m9$ . The entire eclipse event can not be observed during a single night. In about 7 hours, the brightness of  $\lambda$  Tau falls  $0.^m4$  below  $\epsilon$  Tau,  $0.^m3$  below  $\sigma$  Tau,  $27$  Tau and  $\gamma$  Tau,  $0.^m2$  below 3 Ori, 17 Tau and  $\delta$  Tau, as well as between  $0.^m1$  and  $0.^m2$  below  $\zeta$  Tau. Some of these magnitude differences could be observed with naked eyes at the upper culmination of  $\lambda$  Tau which was  $a_{\max} = 62^\circ$  in 1224 B.C. But at  $a = 30^\circ$ , the differential extinction between two objects separated by  $10^\circ$  in altitude is already  $0.^m25$ . Variable extinction therefore certainly misleads these comparisons as the altitude changes during 7 hours. Even during the best observing nights in 1224 B.C., this variable star candidate  $\lambda$  Tau rose above  $30^\circ$  for 8 hours a night (Table 10). The eclipse of  $\lambda$  Tau (5th brightest) does not change the constellation pattern as strongly as that of Algol (2nd brightest). The period of  $\lambda$  Tau is only about an hour less than four days. Once the primary eclipse begins to occur at the nighttime, it will be repeated every fourth night over about one month. During the next month, the epoch of the light minimum of  $\lambda$  Tau can not be observed and for a week or two the brightness appears to be more or less constant (see Fig. 6b: open diamonds and vertical lines).

Atmospheric extinction did not cause problems in observing the first cepheid variable star candidate  $\zeta$  Gem (Fig. 7c:  $a_{\max} = 80^\circ$ ), but the only two suitable comparison stars are  $\iota$  Gem and  $\nu$  Gem. These comparison stars are not variables themselves (Table 11:  $\Delta m = -$ ). This variable star candidate  $\zeta$  Gem can be  $0.^m2$  brighter than  $\iota$  Gem or  $0.^m1$  dimmer than  $\nu$  Gem. Both of these magnitude differences are just on the limit of human eye detection. It is therefore not likely that the Egyptians would have identified these two particular comparison stars among the twelve brighter stars around  $\zeta$  Gem. Only one of these brighter stars,  $\beta$  CMi, does not belong to the modern constellation of Gemini. The variability of  $\zeta$  Gem does not therefore cause major changes in the constellation pattern, were it ancient or modern. It has been noted that  $\zeta$  Gem “presents a challenge even for experienced observers” (Turner 1999).

The field around the second cepheid variable, 1 Car, has eleven brighter stars, as well as numerous suitable comparison stars (Fig. 7d). The changes of this variable would not therefore alter the general constellation pattern, were it modern or ancient. Three comparison stars are variable (Table 11: q Car, X Car and  $\sigma$  Vel). However, atmospheric extinction prevented accurate observations, because the upper culmination of 1 Car was  $a_{\max} = 14^\circ$  in 1224 B.C. Even at the epoch of this upper culmination, an altitude difference between 1 Car and a comparison star  $8^\circ$  below it causes a differential extinction of  $1.^m5$  with  $k_V = 0.25$ . Because the altitude was below  $a_{\max}$  at all other times, it was impossible to detect the  $\Delta m = 0.^m90$  variability of 1 Car.

Atmospheric extinction did not prevent accurate observations of the third EB,  $\beta$  Lyr, (Table 10:  $a_{\max} = 82^\circ$ ). It is the 4th brightest star in the field, which contains one brighter star not belonging to the modern constellation of Lyra (Fig. 7e:  $\beta$  Cyg). Three of the nine comparison stars are variable (Table 11). The strong variability of the two comparison stars R Lyr ( $\Delta m = 1.^m1$ ) and  $\chi$  Cyg ( $\Delta m = 10.^m9$ ) would have mislead observations of  $\beta$

Lyr. The comparison star R Lyr was among the 13 objects in our Table 10, but it was then rejected with the  $C_6$  criterion (i.e. variability unpredictable). The other comparison star  $\chi$  Cyg was rejected with the  $C_4$  criterion, because the period is 408 days. The light curve of the variable star candidate  $\beta$  Lyr is smooth (Fig. 5), i.e. no radical changes occur during a single night (Fig. 6). Although it is an EB, the smooth light curve shape would require continuous long-term differential photometry over 13 days, i.e. a similar observing technique as in the cases of the cepheid variables  $\eta$  Aql and  $\delta$  Cep discussed below. Unlike with the first two EBs, Algol or  $\lambda$  Tau, it is impossible to determine the exact epoch of the primary or secondary minimum of this third EB,  $\beta$  Lyr, from naked eye observations. It is improbable that the Egyptians noticed that during about three days  $\beta$  Lyr first faded  $1.^m0$  below  $\eta$  Cyg and  $\mu$  Her,  $0.^m7$  below  $\xi$  Her,  $0.^m5$  below 109 Her and  $\theta$  Her, and  $0.^m2$  below 110 Her. It then regained its brightness within the next three days and finally went through a weaker secondary eclipse in another 6.5 days. Be that as it may, the Egyptians would have had to reject the two other variables R Lyr and  $\chi$  Cyg as their comparison stars for  $\beta$  Lyr. A more probable discovery in 1224 B.C. would have been that the comparison star  $\chi$  Cyg, which is a Mira variable, sometimes becomes the 5th brightest star in this field, and then disappears completely. The Egyptians may also have noticed other Mira variables, but the periods in this class are longer than 90 days, i.e. not relevant in this study.

The third cepheid variable star candidate,  $\eta$  Aql, is only the 8th brightest star in the field, which contains one brighter star not belonging to the modern constellation of Aquila (Fig. 7f:  $\alpha$  Cap). The variability of this candidate did not therefore cause major changes in the constellation pattern. All four suitable comparison stars have a constant brightness. However, the magnitudes of three comparison stars are the same within  $0.^m01$  ( $i$  Aql,  $\epsilon$  Aql,  $\epsilon$  Del). In about three and a half days, the variable star candidate  $\eta$  Aql fades  $0.^m4$  below these three comparison stars or  $0.^m7$  below  $\beta$  Aql. It is quite implausible that the Egyptians were able to notice this kind of long-term changes lasting several nights. This case also resembles that of the other variable star candidate  $\zeta$  Gem, where the brightness of the variable could be compared to only two fixed magnitude values of comparison stars. This is far from an ideal case for a naked eye variable star observer. Extinction did not prevent accurate observations of  $\zeta$  Gem in 1224 B.C. ( $a_{\max} = 62^\circ$ ). However, the observations of the whole smooth light curve of this cepheid require a week of dedicated continuous differential photometry.

The upper culmination of the fourth cepheid,  $\delta$  Cep, occurred at  $a_{\max} = 73^\circ$ , i.e. extinction did not prevent accurate observations. The field around this variable star candidate has seven brighter stars,  $\beta$  Cas being the only one not belonging to the modern constellation of Cepheus (Fig. 7g). Of the five comparison stars, the two closest ones are also variable stars (Table 11:  $\mu$  Cep with  $\Delta m = 1.^m67$  and  $\epsilon$  Cep with  $\Delta m = 0.^m06$ ). The strongly variable comparison star  $\mu$  Cep has a period of 730 days in GCVS, and was therefore rejected with the  $C_4$  criterion. Of the three constant comparison stars, two are of equal brightness (Table 11:  $\theta$  Cep and 81 Cyg). In about two and a half days, this variable star candidate  $\delta$  Cep fades  $0.^m6$  below  $\alpha$  Lac, about  $0.^m2$  below  $\epsilon$  Cep and  $0.^m1$  below the two other constant comparison stars  $\theta$  Cep and 81 Cyg. It then regains its brightness in another two and a half days. Again, it is unlikely that the Egyptians could notice such long-term variability from one night to another, even with respect to the best comparison star  $\alpha$  Lac. They would also have had to ignore the large changes of the comparison star  $\mu$  Cep, which do in fact alter the constellation more than those of

our candidate  $\delta$  Cep, because the former fades close to the limit of naked eye detection (i.e. to  $5.^m1$ ). The full phase coverage of the smooth light curve of  $\delta$  Cep requires over 5 days of continuous differential photometry.

The 8th selection criterion was:

*C<sub>8</sub>: The variability causes a detectable change in the pattern of the constellation.*

This criterion would eliminate  $\zeta$  Gem (13th brightest),  $\iota$  Car (12th brightest),  $\eta$  Aql (8th brightest) and  $\delta$  Cep (8th brightest). The detection of  $\beta$  Lyr (4th brightest) would have been difficult, because the smooth brightness changes occur during several nights ( $P = 12.9$  days). The presence of other variable stars in the field around some of the above five variables, as well as the effects of differential extinction, would have further interfered with variability detection. The variability of  $\lambda$  Tau (5th brightest) might have been detected, but only from short-term observations (i.e. one night). However, our criterion  $C_8$  would not eliminate Algol, being the 2nd brightest star in the constellation, as it fades below all six comparison stars in less than 5 hours.

The  $C_7$  and  $C_8$  criteria were based on the assumption that the Egyptians could *identify* suitable comparison stars, as well as *eliminate* unsuitable ones. Only in the case of Algol, there would have been no identification problems. But these  $C_7$  and  $C_8$  criteria can lead only to the detection of *variability*. It is yet more challenging to determine the exact *periodicity*.

Let us now make the assumption that the Egyptians were able to identify suitable comparison stars, and eliminate all unsuitable ones. After detecting variability, they would have had to determine the brightness of each constant comparison star, or at least their order of increasing brightness. This is exactly what Goodricke (1783) did. But the Egyptians could not rank these comparison stars with no knowledge about atmospheric extinction. About a thousand years later in the island of Rhodes, Hipparchus (about 190–125 B.C.) compiled the first catalogue of 1080 stars. He classified their magnitudes into six classes (Doig 1950), i.e. his accuracy was  $1.^m0$ . The catalogue by Ptolemy (about 100–160 A.D.), in *Almagest*, aimed to a slightly better accuracy. However, it has been shown that the accuracy within the different magnitude classes of *Almagest* varied between  $0.^m4$  and  $1.^m0$  (Schmidt 1994). The ancient Egyptians drew sketches of the constellations or star groups, where the stars had two or three different sizes (Neugebauer & Parker 1960). Obviously the accuracy of magnitudes in these sketches did not match that of *Almagest*, where the accurate positions of stars were also determined with an instrument called “astrolabe”, which was invented by Ptolemy himself for this particular purpose.

The detection of periodicity in the smooth light curves of the four cepheids ( $\zeta$  Gem,  $\iota$  Car,  $\eta$  Aql and  $\delta$  Cep), as well as in the qualitatively similar light curve of one EB ( $\beta$  Lyr), would have required the determination of magnitudes of the constant comparison stars, preferably with an accuracy of  $0.^m1$ . Then the ancient Egyptian astronomers would have had to tabulate these differential magnitudes as a function of time, i.e. they would have compiled a modern *time series*. But even this modern empirical approach would not have revealed the periodicities in these data. For a modern astronomer, the Cartesian coordinate system offers a simple graphical solution to detect the periodicity in these data. This system was invented by Descartes (1596–1650). Since the Egyptians would not have plotted their differential magnitudes as a function of time (like e.g. in our Fig. 6), they ought to have invented something similar to the modern time series analysis

(e.g. the power spectrum method). Their data would also have contained gaps (e.g. due to cloudy nights), which would have caused additional problems, especially with the longer periods. The longer the period, the more prolonged and dedicated observations are required. Their detection of periodicity from differential photometry does not therefore seem plausible. Furthermore, their measurement of time itself was not precise (see Paper III).

The secondary eclipse of Algol or  $\lambda$  Tau would have been impossible to detect with naked eyes. Both of these stars appear constant, except during a primary eclipse. But their periodicity detection does not require an accurate *time series* (i.e. magnitudes as a function of time), because a *series of time points* will suffice (i.e. epochs of the primary eclipse). If these time point values are found to be multiples of the same number, then periodicity has been detected. There are at least six reasons, why the epoch of the primary eclipse was easier to determine for Algol than for  $\lambda$  Tau:

1. Algol is easier to observe, because it is more than one magnitude brighter than  $\lambda$  Tau.
2. The brightness of Algol falls  $1.^m27$  during the primary eclipse. This amplitude is over two times larger than the  $0.^m54$  amplitude of  $\lambda$  Tau.
3. The primary eclipse of Algol lasts 10 hours and can be observed during a single night. The entire primary eclipse of  $\lambda$  Tau lasts 14 hours and can not be observed during a single night.
4.  $\lambda$  Tau fades  $0.^m4$  below one comparison star,  $0.^m3$  below three comparison stars and  $0.^m2$  below four comparison stars in 7 hours. Algol fades between  $1.^m1$  and  $0.^m4$  below six comparison stars in 5 hours.
5. The timing of the primary minimum of Algol is easier, because  $\lambda$  Tau never reaches its maximum brightness before or after the eclipse during the same night. Furthermore, differential extinction misleads brightness estimates of  $\lambda$  Tau, because the fading or brightening takes 7 hours. The smoother shape of the light curve during the primary eclipse of  $\lambda$  Tau makes it very difficult to determine from naked eye observations when the fading begins (eclipse begins), when the fading is changing into brightening (eclipse epoch occurs) or when the brightening is reaching the level of constant maximum brightness (eclipse has ended).
6. The  $a_0$ ,  $a_{30}$ ,  $a_{60}$  and  $a_{\max}$  values in Table 10 show that it was easier for the ancient Egyptians to observe Algol than  $\lambda$  Tau.

The 9th selection criterion was:

*C<sub>9</sub> The period of variability could be determined from naked eye observations in 1224 B.C.*

This criterion certainly eliminated  $\zeta$  Gem,  $\iota$  Car,  $\eta$  Aql,  $\delta$  Cep and  $\beta$  Lyr. These five stars could have already been rejected with the  $C_7$  or  $C_8$  criterion. Although the  $C_8$  criterion might have rejected  $\lambda$  Tau, it could satisfy the  $C_9$  criterion, but only with accurate differential photometry. Algol is the only known variable star, which satisfies all  $C_1$ , ...,  $C_9$  criteria.

Our last rejection criterion is based on the modern history of variable stars. This history should indicate objectively how difficult the detection of variability and the determination of the period of this variability was for modern astronomers. The variables discussed below are numbered according to their year of discovery (Merrill 1938). The discoverer and the year of discovery are both given in brackets. The first variable discovered was Mira (1st: Fabritius, 1596). The period of variability of this star

is about 332 days. Mira was therefore rejected earlier with our criterion  $C_4$ . Four of the seven variables that were discussed in greater detail (Figs. 5, 6 and 7) were among the eight ones discovered first: Algol (2nd: Montanari, 1669),  $\eta$  Aql (6th: Pigott, 1784),  $\beta$  Lyr (7th: Goodricke, 1784) and  $\delta$  Cep (8th: Goodricke, 1784). Our second best variable star candidate discussed above,  $\lambda$  Tau, was not among the first eight ones discovered.

Incidentally, when Montanari in 1669 discovered the variability of Algol at Bologna, Italy, the upper culmination was  $a_{\max} = 85^\circ$ , i.e. his observing conditions were as favourable as those at Egypt in 1224 B.C. At both sites in these two particular points of history, the eclipse of Algol could be easily noticed by anyone laying on his back and gazing the constellations right above.

Periodicity determinations of these first eight discovered variables followed later. Goodricke determined the period of object Algol in 1783. The variability of our second best candidate,  $\lambda$  Tau, was detected by Baxendell (1848), i.e. 179 years after Montanari discovered Algol. The period of  $\lambda$  Tau was determined immediately after discovery, but it required another 60 years to measure the light curve due to the lack of suitable comparison stars (Stebbins 1920).

The 10th selection criterion between  $\lambda$  Tau and Algol

$C_{10}$  The period of variability was determined first in the modern history of Astronomy.

clearly favoured the latter. The whole sequence of our ten criteria strongly supported the conclusion that Algol is the one out of all currently known over 40 000 variables, where the ancient Egyptians could plausibly have detected predictable variability. It is possible that the eclipses were total or nearly total in those days. In this case, it would have been easier to determine the 2.85 days period that we now detect in CC.

## 6. Discussion

The prognoses of Table 1 were first transformed into series of time points (Sect. 2). We created 24 different SSTP to check, if the period analysis results depend on the chosen transformation between the Egyptian and Gregorian year, on the chosen day division, on the chosen prognoses or on the removal of some prognoses.

We calculated the occurrence of Gregorian January 1st in the Egyptian year for three alternatives separated by four months (Eq. 1:  $N_0 = 62, 187$  or  $307$ ). This gave us three different sets of sunrise and sunset times in Middle Egypt.

It is not known what part of the day exactly each of the three prognoses referred to (Leitz 1994). In our first alternative, we divided daytime into three time intervals of equal length (Fig. 1a). In our second alternative, we divided daytime into two intervals of equal length. The nighttime was the third interval (Fig. 1b). For both alternatives, we used the mid-epochs of these three intervals as the three time points  $t_1, t_2$  and  $t_3$  of each day. Our two alternatives represented the extremes of reasonable choices, because time points in the former were concentrated to the daytime (Fig. 1a) and those in the latter were distributed over 24 hours (Fig. 1b).

We separated the time points of G and S prognoses to SSTP=1–12 and SSTP=13–24, respectively. The  $D = 1$  and 20 prognoses in Table 1 were always GGG and SSS. Because of this regular  $30^d$  spacing, we removed the time points of these prognoses from SSTP = even number (see Table 2).

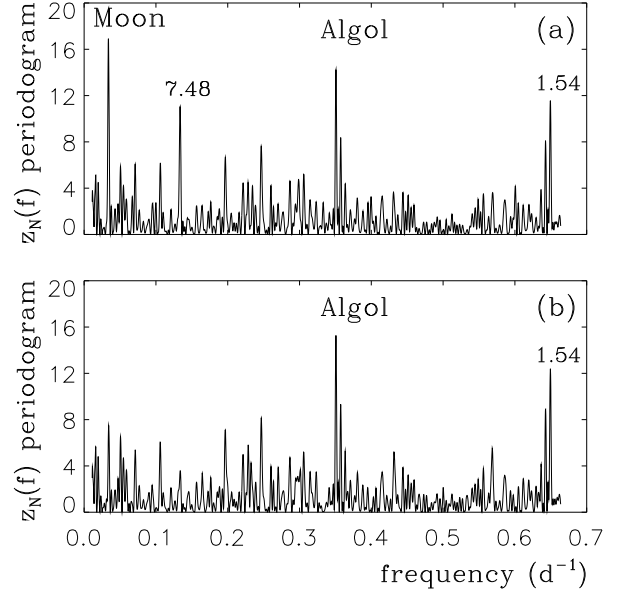


**Fig. 8.** Normalized periodograms  $z_N(f)$  of SSTP=1 (a) and SSTP=2 (b). The peaks of the real (Moon and Algol) and the unreal (7.48 and 1.54 days) significant periods are indicated.

We applied the Rayleigh test to search for periods of  $1.45 \leq P \leq 90^d$  (Sect. 3). The regular spacing of *real* data was three time points a day. We simulated aperiodic data similar to the real data of each SSTP, to test, if the standard  $Q$  estimates were reliable. These *simulated* data had the same regular spacing and the same number of different prognosis combinations as the real data. However, we assigned the prognoses for these simulated aperiodic data in a random order. The “noise periodograms”,  $z^*(f)$ , for these simulated data (e.g. Figs. 2b and 4b) revealed that the standard  $Q$  estimates were not reliable for the real data.

We solved this problem by dividing the  $z(f)$  periodogram of the real data of each SSTP with the noise periodogram  $z^*(f)$  of the same SSTP. This gave us the normalized periodogram  $z_N(f) = z(f)/z^*(f)$ , where the standard Rayleigh test statistic for the real data was converted into noise units at every tested frequency. A similar ratio is utilized in the power spectrum method, where the observed power is the signal-power to noise-power ratio (Scargle 1982). Normalization eliminated many longer unreal periods (Eq. 13). We identified the best periods from the highest peaks of  $z_N(f)$ . The simulated critical level estimates  $Q^*$  of these periods were computed from the  $z_N(f)$  periodogram. We rejected the  $H_0$  hypothesis if  $Q^* < \gamma = 0.001$ , where  $\gamma$  is the preassigned significance level, i.e. the probability of falsely rejecting  $H_0$  when it is in fact true. The error of the best periods was estimated by applying the bootstrap method to  $z_N(f)$  (Jetsu & Pelt 1996).

The  $z_N(f)$  periodograms of SSTP=1 and SSTP=2 are shown in Fig. 8. This figure provides a compact illustration of the main results of our period analysis. Normalization did not eliminate the two significant unreal  $7.48$  and  $1.54$  periods. They were induced by the interplay of the real  $29.46$  and  $2.85$  periods with the regular data spacing (Fig. 8a). This conclusion was supported by the fact that when the lunar  $29.46$  period was removed, the  $7.48$  period vanished (Fig. 8b). The one day window was the obvious connection (Eq. 13) between the unreal  $1.54$  and the real  $2.85$  period, which was  $0.017 \pm 0.002$  shorter than the current  $P_{\text{orb}} = 2.867328$  of Algol. We knew of no other terrestrial or celestial phenomenon that could explain the  $2.85$  period

in CC. Everything indicated that the two best periods in Fig. 8 were the real periods of the Moon and Algol.

The two best periods for all G prognoses were always within  $29.^d6 \pm 0.^d2$  and  $2.^d850 \pm 0.^d002$  (SSTP = 1, 3, 5, 7, 9 and 11). The  $29.^d6$  and  $7.^d48$  periods vanished when the G prognoses of  $D = 1$  were removed. The best period for the remaining G prognoses was always within  $2.^d850 \pm 0.^d002$  reaching  $0.000051 \leq Q^* \leq 0.000160$  (SSTP = 2, 4, 6, 8, 10 and 12). This was indisputable evidence for the  $2.^d850$  period. If the unreliable standard Rayleigh test  $Q$  estimates had been used, like in Paper I, we would not have rejected  $H_0$  with this period. We also checked that this result did not depend on the chosen transformation between the Egyptian and Gregorian year or on the chosen day division. There simply exist no other realistic alternative transformations of CC into series of time points that would alter this main result of our period analysis. Furthermore, we achieved a unique identification of all significant real and unreal periods, and revised the previously detected  $29.^d4$  synodic period of the Moon (Paper I) closer to the correct value of  $29.^d53$ .

No periodicity reaching  $Q^* < \gamma = 0.001$  was detected in the S prognoses (SSTP=13–24).

In Sect. 4, we showed that MT from Algol B to Algol A could explain the  $0.^d017$  increase of  $P_{\text{orb}}$  in three millennia. We dated the  $P_1 = 2.^d850$  period to  $t_1 = 1224$  B.C. An error of  $\pm 200^y$  in  $t_1$  would not have altered our results. The period is now  $P_2 = 2.^d867328$  in  $t_2 = 2012$  A.D. For a constant rate of period change,  $\dot{P}/P = [(P_2 - P_1)/(t_2 - t_1)]/P = 5.1 \times 10^{-9} \text{d}^{-1}$ , the MT relation of Eq. 14 gave  $\dot{m}_B = -2.2 \times 10^{-7} M_\odot$  per year for the mass loss of Algol B. This agreed with  $\dot{m}_B = -2.9 \times 10^{-7} M_\odot$  per year predicted by the best theoretical evolutionary model of Algol in Sarna (1993), as well as with the MT estimates of other EBs (Chaubey 1993; Šimon 1999; Qian 2000). All these results were consistent with that MT could explain the  $P_{\text{orb}}$  increase of  $0.^d017$  since 1224 B.C. More conservative estimates of  $10^{-13} M_\odot \leq |\dot{m}_B| \leq 10^{-8} M_\odot$  per year have been published for Algol (Harnden et al. 1977; Cugier & Chen 1977; Hadrava 1984; Richards 1992), but our  $|\dot{m}_B|$  value could also be an underestimate (Zavala et al. 2002).

We assumed that eclipses of Algol occurred in 1224 B.C. However, Algol C is constantly perturbing the inclination  $i_1$  of the orbital plane of Algol A–B system (Soderhjelm 1975). The current partial eclipse depth is  $\Delta m = 1.^m3$  with  $i_1 = 98.^o6$  (Zavala et al. 2010). Eclipses occur only when  $63.^o < i_1 < 117.^o$ . They become total when  $87.^o3 < i_1 < 92.^o7$ . Because Algol B has a larger diameter than Algol A, no flux from the brighter Algol A is observed during a total eclipse ( $\Delta m = 2.^m8$ ) and the brightness falls to  $5.^m0$ . In this case, a naked eye observer would get the dramatic impression that for half an hour Algol almost disappears from the sky (Csizmadia et al. 2009). Older observations predicted  $i_1$  changes with a period of  $P_{i_1} = 1\,900$  years (Soderhjelm 1975), but the new orbital elements (Zavala et al. 2010) gave  $P_{i_1} = 31\,000$  years (Eq. 15). Thus, only minor  $i_1$  changes may have occurred since 1224 B.C. The two best estimates  $\Phi = 95.^o \pm 3.^o$  (Csizmadia et al. 2009) and  $96.^o \pm 5.^o$  (Zavala et al. 2010), for the angle between the orbital planes of Algol A–B and Algol AB–C systems were too inaccurate to eliminate any of the following three different alternatives in ancient Egypt: total, partial or no eclipses. More accurate future interferometry of Algol may reveal the correct alternative.

Why Algol in particular would have caught the attention of ancient Egyptians? We showed that for naked eye observers, Algol is the star where it is easiest to discover periodic variability (Sect. 5). Only 109 candidates out of all currently known over 40 000 variable stars reach the maximum visual brightness

of  $4.^m0$  and vary more than  $0.^m4$ . Such variability can be discovered with naked eyes (Goodricke 1783; Argelander 1855). Only 13 out of these 109 candidates undergo periodic brightness variations below the upper limit,  $P \leq 90^d$ , of our period analysis (Table 10). Proper motion and precession corrections revealed that three of these candidates could not have been observed in ancient Egypt. Even modern astronomers can not predict the brightness variations of other three candidates. We then compared the light curves of the remaining four cepheids ( $\zeta$  Gem,  $\iota$  Car,  $\eta$  Aql,  $\delta$  Cep) and three EBs (Algol,  $\lambda$  Tau,  $\beta$  Lyr). Algol was the only one, where the ancient Egyptians could certainly have recorded periodic variability. This would have been even easier than nowadays, if they were witnessing total eclipses.

The ancient Egyptian scribes were socially valued professionals in Astronomy, Mathematics and Medicine (Paper III). Their duties included also the measurement of time by observing stars while they conducted the proper nightly rituals that kept the Sun safe during its journey across the underworld (Clagett 1989). The scribes may have considered Algol’s variability to threaten the “cosmic order”. CC describes the repetitive transformation of the Eye of Horus, usually called “Wedjat” or “the Raging one”, from a peaceful to raging personality, with good or bad influence on the life of men (Leitz 1994). A legend existed in which the enraged Eye of Horus nearly destroyed all mankind (Lichtheim 1976). Most likely, the scribes linked Algol’s strange behaviour with this prominent legend. Either they arrived at a numerical period estimate or they merely recorded the observed eclipses and then interpolated the daytime gaps in CC (Paper III).

## 7. Conclusions

We discovered connections between Algol and Egyptian scribes writings that can hardly be a coincidence. All statistical, astrophysical, astronomical and egyptological details matched. The period recorded in CC may represent a valuable constraint for future studies of MT in EBs. Goodricke’s achievement in 1783 was outstanding. The same achievement by the scribes of ancient Egypt, if true, was literally fabulous.

**Acknowledgements.** We have made use of the SIMBAD database at CDS, Strasbourg, France and NASA’s Astrophysics Data System (ADS) bibliographic services. This work was supported by the Vilho, Yrjö and Kalle Väisälä Foundation (P.K.), the Finnish Graduate School in Astronomy and Space Physics (J.L.) and the Academy of Finland (J.T.-V.).

## References

- Aitken, R. 1935, *The Binary Stars* (New York, USA: McGraw-Hill Book Company)
- Applegate, J. H. 1992, *ApJ*, 385, 621
- Argelander, F. W. A. 1855, *AJ*, 4, 57
- Bakir, A. 1966, *The Cairo Calendar No. 86637* (Cairo, Egypt: Government Printing Office)
- Baxendell, J. 1848, *MNRAS*, 9, 37
- Biermann, P. & Hall, D. S. 1973, *A&A*, 27, 249
- Budge, E. 1922, *Facsimiles of Egyptian Hieratic Papyri of the British Museum I* (London, England: Trustees of the British Museum)
- Budge, E. 1923, *Facsimiles of Egyptian Hieratic Papyri of the British Museum II* (London, England: Trustees of the British Museum)
- Chandler, S. C. 1888, *AJ*, 7, 165
- Chaubey, U. S. 1993, *Bulletin of the Astronomical Society of India*, 21, 597
- Clagett, M. 1989, *Ancient Egyptian Science 1: Knowledge and Order* (Philadelphia, USA: American Philosophical Society)
- Clagett, M. 1995, *Ancient Egyptian Science 2: Calendars, Clocks and Astronomy* (Philadelphia, USA: American Philosophical Society)
- Csizmadia, S., Borkovits, T., Paragi, Z., et al. 2009, *ApJ*, 705, 436
- Cugier, H. & Chen, K.-Y. 1977, *Ap&SS*, 52, 169

- Curtiss, R. H. 1908, *ApJ*, 28, 150
- Demaree, R. & Janssen, J. 1982, *Gleanings from Deir el-Medina* (Leiden, Netherlands: Nederlands Instituut voor het Nabije Oosten te Leiden)
- Doig, P. 1950, *A Concise History of Astronomy* (Chapman & Hall, London, England)
- Eggen, O. J. 1948, *ApJ*, 108, 1
- Frieboes-Conde, H., Herczeg, T., & Høg, E. 1970, *A&A*, 4, 78
- Goodricke, J. 1783, *Royal Society of London Philosophical Transactions Series I*, 73, 474
- Hadrava, P. 1984, *Bulletin of the Astronomical Institutes of Czechoslovakia*, 35, 335
- Hall, D. S. 1989, *Space Sci. Rev.*, 50, 219
- Hamden, Jr., F. R., Fabricant, D., Topka, K., et al. 1977, *ApJ*, 214, 418
- Heck, A., Mathys, G., & Manfroid, J. 1987, *A&AS*, 70, 33
- Helck, W., Otto, E., & Westendorf, W. 1975–1992, *Läxikon der Ägyptologie*, I–VI (Wiesbaden, Germany: Harrassowitz)
- Hill, G., Barnes, J. V., Hutchings, J. B., & Pearce, J. A. 1971, *ApJ*, 168, 443
- Hoffleit, D. 1984, *Journal of the American Association of Variable Star Observers*, 13, 67
- Hoffleit, D. & Jaschek, C. . 1991, *The Bright Star Catalogue* (Yale Univ. Observatory, ed. 5, New Haven, USA)
- Isles, J. 1997, *S&T*, 93, 80
- Jetsu, L. & Pelt, J. 1996, *A&AS*, 118, 587
- Jetsu, L. & Pelt, J. 2000, *A&A*, 353, 409
- Kiseleva, L. G., Eggleton, P. P., & Mikkola, S. 1998, *MNRAS*, 300, 292
- Kruger, A. T., Lored, T. J., & Wasserman, I. 2002, *ApJ*, 576, 932
- Lanza, A. F. 2005, *MNRAS*, 364, 238
- Lanza, A. F. 2006, *MNRAS*, 369, 1773
- Leitz, C. 1994, *Tagewählerei* (Wiesbaden, Germany: Ägyptologische Abhandlungen 55, Harrassowitz Verlag)
- Lestrade, J.-F., Phillips, R. B., Hodges, M. W., & Preston, R. A. 1993, *ApJ*, 410, 808
- Liao, W.-P. & Qian, S.-B. 2010, *MNRAS*, 405, 1930
- Lichtheim, M. 1976, *Ancient Egyptian Literature II: The New Kingdom* (Los Angeles, USA: Univ. of California Press)
- Luyten, W. J. 1938, *ZAp*, 15, 97
- Mallama, A. D. 1978, *PASP*, 90, 706
- Merrill, P. W. 1938, *The Nature of Variable Stars* (New York, USA: MacMillan Co.)
- Mikhail, J. S. 1979, *Ap&SS*, 66, 349
- Mikhail, J. S. & Haubold, H. J. 1995, *Ap&SS*, 228, D7
- Neugebauer, O. & Parker, R. 1960, *Egyptian Astronomical Texts I* (London, England: Brown Univ. Press)
- Pavel, F. 1949, *Astronomische Nachrichten*, 278, 57
- Percy, J. R., Desjardins, A., Yu, L., & Landis, H. J. 1996, *PASP*, 108, 139
- Percy, J. R., Ralli, J. A., & Sen, L. V. 1993, *PASP*, 105, 287
- Percy, J. R., Wilson, J. B., & Henry, G. W. 2001, *PASP*, 113, 983
- Perry, C. L., Olsen, E. H., & Crawford, D. L. 1987, *PASP*, 99, 1184
- Perryman, M. A. C. & ESA, eds. 1997, *ESA Special Publication*, Vol. 1200, The HIPPARCOS and TYCHO catalogues. Astrometric and photometric star catalogues derived from the ESA HIPPARCOS Space Astrometry Mission
- Peterson, W. M., Mutel, R. L., Güdel, M., & Goss, W. M. 2010, *Nature*, 463, 207
- Porceddu, S., Jetsu, L., Lyytinen, J., et al. 2012, *Cambridge Archaeol. J.*, to be submitted
- Porceddu, S., Jetsu, L., Markkanen, T., & Toivari-Viitala, J. 2008, *Cambridge Archaeol. J.*, 18:3, 327
- Pustyl'nik, I. 1998, *Astronomical and Astrophysical Transactions*, 15, 357
- Qian, S. 2000, *A&AS*, 146, 377
- Renson, P., Manfroid, J., & Heck, A. 1976, *A&AS*, 23, 413
- Richards, M. T. 1992, *ApJ*, 387, 329
- Richards, M. T. 1993, *ApJS*, 86, 255
- Rudy, R. J. 1979, *MNRAS*, 186, 473
- Sarna, M. J. 1993, *MNRAS*, 262, 534
- Scargle, J. D. 1982, *ApJ*, 263, 835
- Schmidt, H. 1994, *A&AS*, 106, 581
- Soderhjelm, S. 1975, *A&A*, 42, 229
- Soderhjelm, S. 1980, *A&A*, 89, 100
- Stebbins, J. 1920, *ApJ*, 51, 193
- Stephenson, F. R. 1997, *Historical Eclipses and Earth's Rotation* (Cambridge University Press, UK)
- Stephenson, F. R. & Baolin, L. 1991, *The Observatory*, 111, 21
- Tanner, R. W. 1948, *JRASC*, 42, 177
- Turner, D. G. 1999, *JRASC*, 93, 228
- Šimon, V. 1999, *A&AS*, 134, 1
- Zavala, R. T., Hummel, C. A., Boboltz, D. A., et al. 2010, *ApJ*, 715, L44
- Zavala, R. T., McNamara, B. J., Harrison, T. E., et al. 2002, *AJ*, 123, 450

## Acronyms used

EB	=	Eclipsing Binary
MT	=	Mass Transfer
APC	=	Alternate Period Changes
$O - C$	=	Observed (O) minus Calculated (C) eclipse epochs
CC	=	Cairo Calendar
G	=	Good prognosis
S	=	Bad prognosis
SSTP	=	Sample of Series of Time Points
LTTE	=	Light Travel Time Effect
GCVS	=	General Catalogue of Variable Stars
BSC	=	Bright Star Catalogue

## Selected words in ancient Egyptian language

flood season ..	<i>ḥt</i>
winter season	<i>prt</i>
harvest season	<i>šmw</i>
good .....	<i>nfr</i>
bad .....	<i>ḥj</i>
night .....	<i>grh</i>
evening .....	<i>rwhj</i>
hour-watcher .	<i>imy wnw</i>
cosmic order .	<i>mjt</i>
Wedjat .....	<i>wdj</i>
Raging one ...	<i>nsny</i>



**Table 3.** Time points  $t_i$  for all prognoses of Table 1.

$D$	$M$	$N_E$	$X$	Div: Eq. 4			Div: Eq. 5		
				$N_0 = 62$ (days)	$N_0 = 187$ (days)	$N_0 = 307$ (days)	$N_0 = 62$ (days)	$N_0 = 187$ (days)	$N_0 = 307$ (days)
1	1	1	G	0.080	0.095	0.076	0.120	0.142	0.114
1	1	1	G	0.239	0.284	0.227	0.359	0.426	0.341
1	1	1	G	0.399	0.473	0.379	0.739	0.784	0.727
2	1	2	G	1.080	1.095	1.076	1.120	1.142	1.113
2	1	2	G	1.240	1.284	1.227	1.360	1.425	1.340
2	1	2	G	1.400	1.473	1.378	1.740	1.784	1.727
3	1	3	G	2.080	2.094	2.075	2.120	2.142	2.113
3	1	3	G	2.240	2.283	2.226	2.361	2.425	2.340
3	1	3	S	2.401	2.472	2.377	2.740	2.783	2.726
4	1	4	G	3.080	3.094	3.075	3.120	3.142	3.113
4	1	4	G	3.241	3.283	3.226	3.361	3.425	3.339
4	1	4	S	3.401	3.472	3.377	3.741	3.783	3.726
5	1	5	G	4.080	4.094	4.075	4.121	4.142	4.113
5	1	5	G	4.241	4.283	4.225	4.362	4.425	4.338
5	1	5	G	4.402	4.472	4.376	4.741	4.783	4.725
6	1	6	S	5.081	5.094	5.075	5.121	5.141	5.113
6	1	6	S	5.242	5.283	5.225	5.363	5.424	5.338
6	1	6	G	5.403	5.471	5.375	5.742	5.783	5.725
7	1	7	G	6.081	6.094	6.075	6.121	6.141	6.112
7	1	7	G	6.243	6.283	6.225	6.364	6.424	6.337
7	1	7	G	6.404	6.471	6.374	6.743	6.783	6.725
8	1	8	G	7.081	7.094	7.075	7.122	7.141	7.112
8	1	8	G	7.243	7.282	7.224	7.365	7.424	7.336
8	1	8	S	7.405	7.471	7.374	7.743	7.782	7.724
9	1	9	G	8.081	8.094	8.075	8.122	8.141	8.112
9	1	9	G	8.244	8.282	8.224	8.365	8.423	8.336
9	1	9	G	8.406	8.470	8.373	8.744	8.782	8.724
10	1	10	G	9.081	9.094	9.074	9.122	9.141	9.112
10	1	10	G	9.244	9.282	9.223	9.366	9.423	9.335
10	1	10	G	9.407	9.470	9.372	9.744	9.782	9.723
11	1	11	S	10.082	10.094	10.074	10.122	10.141	10.112
11	1	11	S	10.245	10.282	10.223	10.367	10.422	10.335
11	1	11	S	10.408	10.469	10.372	10.745	10.782	10.723
12	1	12	S	11.082	11.094	11.074	11.123	11.141	11.111
12	1	12	S	11.245	11.281	11.223	11.368	11.422	11.334
12	1	12	S	11.409	11.469	11.371	11.745	11.781	11.723
13	1	13	G	12.082	12.094	12.074	12.123	12.141	12.111
13	1	13	S	12.246	12.281	12.222	12.369	12.422	12.333
13	1	13	S	12.410	12.468	12.370	12.746	12.781	12.722
15	1	15	G	14.082	14.093	14.074	14.124	14.140	14.111
15	1	15	S	14.247	14.280	14.222	14.371	14.421	14.332
15	1	15	S	14.412	14.467	14.369	14.747	14.780	14.722
16	1	16	S	15.083	15.093	15.074	15.124	15.140	15.111
16	1	16	S	15.248	15.280	15.221	15.371	15.420	15.332
16	1	16	S	15.413	15.467	15.369	15.748	15.780	15.721
17	1	17	S	16.083	16.093	16.074	16.124	16.140	16.110
17	1	17	S	16.248	16.280	16.221	16.372	16.420	16.331
17	1	17	S	16.414	16.466	16.368	16.748	16.780	16.721
18	1	18	G	17.083	17.093	17.073	17.124	17.140	17.110
18	1	18	G	17.249	17.279	17.220	17.373	17.419	17.331
18	1	18	G	17.414	17.466	17.367	17.749	17.779	17.720
19	1	19	G	18.083	18.093	18.073	18.125	18.140	18.110
19	1	19	G	18.249	18.279	18.220	18.374	18.419	18.330
19	1	19	G	18.415	18.465	18.367	18.749	18.779	18.720
20	1	20	S	19.083	19.093	19.073	19.125	19.139	19.110
20	1	20	S	19.250	19.279	19.220	19.375	19.418	19.330
20	1	20	S	19.416	19.465	19.366	19.750	19.779	19.720
21	1	21	G	20.083	20.093	20.073	20.125	20.139	20.110
21	1	21	G	20.250	20.278	20.220	20.376	20.418	20.329
21	1	21	G	20.417	20.464	20.366	20.750	20.778	20.720
22	1	22	S	21.084	21.093	21.073	21.125	21.139	21.110
22	1	22	S	21.251	21.278	21.219	21.376	21.417	21.329
22	1	22	S	21.418	21.463	21.365	21.751	21.778	21.719
23	1	23	S	22.084	22.093	22.073	22.126	22.139	22.109
23	1	23	S	22.252	22.278	22.219	22.377	22.417	22.328
23	1	23	S	22.419	22.463	22.365	22.752	22.778	22.719
24	1	24	G	23.084	23.092	23.073	23.126	23.139	23.109
24	1	24	G	23.252	23.277	23.219	23.378	23.416	23.328
24	1	24	G	23.420	23.462	23.364	23.752	23.777	23.719
25	1	25	G	24.084	24.092	24.073	24.126	24.138	24.109
25	1	25	G	24.253	24.277	24.218	24.379	24.415	24.328
25	1	25	S	24.421	24.462	24.364	24.753	24.777	24.718
26	1	26	S	25.084	25.092	25.073	25.127	25.138	25.109
26	1	26	S	25.253	25.277	25.218	25.380	25.415	25.327
26	1	26	S	25.422	25.461	25.364	25.753	25.777	25.718
27	1	27	G	26.085	26.092	26.073	26.127	26.138	26.109
27	1	27	G	26.254	26.276	26.218	26.381	26.414	26.327
27	1	27	G	26.423	26.460	26.363	26.754	26.776	26.718
28	1	28	G	27.085	27.092	27.073	27.127	27.138	27.109
28	1	28	G	27.254	27.276	27.218	27.381	27.414	27.326
28	1	28	G	27.424	27.460	27.363	27.754	27.776	27.718
29	1	29	S	28.085	28.092	28.072	28.127	28.138	28.109
29	1	29	G	28.255	28.275	28.217	28.382	28.413	28.326
29	1	29	G	28.425	28.459	28.362	28.755	28.775	28.717
30	1	30	G	29.085	29.092	29.072	29.128	29.137	29.109
30	1	30	G	29.255	29.275	29.217	29.383	29.412	29.326
30	1	30	G	29.426	29.458	29.362	29.755	29.775	29.717

<i>D</i>	<i>M</i>	<i>N<sub>E</sub></i>	<i>X</i>	Div: Eq. 4			Div: Eq. 5		
				<i>N<sub>0</sub></i> = 62 (days)	<i>N<sub>0</sub></i> = 187 (days)	<i>N<sub>0</sub></i> = 307 (days)	<i>N<sub>0</sub></i> = 62 (days)	<i>N<sub>0</sub></i> = 187 (days)	<i>N<sub>0</sub></i> = 307 (days)
1	2	31	G	30.085	30.091	30.072	30.128	30.137	30.108
1	2	31	G	30.256	30.274	30.217	30.384	30.412	30.325
1	2	31	G	30.427	30.457	30.362	30.756	30.774	30.717
2	2	32	G	31.086	31.091	31.072	31.128	31.137	31.108
2	2	32	G	31.257	31.274	31.217	31.385	31.411	31.325
2	2	32	G	31.428	31.457	31.361	31.757	31.774	31.717
3	2	33	G	32.086	32.091	32.072	32.129	32.137	32.108
3	2	33	G	32.257	32.274	32.217	32.386	32.410	32.325
3	2	33	G	32.429	32.456	32.361	32.757	32.774	32.717
4	2	34	S	33.086	33.091	33.072	33.129	33.137	33.108
4	2	34	G	33.258	33.273	33.216	33.386	33.410	33.325
4	2	34	S	33.429	33.455	33.361	33.758	33.773	33.716
5	2	35	S	34.086	34.091	34.072	34.129	34.136	34.108
5	2	35	S	34.258	34.273	34.216	34.387	34.409	34.324
5	2	35	S	34.430	34.454	34.360	34.758	34.773	34.716
6	2	36	G	35.086	35.091	35.072	35.129	35.136	35.108
6	2	36	G	35.259	35.272	35.216	35.388	35.408	35.324
6	2	36	G	35.431	35.454	35.360	35.759	35.772	35.716
7	2	37	S	36.086	36.091	36.072	36.130	36.136	36.108
7	2	37	S	36.259	36.272	36.216	36.389	36.408	36.324
7	2	37	S	36.432	36.453	36.360	36.759	36.772	36.716
8	2	38	G	37.087	37.090	37.072	37.130	37.136	37.108
8	2	38	G	37.260	37.271	37.216	37.390	37.407	37.324
8	2	38	G	37.433	37.452	37.360	37.760	37.771	37.716
9	2	39	G	38.087	38.090	38.072	38.130	38.135	38.108
9	2	39	G	38.260	38.271	38.216	38.391	38.406	38.323
9	2	39	G	38.434	38.451	38.359	38.760	38.771	38.716
10	2	40	G	39.087	39.090	39.072	39.130	39.135	39.108
10	2	40	G	39.261	39.270	39.216	39.391	39.406	39.323
10	2	40	G	39.435	39.451	39.359	39.761	39.770	39.716
11	2	41	G	40.087	40.090	40.072	40.131	40.135	40.108
11	2	41	G	40.261	40.270	40.215	40.392	40.405	40.323
11	2	41	G	40.436	40.450	40.359	40.761	40.770	40.715
12	2	42	S	41.087	41.090	41.072	41.131	41.135	41.108
12	2	42	S	41.262	41.269	41.215	41.393	41.404	41.323
12	2	42	S	41.437	41.449	41.359	41.762	41.769	41.715
13	2	43	G	42.088	42.090	42.072	42.131	42.134	42.108
13	2	43	G	42.263	42.269	42.215	42.394	42.403	42.323
13	2	43	G	42.438	42.448	42.359	42.763	42.769	42.715
14	2	44	G	43.088	43.089	43.072	43.132	43.134	43.108
14	2	44	G	43.263	43.268	43.215	43.395	43.403	43.323
14	2	44	G	43.439	43.447	43.359	43.763	43.768	43.715
15	2	45	G	44.088	44.089	44.072	44.132	44.134	44.108
15	2	45	S	44.264	44.268	44.215	44.395	44.402	44.323
15	2	45	S	44.439	44.446	44.359	44.764	44.768	44.715
16	2	46	G	45.088	45.089	45.072	45.132	45.134	45.108
16	2	46	G	45.264	45.267	45.215	45.396	45.401	45.323
16	2	46	G	45.440	45.446	45.358	45.764	45.767	45.715
17	2	47	G	46.088	46.089	46.072	46.132	46.133	46.108
17	2	47	G	46.265	46.267	46.215	46.397	46.400	46.323
17	2	47	G	46.441	46.445	46.358	46.765	46.767	46.715
18	2	48	S	47.088	47.089	47.072	47.133	47.133	47.108
18	2	48	S	47.265	47.266	47.215	47.398	47.400	47.323
18	2	48	S	47.442	47.444	47.358	47.765	47.766	47.715
19	2	49	G	48.089	48.089	48.072	48.133	48.133	48.108
19	2	49	G	48.266	48.266	48.215	48.399	48.399	48.323
19	2	49	G	48.443	48.443	48.358	48.766	48.766	48.715
20	2	50	S	49.089	49.088	49.072	49.133	49.133	49.108
20	2	50	S	49.266	49.265	49.215	49.399	49.398	49.323
20	2	50	S	49.444	49.442	49.358	49.766	49.765	49.715
21	2	51	S	50.089	50.088	50.072	50.133	50.132	50.108
21	2	51	S	50.267	50.265	50.215	50.400	50.397	50.323
21	2	51	G	50.445	50.441	50.358	50.767	50.765	50.715
24	2	54	S	53.089	53.088	53.072	53.134	53.132	53.108
24	2	54	S	53.268	53.263	53.215	53.402	53.395	53.323
24	2	54	S	53.447	53.439	53.359	53.768	53.763	53.715
25	2	55	S	54.090	54.088	54.072	54.134	54.131	54.108
25	2	55	S	54.269	54.263	54.215	54.403	54.394	54.323
25	2	55	S	54.448	54.438	54.359	54.769	54.763	54.715
26	2	56	S	55.090	55.087	55.072	55.135	55.131	55.108
26	2	56	S	55.269	55.262	55.215	55.404	55.393	55.323
26	2	56	S	55.449	55.437	55.359	55.769	55.762	55.715
27	2	57	S	56.090	56.087	56.072	56.135	56.131	56.108
27	2	57	S	56.270	56.262	56.215	56.405	56.392	56.323
27	2	57	S	56.450	56.436	56.359	56.770	56.762	56.715
28	2	58	G	57.090	57.087	57.072	57.135	57.131	57.108
28	2	58	G	57.270	57.261	57.215	57.405	57.392	57.323
28	2	58	G	57.450	57.435	57.359	57.770	57.761	57.715
29	2	59	G	58.090	58.087	58.072	58.135	58.130	58.108
29	2	59	G	58.271	58.261	58.216	58.406	58.391	58.323
29	2	59	G	58.451	58.434	58.359	58.771	58.761	58.716
30	2	60	G	59.090	59.087	59.072	59.136	59.130	59.108
30	2	60	G	59.271	59.260	59.216	59.407	59.390	59.324
30	2	60	G	59.452	59.433	59.360	59.771	59.760	59.716

<i>D</i>	<i>M</i>	<i>N<sub>E</sub></i>	<i>X</i>	Div: Eq. 4			Div: Eq. 5		
				<i>N<sub>0</sub></i> = 62 (days)	<i>N<sub>0</sub></i> = 187 (days)	<i>N<sub>0</sub></i> = 307 (days)	<i>N<sub>0</sub></i> = 62 (days)	<i>N<sub>0</sub></i> = 187 (days)	<i>N<sub>0</sub></i> = 307 (days)
1	3	61	G	60.091	60.086	60.072	60.136	60.130	60.108
1	3	61	G	60.272	60.259	60.216	60.407	60.389	60.324
1	3	61	G	60.453	60.432	60.360	60.772	60.759	60.716
3	3	63	G	62.091	62.086	62.072	62.136	62.129	62.108
3	3	63	G	62.273	62.258	62.216	62.409	62.388	62.324
3	3	63	G	62.454	62.431	62.360	62.773	62.758	62.716
6	3	66	G	65.091	65.086	65.072	65.137	65.128	65.108
6	3	66	G	65.274	65.257	65.217	65.411	65.385	65.325
6	3	66	G	65.457	65.428	65.361	65.774	65.757	65.717
7	3	67	G	66.091	66.085	66.072	66.137	66.128	66.108
7	3	67	G	66.274	66.256	66.217	66.412	66.384	66.325
7	3	67	G	66.457	66.427	66.361	66.774	66.756	66.717
9	3	69	S	68.092	68.085	68.072	68.138	68.128	68.109
9	3	69	S	68.275	68.255	68.217	68.413	68.383	68.326
9	3	69	S	68.459	68.425	68.362	68.775	68.755	68.717
10	3	70	G	69.092	69.085	69.073	69.138	69.127	69.109
10	3	70	G	69.276	69.254	69.218	69.413	69.382	69.326
10	3	70	G	69.459	69.424	69.363	69.776	69.754	69.718
11	3	71	G	70.092	70.085	70.073	70.138	70.127	70.109
11	3	71	G	70.276	70.254	70.218	70.414	70.381	70.327
11	3	71	G	70.460	70.423	70.363	70.776	70.754	70.718
13	3	73	S	72.092	72.084	72.073	72.138	72.126	72.109
13	3	73	S	72.277	72.253	72.218	72.415	72.379	72.327
13	3	73	S	72.461	72.421	72.364	72.777	72.753	72.718
14	3	74	S	73.092	73.084	73.073	73.139	73.126	73.109
14	3	74	S	73.277	73.252	73.219	73.416	73.378	73.328
14	3	74	S	73.462	73.420	73.364	73.777	73.752	73.719
15	3	75	S	74.093	74.084	74.073	74.139	74.126	74.109
15	3	75	S	74.278	74.252	74.219	74.416	74.377	74.328
15	3	75	S	74.463	74.419	74.365	74.778	74.752	74.719
16	3	76	G	75.093	75.084	75.073	75.139	75.126	75.110
16	3	76	G	75.278	75.251	75.219	75.417	75.377	75.329
16	3	76	G	75.463	75.418	75.365	75.778	75.751	75.719
18	3	78	S	77.093	77.083	77.073	77.139	77.125	77.110
18	3	78	S	77.279	77.250	77.220	77.418	77.375	77.330
18	3	78	S	77.464	77.417	77.366	77.779	77.750	77.720
19	3	79	S	78.093	78.083	78.073	78.140	78.125	78.110
19	3	79	S	78.279	78.249	78.220	78.419	78.374	78.330
19	3	79	S	78.465	78.416	78.367	78.779	78.749	78.720
20	3	80	S	79.093	79.083	79.073	79.140	79.124	79.110
20	3	80	S	79.279	79.249	79.220	79.419	79.373	79.331
20	3	80	S	79.466	79.415	79.367	79.779	79.749	79.720
21	3	81	G	80.093	80.083	80.074	80.140	80.124	80.110
21	3	81	G	80.280	80.248	80.221	80.420	80.372	80.331
21	3	81	G	80.466	80.414	80.368	80.780	80.748	80.721
23	3	83	S	82.093	82.082	82.074	82.140	82.124	82.111
23	3	83	S	82.280	82.247	82.221	82.421	82.371	82.332
23	3	83	S	82.467	82.412	82.369	82.780	82.747	82.721
24	3	84	G	83.094	83.082	83.074	83.140	83.123	83.111
24	3	84	G	83.281	83.247	83.222	83.421	83.370	83.333
24	3	84	G	83.468	83.411	83.370	83.781	83.747	83.722
25	3	85	G	84.094	84.082	84.074	84.140	84.123	84.111
25	3	85	G	84.281	84.246	84.222	84.421	84.369	84.333
25	3	85	G	84.468	84.410	84.370	84.781	84.746	84.722
26	3	86	G	85.094	85.082	85.074	85.141	85.123	85.111
26	3	86	G	85.281	85.245	85.223	85.422	85.368	85.334
26	3	86	G	85.469	85.409	85.371	85.781	85.745	85.723
27	3	87	G	86.094	86.082	86.074	86.141	86.122	86.111
27	3	87	G	86.282	86.245	86.223	86.422	86.367	86.334
27	3	87	G	86.469	86.408	86.372	86.782	86.745	86.723
28	3	88	G	87.094	87.081	87.074	87.141	87.122	87.112
28	3	88	G	87.282	87.244	87.223	87.423	87.367	87.335
28	3	88	G	87.470	87.407	87.372	87.782	87.744	87.723
29	3	89	G	88.094	88.081	88.075	88.141	88.122	88.112
29	3	89	G	88.282	88.244	88.224	88.423	88.366	88.336
29	3	89	G	88.470	88.406	88.373	88.782	88.744	88.724
30	3	90	G	89.094	89.081	89.075	89.141	89.122	89.112
30	3	90	G	89.282	89.243	89.224	89.423	89.365	89.336
30	3	90	G	89.470	89.405	89.374	89.782	89.743	89.724

$D$	$M$	$N_E$	$X$	Div: Eq. 4			Div: Eq. 5		
				$N_0 = 62$ (days)	$N_0 = 187$ (days)	$N_0 = 307$ (days)	$N_0 = 62$ (days)	$N_0 = 187$ (days)	$N_0 = 307$ (days)
1	4	91	G	90.094	90.081	90.075	90.141	90.121	90.112
1	4	91	G	90.283	90.243	90.225	90.424	90.364	90.337
1	4	91	G	90.471	90.404	90.374	90.783	90.743	90.725
2	4	92	G	91.094	91.081	91.075	91.141	91.121	91.112
2	4	92	G	91.283	91.242	91.225	91.424	91.363	91.337
2	4	92	G	91.471	91.404	91.375	91.783	91.742	91.725
3	4	93	S	92.094	92.081	92.075	92.141	92.121	92.113
3	4	93	S	92.283	92.242	92.225	92.424	92.362	92.338
3	4	93	S	92.472	92.403	92.376	92.783	92.742	92.725
4	4	94	G	93.094	93.080	93.075	93.142	93.121	93.113
4	4	94	G	93.283	93.241	93.226	93.425	93.362	93.339
4	4	94	G	93.472	93.402	93.376	93.783	93.741	93.726
5	4	95	G	94.094	94.080	94.075	94.142	94.120	94.113
5	4	95	G	94.283	94.240	94.226	94.425	94.361	94.339
5	4	95	G	94.472	94.401	94.377	94.783	94.740	94.726
6	4	96	S	95.095	95.080	95.076	95.142	95.120	95.113
6	4	96	S	95.284	95.240	95.227	95.425	95.360	95.340
6	4	96	S	95.473	95.400	95.378	95.784	95.740	95.727
7	4	97	S	96.095	96.080	96.076	96.142	96.120	96.114
7	4	97	S	96.284	96.239	96.227	96.426	96.359	96.341
7	4	97	S	96.473	96.399	96.379	96.784	96.739	96.727
8	4	98	G	97.095	97.080	97.076	97.142	97.119	97.114
8	4	98	G	97.284	97.239	97.228	97.426	97.358	97.341
8	4	98	G	97.473	97.398	97.379	97.784	97.739	97.728
9	4	99	G	98.095	98.079	98.076	98.142	98.119	98.114
9	4	99	G	98.284	98.238	98.228	98.426	98.357	98.342
9	4	99	G	98.473	98.397	98.380	98.784	98.738	98.728
10	4	100	G	99.095	99.079	99.076	99.142	99.119	99.114
10	4	100	G	99.284	99.238	99.229	99.426	99.357	99.343
10	4	100	G	99.474	99.396	99.381	99.784	99.738	99.729
11	4	101	G	100.095	100.079	100.076	100.142	100.119	100.114
11	4	101	G	100.284	100.237	100.229	100.426	100.356	100.343
11	4	101	G	100.474	100.395	100.382	100.784	100.737	100.729
12	4	102	S	101.095	101.079	101.076	101.142	101.118	101.115
12	4	102	S	101.284	101.237	101.229	101.427	101.355	101.344
12	4	102	S	101.474	101.394	101.382	101.784	101.737	101.729
13	4	103	G	102.095	102.079	102.077	102.142	102.118	102.115
13	4	103	G	102.285	102.236	102.230	102.427	102.354	102.345
13	4	103	G	102.474	102.394	102.383	102.785	102.736	102.730
14	4	104	G	103.095	103.079	103.077	103.142	103.118	103.115
14	4	104	G	103.285	103.236	103.230	103.427	103.353	103.346
14	4	104	G	103.474	103.393	103.384	103.785	103.736	103.730
16	4	106	G	105.095	105.078	105.077	105.142	105.117	105.116
16	4	106	G	105.285	105.235	105.231	105.427	105.352	105.347
16	4	106	G	105.475	105.391	105.386	105.785	105.735	105.731
18	4	108	S	107.095	107.078	107.077	107.142	107.117	107.116
18	4	108	S	107.285	107.234	107.232	107.427	107.350	107.349
18	4	108	S	107.475	107.389	107.387	107.785	107.734	107.732
19	4	109	S	108.095	108.078	108.078	108.142	108.117	108.116
19	4	109	S	108.285	108.233	108.233	108.427	108.350	108.349
19	4	109	S	108.475	108.388	108.388	108.785	108.733	108.733
20	4	110	S	109.095	109.078	109.078	109.142	109.116	109.117
20	4	110	S	109.285	109.233	109.233	109.427	109.349	109.350
20	4	110	S	109.475	109.388	109.389	109.785	109.733	109.733
21	4	111	S	110.095	110.077	110.078	110.142	110.116	110.117
21	4	111	S	110.285	110.232	110.234	110.427	110.348	110.351
21	4	111	G	110.475	110.387	110.390	110.785	110.732	110.734
22	4	112	G	111.095	111.077	111.078	111.142	111.116	111.117
22	4	112	G	111.285	111.232	111.234	111.427	111.347	111.352
22	4	112	G	111.475	111.386	111.391	111.785	111.732	111.734
23	4	113	G	112.095	112.077	112.078	112.142	112.116	112.117
23	4	113	G	112.285	112.231	112.235	112.427	112.347	112.352
23	4	113	S	112.475	112.385	112.392	112.785	112.731	112.735
26	4	116	G	115.095	115.077	115.079	115.142	115.115	115.118
26	4	116	G	115.285	115.230	115.237	115.427	115.344	115.355
26	4	116	G	115.475	115.383	115.394	115.785	115.730	115.737
27	4	117	G	116.095	116.076	116.079	116.142	116.115	116.119
27	4	117	G	116.285	116.229	116.237	116.427	116.344	116.356
27	4	117	S	116.475	116.382	116.395	116.785	116.729	116.737
28	4	118	S	117.095	117.076	117.079	117.142	117.114	117.119
28	4	118	S	117.285	117.229	117.238	117.427	117.343	117.356
28	4	118	S	117.475	117.381	117.396	117.785	117.729	117.738
29	4	119	S	118.095	118.076	118.079	118.142	118.114	118.119
29	4	119	S	118.285	118.228	118.238	118.427	118.342	118.357
29	4	119	S	118.474	118.380	118.397	118.785	118.728	118.738
30	4	120	G	119.095	119.076	119.080	119.142	119.114	119.119
30	4	120	G	119.285	119.228	119.239	119.427	119.342	119.358
30	4	120	G	119.474	119.380	119.398	119.785	119.728	119.739

<i>D</i>	<i>M</i>	<i>N<sub>E</sub></i>	<i>X</i>	Div: Eq. 4			Div: Eq. 5		
				<i>N<sub>0</sub></i> = 62 (days)	<i>N<sub>0</sub></i> = 187 (days)	<i>N<sub>0</sub></i> = 307 (days)	<i>N<sub>0</sub></i> = 62 (days)	<i>N<sub>0</sub></i> = 187 (days)	<i>N<sub>0</sub></i> = 307 (days)
1	5	121	G	120.095	120.076	120.080	120.142	120.114	120.120
1	5	121	G	120.284	120.227	120.239	120.427	120.341	120.359
1	5	121	G	120.474	120.379	120.399	120.784	120.727	120.739
2	5	122	G	121.095	121.076	121.080	121.142	121.113	121.120
2	5	122	G	121.284	121.227	121.240	121.427	121.340	121.360
2	5	122	G	121.474	121.378	121.400	121.784	121.727	121.740
3	5	123	G	122.095	122.075	122.080	122.142	122.113	122.120
3	5	123	G	122.284	122.226	122.240	122.426	122.340	122.361
3	5	123	G	122.474	122.377	122.401	122.784	122.726	122.740
4	5	124	G	123.095	123.075	123.080	123.142	123.113	123.120
4	5	124	G	123.284	123.226	123.241	123.426	123.339	123.361
4	5	124	G	123.473	123.377	123.401	123.784	123.726	123.741
5	5	125	G	124.095	124.075	124.080	124.142	124.113	124.121
5	5	125	S	124.284	124.225	124.241	124.426	124.338	124.362
5	5	125	S	124.473	124.376	124.402	124.784	124.725	124.741
6	5	126	G	125.095	125.075	125.081	125.142	125.113	125.121
6	5	126	G	125.284	125.225	125.242	125.426	125.338	125.363
6	5	126	G	125.473	125.375	125.403	125.784	125.725	125.742
7	5	127	S	126.095	126.075	126.081	126.142	126.112	126.121
7	5	127	S	126.284	126.225	126.243	126.425	126.337	126.364
7	5	127	S	126.473	126.374	126.404	126.784	126.725	126.743
8	5	128	G	127.094	127.075	127.081	127.142	127.112	127.122
8	5	128	G	127.283	127.224	127.243	127.425	127.336	127.365
8	5	128	G	127.472	127.374	127.405	127.783	127.724	127.743
9	5	129	G	128.094	128.075	128.081	128.142	128.112	128.122
9	5	129	G	128.283	128.224	128.244	128.425	128.336	128.365
9	5	129	G	128.472	128.373	128.406	128.783	128.724	128.744
10	5	130	S	129.094	129.074	129.081	129.142	129.112	129.122
10	5	130	S	129.283	129.223	129.244	129.425	129.335	129.366
10	5	130	S	129.472	129.372	129.407	129.783	129.723	129.744
11	5	131	S	130.094	130.074	130.082	130.141	130.112	130.122
11	5	131	S	130.283	130.223	130.245	130.424	130.335	130.367
11	5	131	S	130.471	130.372	130.408	130.783	130.723	130.745
13	5	133	G	132.094	132.074	132.082	132.141	132.111	132.123
13	5	133	G	132.282	132.222	132.246	132.424	132.333	132.369
13	5	133	G	132.471	132.370	132.410	132.782	132.722	132.746
14	5	134	S	133.094	133.074	133.082	133.141	133.111	133.123
14	5	134	S	133.282	133.222	133.246	133.423	133.333	133.370
14	5	134	S	133.470	133.370	133.411	133.782	133.722	133.746
15	5	135	G	134.094	134.074	134.082	134.141	134.111	134.124
15	5	135	G	134.282	134.222	134.247	134.423	134.332	134.371
15	5	135	G	134.470	134.369	134.412	134.782	134.722	134.747
16	5	136	G	135.094	135.074	135.083	135.141	135.111	135.124
16	5	136	G	135.282	135.221	135.248	135.422	135.332	135.371
16	5	136	G	135.469	135.369	135.413	135.782	135.721	135.748
17	5	137	S	136.094	136.074	136.083	136.141	136.110	136.124
17	5	137	S	136.281	136.221	136.248	136.422	136.331	136.372
17	5	137	S	136.469	136.368	136.414	136.781	136.721	136.748
18	5	138	G	137.094	137.073	137.083	137.141	137.110	137.124
18	5	138	G	137.281	137.220	137.249	137.422	137.331	137.373
18	5	138	G	137.468	137.367	137.414	137.781	137.720	137.749
19	5	139	S	138.094	138.073	138.083	138.140	138.110	138.125
19	5	139	S	138.281	138.220	138.249	138.421	138.330	138.374
19	5	139	S	138.468	138.367	138.415	138.781	138.720	138.749
20	5	140	S	139.093	139.073	139.083	139.140	139.110	139.125
20	5	140	S	139.280	139.220	139.250	139.421	139.330	139.375
20	5	140	S	139.467	139.366	139.416	139.780	139.720	139.750
21	5	141	G	140.093	140.073	140.083	140.140	140.110	140.125
21	5	141	G	140.280	140.220	140.250	140.420	140.329	140.376
21	5	141	G	140.467	140.366	140.417	140.780	140.720	140.750
22	5	142	G	141.093	141.073	141.084	141.140	141.110	141.125
22	5	142	G	141.280	141.219	141.251	141.420	141.329	141.376
22	5	142	G	141.466	141.365	141.418	141.780	141.719	141.751
23	5	143	G	142.093	142.073	142.084	142.140	142.109	142.126
23	5	143	G	142.279	142.219	142.252	142.419	142.328	142.377
23	5	143	G	142.466	142.365	142.419	142.779	142.719	142.752
24	5	144	G	143.093	143.073	143.084	143.140	143.109	143.126
24	5	144	G	143.279	143.219	143.252	143.419	143.328	143.378
24	5	144	G	143.465	143.364	143.420	143.779	143.719	143.752
25	5	145	G	144.093	144.073	144.084	144.139	144.109	144.126
25	5	145	G	144.279	144.218	144.253	144.418	144.328	144.379
25	5	145	G	144.465	144.364	144.421	144.779	144.718	144.753
26	5	146	S	145.093	145.073	145.084	145.139	145.109	145.127
26	5	146	S	145.278	145.218	145.253	145.418	145.327	145.380
26	5	146	S	145.464	145.364	145.422	145.778	145.718	145.753
27	5	147	G	146.093	146.073	146.085	146.139	146.109	146.127
27	5	147	G	146.278	146.218	146.254	146.417	146.327	146.381
27	5	147	G	146.463	146.363	146.423	146.778	146.718	146.754
28	5	148	G	147.093	147.073	147.085	147.139	147.109	147.127
28	5	148	G	147.278	147.218	147.254	147.417	147.326	147.381
28	5	148	G	147.463	147.363	147.424	147.778	147.718	147.754
29	5	149	G	148.092	148.072	148.085	148.139	148.109	148.127
29	5	149	G	148.277	148.217	148.255	148.416	148.326	148.382
29	5	149	G	148.462	148.362	148.425	148.777	148.717	148.755
30	5	150	G	149.092	149.072	149.085	149.138	149.109	149.128
30	5	150	G	149.277	149.217	149.255	149.415	149.326	149.383
30	5	150	G	149.462	149.362	149.426	149.777	149.717	149.755

<i>D</i>	<i>M</i>	<i>N<sub>E</sub></i>	<i>X</i>	Div: Eq. 4			Div: Eq. 5		
				<i>N<sub>0</sub></i> = 62 (days)	<i>N<sub>0</sub></i> = 187 (days)	<i>N<sub>0</sub></i> = 307 (days)	<i>N<sub>0</sub></i> = 62 (days)	<i>N<sub>0</sub></i> = 187 (days)	<i>N<sub>0</sub></i> = 307 (days)
1	6	151	G	150.092	150.072	150.085	150.138	150.108	150.128
1	6	151	G	150.277	150.217	150.256	150.415	150.325	150.384
1	6	151	G	150.461	150.362	150.427	150.777	150.717	150.756
2	6	152	G	151.092	151.072	151.086	151.138	151.108	151.128
2	6	152	G	151.276	151.217	151.257	151.414	151.325	151.385
2	6	152	G	151.460	151.361	151.428	151.776	151.717	151.757
4	6	154	G	153.092	153.072	153.086	153.138	153.108	153.129
4	6	154	G	153.275	153.216	153.258	153.413	153.325	153.386
4	6	154	G	153.459	153.361	153.429	153.775	153.716	153.758
5	6	155	G	154.092	154.072	154.086	154.137	154.108	154.129
5	6	155	G	154.275	154.216	154.258	154.412	154.324	154.387
5	6	155	G	154.458	154.360	154.430	154.775	154.716	154.758
7	6	157	G	156.091	156.072	156.086	156.137	156.108	156.130
7	6	157	G	156.274	156.216	156.259	156.411	156.324	156.389
7	6	157	G	156.457	156.360	156.432	156.774	156.716	156.759
8	6	158	G	157.091	157.072	157.087	157.137	157.108	157.130
8	6	158	G	157.274	157.216	157.260	157.410	157.324	157.390
8	6	158	G	157.456	157.360	157.433	157.774	157.716	157.760
9	6	159	G	158.091	158.072	158.087	158.137	158.108	158.130
9	6	159	G	158.273	158.216	158.260	158.410	158.323	158.391
9	6	159	G	158.455	158.359	158.434	158.773	158.716	158.760
10	6	160	S	159.091	159.072	159.087	159.136	159.108	159.130
10	6	160	S	159.273	159.216	159.261	159.409	159.323	159.391
10	6	160	S	159.454	159.359	159.435	159.773	159.716	159.761
11	6	161	G	160.091	160.072	160.087	160.136	160.108	160.131
11	6	161	G	160.272	160.215	160.261	160.408	160.323	160.392
11	6	161	G	160.454	160.359	160.436	160.772	160.715	160.761
12	6	162	G	161.091	161.072	161.087	161.136	161.108	161.131
12	6	162	G	161.272	161.215	161.262	161.408	161.323	161.393
12	6	162	G	161.453	161.359	161.437	161.772	161.715	161.762
13	6	163	S	162.090	162.072	162.088	162.136	162.108	162.131
13	6	163	S	162.271	162.215	162.263	162.407	162.323	162.394
13	6	163	S	162.452	162.359	162.438	162.771	162.715	162.763
14	6	164	S	163.090	163.072	163.088	163.135	163.108	163.132
14	6	164	G	163.271	163.215	163.263	163.406	163.323	163.395
14	6	164	G	163.451	163.359	163.439	163.771	163.715	163.763
17	6	167	G	166.090	166.072	166.088	166.135	166.108	166.132
17	6	167	G	166.269	166.215	166.265	166.404	166.323	166.397
17	6	167	G	166.449	166.358	166.441	166.769	166.715	166.765
18	6	168	S	167.090	167.072	167.088	167.134	167.108	167.133
18	6	168	S	167.269	167.215	167.265	167.403	167.323	167.398
18	6	168	S	167.448	167.358	167.442	167.769	167.715	167.765
19	6	169	G	168.089	168.072	168.089	168.134	168.108	168.133
19	6	169	S	168.268	168.215	168.266	168.403	168.323	168.399
19	6	169	S	168.447	168.358	168.443	168.768	168.715	168.766
20	6	170	S	169.089	169.072	169.089	169.134	169.108	169.133
20	6	170	S	169.268	169.215	169.266	169.402	169.323	169.399
20	6	170	S	169.446	169.358	169.444	169.768	169.715	169.766
22	6	172	G	171.089	171.072	171.089	171.133	171.108	171.134
22	6	172	G	171.267	171.215	171.267	171.400	171.323	171.401
22	6	172	G	171.445	171.358	171.445	171.767	171.715	171.767
23	6	173	G	172.089	172.072	172.089	172.133	172.108	172.134
23	6	173	G	172.266	172.215	172.268	172.400	172.323	172.402
23	6	173	G	172.444	172.359	172.446	172.766	172.715	172.768
24	6	174	S	173.089	173.072	173.089	173.133	173.108	173.134
24	6	174	S	173.266	173.215	173.268	173.399	173.323	173.402
24	6	174	S	173.443	173.359	173.447	173.766	173.715	173.768
25	6	175	G	174.088	174.072	174.090	174.133	174.108	174.134
25	6	175	G	174.265	174.215	174.269	174.398	174.323	174.403
25	6	175	G	174.442	174.359	174.448	174.765	174.715	174.769
28	6	178	G	177.088	177.072	177.090	177.132	177.108	177.135
28	6	178	G	177.264	177.215	177.270	177.396	177.323	177.405
28	6	178	G	177.440	177.359	177.450	177.764	177.715	177.770
29	6	179	S	178.088	178.072	178.090	178.132	178.108	178.135
29	6	179	S	178.263	178.216	178.271	178.395	178.323	178.406
29	6	179	S	178.439	178.359	178.451	178.763	178.716	178.771
30	6	180	S	179.088	179.072	179.090	179.131	179.108	179.136
30	6	180	S	179.263	179.216	179.271	179.394	179.324	179.407
30	6	180	S	179.438	179.360	179.452	179.763	179.716	179.771

<i>D</i>	<i>M</i>	<i>N<sub>E</sub></i>	<i>X</i>	Div: Eq. 4			Div: Eq. 5		
				<i>N<sub>0</sub></i> = 62 (days)	<i>N<sub>0</sub></i> = 187 (days)	<i>N<sub>0</sub></i> = 307 (days)	<i>N<sub>0</sub></i> = 62 (days)	<i>N<sub>0</sub></i> = 187 (days)	<i>N<sub>0</sub></i> = 307 (days)
1	7	181	G	180.087	180.072	180.091	180.131	180.108	180.136
1	7	181	G	180.262	180.216	180.272	180.393	180.324	180.407
1	7	181	G	180.437	180.360	180.453	180.762	180.716	180.772
2	7	182	G	181.087	181.072	181.091	181.131	181.108	181.136
2	7	182	G	181.262	181.216	181.272	181.392	181.324	181.408
2	7	182	G	181.436	181.360	181.454	181.762	181.716	181.772
4	7	184	G	183.087	183.072	183.091	183.130	183.108	183.137
4	7	184	S	183.261	183.216	183.273	183.391	183.324	183.410
4	7	184	S	183.434	183.361	183.455	183.761	183.716	183.773
5	7	185	G	184.087	184.072	184.091	184.130	184.108	184.137
5	7	185	G	184.260	184.217	184.273	184.390	184.325	184.410
5	7	185	G	184.433	184.361	184.456	184.760	184.717	184.773
6	7	186	G	185.086	185.072	185.091	185.130	185.108	185.137
6	7	186	G	185.259	185.217	185.274	185.389	185.325	185.411
6	7	186	G	185.432	185.361	185.457	185.759	185.717	185.774
7	7	187	S	186.086	186.072	186.091	186.129	186.108	186.137
7	7	187	S	186.259	186.217	186.274	186.388	186.325	186.412
7	7	187	S	186.432	186.361	186.457	186.759	186.717	186.774
8	7	188	G	187.086	187.072	187.092	187.129	187.109	187.137
8	7	188	G	187.258	187.217	187.275	187.388	187.326	187.412
8	7	188	G	187.431	187.362	187.458	187.758	187.717	187.775
9	7	189	G	188.086	188.072	188.092	188.129	188.109	188.138
9	7	189	G	188.258	188.217	188.275	188.387	188.326	188.413
9	7	189	G	188.430	188.362	188.459	188.758	188.717	188.775
10	7	190	S	189.086	189.073	189.092	189.129	189.109	189.138
10	7	190	S	189.257	189.218	189.276	189.386	189.326	189.413
10	7	190	S	189.429	189.363	189.459	189.757	189.718	189.776
11	7	191	G	190.086	190.073	190.092	190.128	190.109	190.138
11	7	191	G	190.257	190.218	190.276	190.385	190.327	190.414
11	7	191	G	190.428	190.363	190.460	190.757	190.718	190.776
12	7	192	G	191.085	191.073	191.092	191.128	191.109	191.138
12	7	192	G	191.256	191.218	191.276	191.384	191.327	191.415
12	7	192	G	191.427	191.363	191.461	191.756	191.718	191.776
13	7	193	G	192.085	192.073	192.092	192.128	192.109	192.138
13	7	193	G	192.256	192.218	192.277	192.383	192.327	192.415
13	7	193	G	192.426	192.364	192.461	192.756	192.718	192.777
15	7	195	S	194.085	194.073	194.093	194.127	194.109	194.139
15	7	195	S	194.254	194.219	194.278	194.382	194.328	194.416
15	7	195	S	194.424	194.365	194.463	194.754	194.719	194.778
16	7	196	S	195.085	195.073	195.093	195.127	195.110	195.139
16	7	196	S	195.254	195.219	195.278	195.381	195.329	195.417
16	7	196	S	195.423	195.365	195.463	195.754	195.719	195.778
17	7	197	S	196.084	196.073	196.093	196.127	196.110	196.139
17	7	197	S	196.253	196.219	196.278	196.380	196.329	196.418
17	7	197	S	196.422	196.366	196.464	196.753	196.719	196.778
18	7	198	G	197.084	197.073	197.093	197.126	197.110	197.139
18	7	198	G	197.253	197.220	197.279	197.379	197.330	197.418
18	7	198	G	197.421	197.366	197.464	197.753	197.720	197.779
20	7	200	S	199.084	199.073	199.093	199.126	199.110	199.140
20	7	200	S	199.252	199.220	199.279	199.377	199.331	199.419
20	7	200	S	199.419	199.367	199.466	199.752	199.720	199.779
22	7	202	S	201.084	201.074	201.093	201.125	201.111	201.140
22	7	202	S	201.251	201.221	201.280	201.376	201.332	201.420
22	7	202	S	201.418	201.368	201.467	201.751	201.721	201.780
23	7	203	G	202.083	202.074	202.093	202.125	202.111	202.140
23	7	203	G	202.250	202.221	202.280	202.375	202.332	202.421
23	7	203	G	202.417	202.369	202.467	202.750	202.721	202.780
24	7	204	S	203.083	203.074	203.094	203.125	203.111	203.140
24	7	204	S	203.249	203.222	203.281	203.374	203.333	203.421
24	7	204	S	203.416	203.370	203.468	203.749	203.722	203.781
26	7	206	S	205.083	205.074	205.094	205.124	205.111	205.141
26	7	206	S	205.248	205.223	205.281	205.372	205.334	205.422
26	7	206	S	205.414	205.371	205.469	205.748	205.723	205.781
27	7	207	S	206.083	206.074	206.094	206.124	206.111	206.141
27	7	207	S	206.248	206.223	206.282	206.372	206.334	206.422
27	7	207	S	206.413	206.372	206.469	206.748	206.723	206.782
28	7	208	G	207.082	207.074	207.094	207.124	207.112	207.141
28	7	208	G	207.247	207.223	207.282	207.371	207.335	207.423
28	7	208	G	207.412	207.372	207.470	207.747	207.723	207.782
29	7	209	G	208.082	208.075	208.094	208.123	208.112	208.141
29	7	209	G	208.247	208.224	208.282	208.370	208.336	208.423
29	7	209	G	208.411	208.373	208.470	208.747	208.724	208.782
30	7	210	G	209.082	209.075	209.094	209.123	209.112	209.141
30	7	210	G	209.246	209.224	209.282	209.369	209.336	209.423
30	7	210	G	209.410	209.374	209.470	209.746	209.724	209.782

$D$	$M$	$N_E$	$X$	Div: Eq. 4			Div: Eq. 5		
				$N_0 = 62$ (days)	$N_0 = 187$ (days)	$N_0 = 307$ (days)	$N_0 = 62$ (days)	$N_0 = 187$ (days)	$N_0 = 307$ (days)
1	8	211	G	210.082	210.075	210.094	210.123	210.112	210.141
1	8	211	G	210.245	210.225	210.283	210.368	210.337	210.424
1	8	211	G	210.409	210.374	210.471	210.745	210.725	210.783
2	8	212	G	211.082	211.075	211.094	211.122	211.112	211.141
2	8	212	G	211.245	211.225	211.283	211.367	211.337	211.424
2	8	212	G	211.408	211.375	211.471	211.745	211.725	211.783
3	8	213	S	212.081	212.075	212.094	212.122	212.113	212.141
3	8	213	S	212.244	212.225	212.283	212.367	212.338	212.424
3	8	213	S	212.407	212.376	212.472	212.744	212.725	212.783
4	8	214	G	213.081	213.075	213.094	213.122	213.113	213.142
4	8	214	G	213.244	213.226	213.283	213.366	213.339	213.425
4	8	214	G	213.406	213.376	213.472	213.744	213.726	213.783
5	8	215	S	214.081	214.075	214.094	214.122	214.113	214.142
5	8	215	S	214.243	214.226	214.283	214.365	214.339	214.425
5	8	215	S	214.405	214.377	214.472	214.743	214.726	214.783
6	8	216	S	215.081	215.076	215.095	215.121	215.113	215.142
6	8	216	S	215.243	215.227	215.284	215.364	215.340	215.425
6	8	216	S	215.404	215.378	215.473	215.743	215.727	215.784
7	8	217	G	216.081	216.076	216.095	216.121	216.114	216.142
7	8	217	G	216.242	216.227	216.284	216.363	216.341	216.426
7	8	217	G	216.404	216.379	216.473	216.742	216.727	216.784
8	8	218	G	217.081	217.076	217.095	217.121	217.114	217.142
8	8	218	G	217.242	217.228	217.284	217.362	217.341	217.426
8	8	218	G	217.403	217.379	217.473	217.742	217.728	217.784
11	8	221	S	220.080	220.076	220.095	220.120	220.114	220.142
11	8	221	S	220.240	220.229	220.284	220.360	220.343	220.426
11	8	221	S	220.400	220.382	220.474	220.740	220.729	220.784
12	8	222	S	221.080	221.076	221.095	221.120	221.115	221.142
12	8	222	S	221.239	221.229	221.284	221.359	221.344	221.427
12	8	222	S	221.399	221.382	221.474	221.739	221.729	221.784
13	8	223	S	222.080	222.077	222.095	222.119	222.115	222.142
13	8	223	S	222.239	222.230	222.285	222.358	222.345	222.427
13	8	223	S	222.398	222.383	222.474	222.739	222.730	222.785
15	8	225	G	224.079	224.077	224.095	224.119	224.115	224.142
15	8	225	G	224.238	224.231	224.285	224.357	224.346	224.427
15	8	225	G	224.396	224.385	224.475	224.738	224.731	224.785
16	8	226	G	225.079	225.077	225.095	225.119	225.116	225.142
16	8	226	G	225.237	225.231	225.285	225.356	225.347	225.427
16	8	226	G	225.395	225.386	225.475	225.737	225.731	225.785
17	8	227	S	226.079	226.077	226.095	226.118	226.116	226.142
17	8	227	S	226.237	226.232	226.285	226.355	226.348	226.427
17	8	227	S	226.394	226.387	226.475	226.737	226.732	226.785
19	8	229	G	228.079	228.078	228.095	228.118	228.116	228.142
19	8	229	G	228.236	228.233	228.285	228.353	228.349	228.427
19	8	229	G	228.393	228.388	228.475	228.736	228.733	228.785
22	8	232	S	231.078	231.078	231.095	231.117	231.117	231.142
22	8	232	S	231.234	231.234	231.285	231.351	231.352	231.427
22	8	232	S	231.390	231.391	231.475	231.734	231.734	231.785
24	8	234	S	233.078	233.079	233.095	233.117	233.118	233.142
24	8	234	S	233.233	233.236	233.285	233.350	233.353	233.427
24	8	234	S	233.388	233.393	233.475	233.733	233.736	233.785
25	8	235	S	234.078	234.079	234.095	234.116	234.118	234.142
25	8	235	S	234.233	234.236	234.285	234.349	234.354	234.427
25	8	235	S	234.388	234.393	234.475	234.733	234.736	234.785
27	8	237	S	236.077	236.079	236.095	236.116	236.119	236.142
27	8	237	S	236.232	236.237	236.285	236.347	236.356	236.427
27	8	237	S	236.386	236.395	236.475	236.732	236.737	236.785
28	8	238	G	237.077	237.079	237.095	237.116	237.119	237.142
28	8	238	G	237.231	237.238	237.285	237.347	237.356	237.427
28	8	238	G	237.385	237.396	237.475	237.731	237.738	237.785
29	8	239	G	238.077	238.079	238.095	238.115	238.119	238.142
29	8	239	G	238.231	238.238	238.285	238.346	238.357	238.427
29	8	239	G	238.384	238.397	238.474	238.731	238.738	238.785
30	8	240	G	239.077	239.080	239.095	239.115	239.119	239.142
30	8	240	G	239.230	239.239	239.285	239.345	239.358	239.427
30	8	240	G	239.383	239.398	239.474	239.730	239.739	239.785



<i>D</i>	<i>M</i>	<i>N<sub>E</sub></i>	<i>X</i>	Div: Eq. 4			Div: Eq. 5		
				<i>N<sub>0</sub></i> = 62 (days)	<i>N<sub>0</sub></i> = 187 (days)	<i>N<sub>0</sub></i> = 307 (days)	<i>N<sub>0</sub></i> = 62 (days)	<i>N<sub>0</sub></i> = 187 (days)	<i>N<sub>0</sub></i> = 307 (days)
1	9	241	G	240.077	240.080	240.095	240.115	240.120	240.142
1	9	241	G	240.230	240.239	240.284	240.344	240.359	240.427
1	9	241	G	240.383	240.399	240.474	240.730	240.739	240.784
3	9	243	G	242.076	242.080	242.095	242.114	242.120	242.142
3	9	243	G	242.229	242.240	242.284	242.343	242.361	242.426
3	9	243	G	242.381	242.401	242.474	242.729	242.740	242.784
4	9	244	S	243.076	243.080	243.095	243.114	243.120	243.142
4	9	244	S	243.228	243.241	243.284	243.342	243.361	243.426
4	9	244	S	243.380	243.401	243.473	243.728	243.741	243.784
6	9	246	G	245.076	245.081	245.095	245.114	245.121	245.142
6	9	246	G	245.227	245.242	245.284	245.341	245.363	245.426
6	9	246	G	245.379	245.403	245.473	245.727	245.742	245.784
7	9	247	G	246.076	246.081	246.095	246.113	246.121	246.142
7	9	247	G	246.227	246.243	246.284	246.340	246.364	246.425
7	9	247	G	246.378	246.404	246.473	246.727	246.743	246.784
9	9	249	G	248.075	248.081	248.094	248.113	248.122	248.142
9	9	249	G	248.226	248.244	248.283	248.339	248.365	248.425
9	9	249	G	248.377	248.406	248.472	248.726	248.744	248.783
16	9	256	G	255.074	255.083	255.094	255.112	255.124	255.141
16	9	256	G	255.223	255.248	255.282	255.335	255.371	255.422
16	9	256	G	255.372	255.413	255.469	255.723	255.748	255.782
17	9	257	G	256.074	256.083	256.094	256.111	256.124	256.141
17	9	257	G	256.223	256.248	256.281	256.334	256.372	256.422
17	9	257	G	256.371	256.414	256.469	256.723	256.748	256.781
18	9	258	G	257.074	257.083	257.094	257.111	257.124	257.141
18	9	258	G	257.222	257.249	257.281	257.333	257.373	257.422
18	9	258	G	257.370	257.414	257.468	257.722	257.749	257.781
19	9	259	G	258.074	258.083	258.094	258.111	258.125	258.140
19	9	259	G	258.222	258.249	258.281	258.333	258.374	258.421
19	9	259	G	258.370	258.415	258.468	258.722	258.749	258.781
20	9	260	S	259.074	259.083	259.093	259.111	259.125	259.140
20	9	260	S	259.222	259.250	259.280	259.332	259.375	259.421
20	9	260	S	259.369	259.416	259.467	259.722	259.750	259.780
21	9	261	S	260.074	260.083	260.093	260.111	260.125	260.140
21	9	261	S	260.221	260.250	260.280	260.332	260.376	260.420
21	9	261	S	260.369	260.417	260.467	260.721	260.750	260.780
22	9	262	G	261.074	261.084	261.093	261.110	261.125	261.140
22	9	262	G	261.221	261.251	261.280	261.331	261.376	261.420
22	9	262	G	261.368	261.418	261.466	261.721	261.751	261.780
23	9	263	G	262.073	262.084	262.093	262.110	262.126	262.140
23	9	263	G	262.220	262.252	262.279	262.331	262.377	262.419
23	9	263	G	262.367	262.419	262.466	262.720	262.752	262.779
25	9	265	G	264.073	264.084	264.093	264.110	264.126	264.139
25	9	265	G	264.220	264.253	264.279	264.330	264.379	264.418
25	9	265	G	264.366	264.421	264.465	264.720	264.753	264.779
26	9	266	G	265.073	265.084	265.093	265.110	265.127	265.139
26	9	266	G	265.220	265.253	265.278	265.329	265.380	265.418
26	9	266	G	265.366	265.422	265.464	265.720	265.753	265.778
29	9	269	G	268.073	268.085	268.092	268.109	268.127	268.139
29	9	269	G	268.219	268.255	268.277	268.328	268.382	268.416
29	9	269	G	268.364	268.425	268.462	268.719	268.755	268.777
30	9	270	G	269.073	269.085	269.092	269.109	269.128	269.138
30	9	270	G	269.218	269.255	269.277	269.328	269.383	269.415
30	9	270	G	269.364	269.426	269.462	269.718	269.755	269.777

<i>D</i>	<i>M</i>	<i>N<sub>E</sub></i>	<i>X</i>	Div: Eq. 4			Div: Eq. 5		
				<i>N<sub>0</sub></i> = 62 (days)	<i>N<sub>0</sub></i> = 187 (days)	<i>N<sub>0</sub></i> = 307 (days)	<i>N<sub>0</sub></i> = 62 (days)	<i>N<sub>0</sub></i> = 187 (days)	<i>N<sub>0</sub></i> = 307 (days)
1	10	271	G	270.073	270.085	270.092	270.109	270.128	270.138
1	10	271	G	270.218	270.256	270.277	270.327	270.384	270.415
1	10	271	G	270.364	270.427	270.461	270.718	270.756	270.777
3	10	273	G	272.073	272.086	272.092	272.109	272.129	272.138
3	10	273	G	272.218	272.257	272.276	272.326	272.386	272.414
3	10	273	G	272.363	272.429	272.460	272.718	272.757	272.776
4	10	274	S	273.072	273.086	273.092	273.109	273.129	273.138
4	10	274	S	273.217	273.258	273.275	273.326	273.386	273.413
4	10	274	S	273.362	273.429	273.459	273.717	273.758	273.775
5	10	275	G	274.072	274.086	274.092	274.109	274.129	274.137
5	10	275	G	274.217	274.258	274.275	274.326	274.387	274.412
5	10	275	G	274.362	274.430	274.458	274.717	274.758	274.775
7	10	277	S	276.072	276.086	276.091	276.108	276.130	276.137
7	10	277	S	276.217	276.259	276.274	276.325	276.389	276.411
7	10	277	S	276.361	276.432	276.457	276.717	276.759	276.774
8	10	278	G	277.072	277.087	277.091	277.108	277.130	277.137
8	10	278	G	277.217	277.260	277.274	277.325	277.390	277.410
8	10	278	G	277.361	277.433	277.456	277.717	277.760	277.774
9	10	279	G	278.072	278.087	278.091	278.108	278.130	278.137
9	10	279	G	278.216	278.260	278.273	278.325	278.391	278.410
9	10	279	G	278.361	278.434	278.455	278.716	278.760	278.773
10	10	280	G	279.072	279.087	279.091	279.108	279.130	279.136
10	10	280	G	279.216	279.261	279.273	279.324	279.391	279.409
10	10	280	G	279.360	279.435	279.454	279.716	279.761	279.773
11	10	281	S	280.072	280.087	280.091	280.108	280.131	280.136
11	10	281	S	280.216	280.261	280.272	280.324	280.392	280.408
11	10	281	S	280.360	280.436	280.454	280.716	280.761	280.772
12	10	282	G	281.072	281.087	281.091	281.108	281.131	281.136
12	10	282	G	281.216	281.262	281.272	281.324	281.393	281.408
12	10	282	G	281.360	281.437	281.453	281.716	281.762	281.772
13	10	283	G	282.072	282.088	282.090	282.108	282.131	282.136
13	10	283	G	282.216	282.263	282.271	282.324	282.394	282.407
13	10	283	G	282.360	282.438	282.452	282.716	282.763	282.771
14	10	284	G	283.072	283.088	283.090	283.108	283.132	283.135
14	10	284	G	283.216	283.263	283.271	283.323	283.395	283.406
14	10	284	G	283.359	283.439	283.451	283.716	283.763	283.771
15	10	285	S	284.072	284.088	284.090	284.108	284.132	284.135
15	10	285	S	284.216	284.264	284.270	284.323	284.395	284.406
15	10	285	S	284.359	284.439	284.451	284.716	284.764	284.770
16	10	286	G	285.072	285.088	285.090	285.108	285.132	285.135
16	10	286	G	285.215	285.264	285.270	285.323	285.396	285.405
16	10	286	G	285.359	285.440	285.450	285.715	285.764	285.770
17	10	287	S	286.072	286.088	286.090	286.108	286.132	286.135
17	10	287	S	286.215	286.265	286.269	286.323	286.397	286.404
17	10	287	S	286.359	286.441	286.449	286.715	286.765	286.769
18	10	288	S	287.072	287.088	287.090	287.108	287.133	287.134
18	10	288	S	287.215	287.265	287.269	287.323	287.398	287.403
18	10	288	S	287.359	287.442	287.448	287.715	287.765	287.769
19	10	289	S	288.072	288.089	288.089	288.108	288.133	288.134
19	10	289	S	288.215	288.266	288.268	288.323	288.399	288.403
19	10	289	S	288.359	288.443	288.447	288.715	288.766	288.768
20	10	290	S	289.072	289.089	289.089	289.108	289.133	289.134
20	10	290	S	289.215	289.266	289.268	289.323	289.399	289.402
20	10	290	S	289.359	289.444	289.446	289.715	289.766	289.768
21	10	291	S	290.072	290.089	290.089	290.108	290.133	290.134
21	10	291	S	290.215	290.267	290.267	290.323	290.400	290.401
21	10	291	G	290.358	290.445	290.446	290.715	290.767	290.767
22	10	292	S	291.072	291.089	291.089	291.108	291.134	291.133
22	10	292	S	291.215	291.267	291.267	291.323	291.401	291.400
22	10	292	S	291.358	291.445	291.445	291.715	291.767	291.767
23	10	293	G	292.072	292.089	292.089	292.108	292.134	292.133
23	10	293	G	292.215	292.268	292.266	292.323	292.402	292.400
23	10	293	G	292.358	292.446	292.444	292.715	292.768	292.766
24	10	294	G	293.072	293.089	293.089	293.108	293.134	293.133
24	10	294	G	293.215	293.268	293.266	293.323	293.402	293.399
24	10	294	G	293.358	293.447	293.443	293.715	293.768	293.766
25	10	295	G	294.072	294.090	294.088	294.108	294.134	294.133
25	10	295	G	294.215	294.269	294.265	294.323	294.403	294.398
25	10	295	G	294.358	294.448	294.442	294.715	294.769	294.765
26	10	296	S	295.072	295.090	295.088	295.108	295.135	295.132
26	10	296	S	295.215	295.269	295.265	295.323	295.404	295.397
26	10	296	S	295.358	295.449	295.441	295.715	295.769	295.765
27	10	297	S	296.072	296.090	296.088	296.108	296.135	296.132
27	10	297	S	296.215	296.270	296.264	296.323	296.405	296.396
27	10	297	S	296.358	296.450	296.440	296.715	296.770	296.764
28	10	298	G	297.072	297.090	297.088	297.108	297.135	297.132
28	10	298	G	297.215	297.270	297.264	297.323	297.405	297.396
28	10	298	G	297.359	297.450	297.440	297.715	297.770	297.764
29	10	299	G	298.072	298.090	298.088	298.108	298.135	298.132
29	10	299	G	298.215	298.271	298.263	298.323	298.406	298.395
29	10	299	G	298.359	298.451	298.439	298.715	298.771	298.763
30	10	300	G	299.072	299.090	299.088	299.108	299.136	299.131
30	10	300	G	299.215	299.271	299.263	299.323	299.407	299.394
30	10	300	G	299.359	299.452	299.438	299.715	299.771	299.763

<i>D</i>	<i>M</i>	<i>N<sub>E</sub></i>	<i>X</i>	Div: Eq. 4			Div: Eq. 5		
				<i>N<sub>0</sub></i> = 62 (days)	<i>N<sub>0</sub></i> = 187 (days)	<i>N<sub>0</sub></i> = 307 (days)	<i>N<sub>0</sub></i> = 62 (days)	<i>N<sub>0</sub></i> = 187 (days)	<i>N<sub>0</sub></i> = 307 (days)
1	11	301	G	300.072	300.091	300.087	300.108	300.136	300.131
1	11	301	G	300.215	300.272	300.262	300.323	300.407	300.393
1	11	301	G	300.359	300.453	300.437	300.715	300.772	300.762
2	11	302	G	301.072	301.091	301.087	301.108	301.136	301.131
2	11	302	G	301.215	301.272	301.262	301.323	301.408	301.392
2	11	302	G	301.359	301.454	301.436	301.715	301.772	301.762
3	11	303	S	302.072	302.091	302.087	302.108	302.136	302.131
3	11	303	S	302.215	302.273	302.261	302.323	302.409	302.392
3	11	303	S	302.359	302.454	302.435	302.715	302.773	302.761
4	11	304	G	303.072	303.091	303.087	303.108	303.137	303.130
4	11	304	G	303.216	303.273	303.261	303.323	303.410	303.391
4	11	304	G	303.359	303.455	303.434	303.716	303.773	303.761
5	11	305	S	304.072	304.091	304.087	304.108	304.137	304.130
5	11	305	S	304.216	304.273	304.260	304.324	304.410	304.390
5	11	305	S	304.360	304.456	304.433	304.716	304.773	304.760
7	11	307	S	306.072	306.091	306.086	306.108	306.137	306.129
7	11	307	S	306.216	306.274	306.259	306.324	306.412	306.388
7	11	307	S	306.360	306.457	306.432	306.716	306.774	306.759
8	11	308	S	307.072	307.092	307.086	307.108	307.137	307.129
8	11	308	S	307.216	307.275	307.258	307.324	307.412	307.388
8	11	308	S	307.360	307.458	307.431	307.716	307.775	307.758
9	11	309	G	308.072	308.092	308.086	308.108	308.138	308.129
9	11	309	G	308.216	308.275	308.258	308.324	308.413	308.387
9	11	309	G	308.361	308.459	308.430	308.716	308.775	308.758
10	11	310	S	309.072	309.092	309.086	309.108	309.138	309.129
10	11	310	S	309.217	309.276	309.257	309.325	309.413	309.386
10	11	310	S	309.361	309.459	309.429	309.717	309.776	309.757
11	11	311	S	310.072	310.092	310.086	310.108	310.138	310.128
11	11	311	S	310.217	310.276	310.257	310.325	310.414	310.385
11	11	311	S	310.361	310.460	310.428	310.717	310.776	310.757
14	11	314	S	313.072	313.092	313.085	313.109	313.139	313.128
14	11	314	S	313.217	313.277	313.255	313.326	313.416	313.383
14	11	314	S	313.362	313.462	313.425	313.717	313.777	313.755
15	11	315	G	314.073	314.093	314.085	314.109	314.139	314.127
15	11	315	G	314.218	314.278	314.254	314.326	314.416	314.382
15	11	315	G	314.363	314.463	314.424	314.718	314.778	314.754
16	11	316	S	315.073	315.093	315.085	315.109	315.139	315.127
16	11	316	S	315.218	315.278	315.254	315.327	315.417	315.381
16	11	316	S	315.363	315.463	315.423	315.718	315.778	315.754
18	11	318	S	317.073	317.093	317.084	317.109	317.139	317.126
18	11	318	S	317.218	317.279	317.253	317.327	317.418	317.379
18	11	318	S	317.364	317.464	317.421	317.718	317.779	317.753
19	11	319	S	318.073	318.093	318.084	318.109	318.140	318.126
19	11	319	S	318.219	318.279	318.252	318.328	318.419	318.378
19	11	319	S	318.364	318.465	318.420	318.719	318.779	318.752
20	11	320	S	319.073	319.093	319.084	319.109	319.140	319.126
20	11	320	S	319.219	319.279	319.252	319.328	319.419	319.377
20	11	320	S	319.365	319.466	319.419	319.719	319.779	319.752
21	11	321	G	320.073	320.093	320.084	320.110	320.140	320.126
21	11	321	G	320.219	320.280	320.251	320.329	320.420	320.377
21	11	321	G	320.365	320.466	320.418	320.719	320.780	320.751
22	11	322	S	321.073	321.093	321.084	321.110	321.140	321.125
22	11	322	S	321.219	321.280	321.251	321.329	321.420	321.376
22	11	322	S	321.366	321.467	321.418	321.719	321.780	321.751
23	11	323	S	322.073	322.093	322.083	322.110	322.140	322.125
23	11	323	S	322.220	322.280	322.250	322.330	322.421	322.375
23	11	323	S	322.366	322.467	322.417	322.720	322.780	322.750
24	11	324	G	323.073	323.094	323.083	323.110	323.140	323.125
24	11	324	G	323.220	323.281	323.249	323.330	323.421	323.374
24	11	324	G	323.367	323.468	323.416	323.720	323.781	323.749
25	11	325	G	324.073	324.094	324.083	324.110	324.140	324.124
25	11	325	S	324.220	324.281	324.249	324.331	324.421	324.373
25	11	325	G	324.367	324.468	324.415	324.720	324.781	324.749
26	11	326	G	325.074	325.094	325.083	325.110	325.141	325.124
26	11	326	G	325.221	325.281	325.248	325.331	325.422	325.372
26	11	326	G	325.368	325.469	325.414	325.721	325.781	325.748
27	11	327	S	326.074	326.094	326.083	326.111	326.141	326.124
27	11	327	S	326.221	326.282	326.248	326.332	326.422	326.372
27	11	327	S	326.368	326.469	326.413	326.721	326.782	326.748
28	11	328	S	327.074	327.094	327.082	327.111	327.141	327.124
28	11	328	S	327.221	327.282	327.247	327.332	327.423	327.371
28	11	328	S	327.369	327.470	327.412	327.721	327.782	327.747
29	11	329	G	328.074	328.094	328.082	328.111	328.141	328.123
29	11	329	G	328.222	328.282	328.247	328.333	328.423	328.370
29	11	329	G	328.370	328.470	328.411	328.722	328.782	328.747
30	11	330	G	329.074	329.094	329.082	329.111	329.141	329.123
30	11	330	G	329.222	329.282	329.246	329.333	329.423	329.369
30	11	330	G	329.370	329.470	329.410	329.722	329.782	329.746

<i>D</i>	<i>M</i>	<i>N<sub>E</sub></i>	<i>X</i>	Div: Eq. 4			Div: Eq. 5		
				<i>N<sub>0</sub></i> = 62 (days)	<i>N<sub>0</sub></i> = 187 (days)	<i>N<sub>0</sub></i> = 307 (days)	<i>N<sub>0</sub></i> = 62 (days)	<i>N<sub>0</sub></i> = 187 (days)	<i>N<sub>0</sub></i> = 307 (days)
1	12	331	G	330.074	330.094	330.082	330.111	330.141	330.123
1	12	331	G	330.223	330.283	330.245	330.334	330.424	330.368
1	12	331	G	330.371	330.471	330.409	330.723	330.783	330.745
2	12	332	G	331.074	331.094	331.082	331.111	331.141	331.122
2	12	332	G	331.223	331.283	331.245	331.334	331.424	331.367
2	12	332	G	331.372	331.471	331.408	331.723	331.783	331.745
3	12	333	S	332.074	332.094	332.081	332.112	332.141	332.122
3	12	333	S	332.223	332.283	332.244	332.335	332.424	332.367
3	12	333	S	332.372	332.472	332.407	332.723	332.783	332.744
4	12	334	S	333.075	333.094	333.081	333.112	333.142	333.122
4	12	334	S	333.224	333.283	333.244	333.336	333.425	333.366
4	12	334	G	333.373	333.472	333.406	333.724	333.783	333.744
5	12	335	G	334.075	334.094	334.081	334.112	334.142	334.122
5	12	335	G	334.224	334.283	334.243	334.336	334.425	334.365
5	12	335	G	334.374	334.472	334.405	334.724	334.783	334.743
6	12	336	S	335.075	335.095	335.081	335.112	335.142	335.121
6	12	336	S	335.225	335.284	335.243	335.337	335.425	335.364
6	12	336	S	335.374	335.473	335.404	335.725	335.784	335.743
8	12	338	G	337.075	337.095	337.081	337.113	337.142	337.121
8	12	338	G	337.225	337.284	337.242	337.338	337.426	337.362
8	12	338	G	337.376	337.473	337.403	337.725	337.784	337.742
9	12	339	G	338.075	338.095	338.080	338.113	338.142	338.121
9	12	339	G	338.226	338.284	338.241	338.339	338.426	338.362
9	12	339	G	338.376	338.473	338.402	338.726	338.784	338.741
10	12	340	G	339.075	339.095	339.080	339.113	339.142	339.120
10	12	340	G	339.226	339.284	339.240	339.339	339.426	339.361
10	12	340	G	339.377	339.474	339.401	339.726	339.784	339.740
11	12	341	S	340.076	340.095	340.080	340.113	340.142	340.120
11	12	341	S	340.227	340.284	340.240	340.340	340.426	340.360
11	12	341	S	340.378	340.474	340.400	340.727	340.784	340.740
12	12	342	G	341.076	341.095	341.080	341.114	341.142	341.120
12	12	342	G	341.227	341.284	341.239	341.341	341.427	341.359
12	12	342	G	341.379	341.474	341.399	341.727	341.784	341.739
13	12	343	G	342.076	342.095	342.080	342.114	342.142	342.119
13	12	343	G	342.228	342.285	342.239	342.341	342.427	342.358
13	12	343	G	342.379	342.474	342.398	342.728	342.785	342.739
14	12	344	G	343.076	343.095	343.079	343.114	343.142	343.119
14	12	344	G	343.228	343.285	343.238	343.342	343.427	343.357
14	12	344	G	343.380	343.474	343.397	343.728	343.785	343.738
15	12	345	S	344.076	344.095	344.079	344.114	344.142	344.119
15	12	345	S	344.229	344.285	344.238	344.343	344.427	344.357
15	12	345	S	344.381	344.475	344.396	344.729	344.785	344.738
16	12	346	G	345.076	345.095	345.079	345.114	345.142	345.119
16	12	346	G	345.229	345.285	345.237	345.343	345.427	345.356
16	12	346	G	345.382	345.475	345.395	345.729	345.785	345.737
17	12	347	G	346.076	346.095	346.079	346.115	346.142	346.118
17	12	347	G	346.229	346.285	346.237	346.344	346.427	346.355
17	12	347	G	346.382	346.475	346.394	346.729	346.785	346.737
18	12	348	S	347.077	347.095	347.079	347.115	347.142	347.118
18	12	348	S	347.230	347.285	347.236	347.345	347.427	347.354
18	12	348	G	347.383	347.475	347.394	347.730	347.785	347.736
19	12	349	G	348.077	348.095	348.079	348.115	348.142	348.118
19	12	349	G	348.230	348.285	348.236	348.346	348.427	348.353
19	12	349	G	348.384	348.475	348.393	348.730	348.785	348.736
21	12	351	G	350.077	350.095	350.078	350.116	350.142	350.117
21	12	351	G	350.231	350.285	350.235	350.347	350.427	350.352
21	12	351	G	350.386	350.475	350.391	350.731	350.785	350.735
22	12	352	G	351.077	351.095	351.078	351.116	351.142	351.117
22	12	352	G	351.232	351.285	351.234	351.348	351.427	351.351
22	12	352	G	351.387	351.475	351.390	351.732	351.785	351.734
23	12	353	S	352.077	352.095	352.078	352.116	352.142	352.117
23	12	353	S	352.232	352.285	352.234	352.349	352.427	352.350
23	12	353	S	352.387	352.475	352.389	352.732	352.785	352.734
24	12	354	G	353.078	353.095	353.078	353.116	353.142	353.117
24	12	354	G	353.233	353.285	353.233	353.349	353.427	353.350
24	12	354	G	353.388	353.475	353.388	353.733	353.785	353.733
25	12	355	G	354.078	354.095	354.078	354.117	354.142	354.116
25	12	355	G	354.233	354.285	354.233	354.350	354.427	354.349
25	12	355	G	354.389	354.475	354.388	354.733	354.785	354.733
26	12	356	G	355.078	355.095	355.077	355.117	355.142	355.116
26	12	356	S	355.234	355.285	355.232	355.351	355.427	355.348
26	12	356	G	355.390	355.475	355.387	355.734	355.785	355.732
27	12	357	S	356.078	356.095	356.077	356.117	356.142	356.116
27	12	357	S	356.234	356.285	356.232	356.352	356.427	356.347
27	12	357	S	356.391	356.475	356.386	356.734	356.785	356.732
28	12	358	G	357.078	357.095	357.077	357.117	357.142	357.116
28	12	358	G	357.235	357.285	357.231	357.352	357.427	357.347
28	12	358	G	357.392	357.475	357.385	357.735	357.785	357.731
29	12	359	G	358.079	358.095	358.077	358.118	358.142	358.115
29	12	359	G	358.236	358.285	358.231	358.353	358.427	358.346
29	12	359	G	358.393	358.474	358.384	358.736	358.785	358.731
30	12	360	G	359.079	359.095	359.077	359.118	359.142	359.115
30	12	360	G	359.236	359.285	359.230	359.354	359.427	359.345
30	12	360	G	359.393	359.474	359.383	359.736	359.785	359.730

**Notes.** Cols. 5–10 have been calculated with  $N_0 = 62, 187$  or  $307$  in Eq. 1 combined with the day divisions Div: Eqs. 4 or 5.